Biochemical and structural analysis of marine polysaccharide lyases

Master thesis written in partial fulfilment of the requirements for the academic degree Master of Science in Microbiology from the Carl von Ossietzky University of Oldenburg.

Submitted by Nadine Gerlach (2187667)

24.05.2017

The presented master thesis was conducted in the department of Dr. Jan-Hendrik Hehemann *Marine Glycobiology* at the Max-Planck-Institute for Marine Microbiology and the MARUM of the University of Bremen in collaboration with the University of Oldenburg and the University of Greifswald.

The thesis was constructed as a draft version of two scientific papers that base on the present study as well as additional background information and an outlook section regarding further research.

1. Reviewer: Dr. Jan-Hendrik Hehemann

Department of Marine Glycobiology at the Max-Planck-Institute for Marine Microbiology and the MARUM, University of Bremen, Germany

2. Reviewer: Prof. Dr. Meinhard Simon

Department of Biology of Geological Processes at the Institute for Chemistry and Biology of the Marine Environment (ICBM), University of Oldenburg, Germany

Table of contents

Acknowledgments

I would like to thank my reviewers Dr. Jan-Hendrik Hehemann and Prof. Dr. Simon Meinhard for the opportunity to introduce me in the field of glyco- and structural biology as well as acquiring so many research skills. I am grateful for the support and guidance of my supervisors Dr. Craig S. Robb and Dr. Matthias Wietz throughout this project. Many thanks go to my collaborators Lukas Reisky and Prof. Uwe Bornscheuer from the University Greifswald, with whom I worked on the structural analysis of the ulvan lyase from *F. agariphila* KM3901^{T}.

I also thank the whole department of Marine Glycobiology for their warm welcome, the nice working atmosphere and especially their support in any way.

Lastly, I am very thankful for my parents and friends - especially Djoana Shopova, Christopher Friedrich & Julian Engel - for all their encouragement and love.

List of abbreviations

ABC	ATP-binding cassette
Aly	alginate lyase
CAPS	N-cyclohexyl-3-aminopropanesulfonic acid
CAZymes	carbohydrate active enzymes
CBM	carbohydrate binding module
DLS	dynamic light scattering
DOM	dissolved organic matter
EDTA	ethylenediaminetetraacetic acid
G	guluronate
GFP	green fluorescent protein
GH	glycoside hydrolase
GlcUA	D-glucuronic acid
GM	guluronate and mannuronate
HEPES	4-(2-hydroyethyl)-1-piperazineethanesulfonic acid
HPLC	high pressure liquid chromatography
IdoUA	L-iduronic acid
IEX	ion exchange chromatography
IPTG	Isopropyl β-D-1-thiogalactopyranoside
IMAC	immobilized metal affinity chromatography
kbp	kilo base pairs
LB	lysogeny broth

LGT	lateral gene transfer
M	mannuronate
MES	2-(N-morpholino)ethane sulfonic acid
MOPS	3-(N-morpholino)propanesulfonic acid
MS	mass spectrometry
NMR	nuclear magnetic resonance
OM	organic matter
PCR	polymerase chain reaction
PL	polysaccharide lyase
POM	particulate organic matter
PUL	polysaccharide utilization loci (or locus)
R3S	3-sulfated rhamnose
SDS-PAGE	sodium dodecyl sulphate polyacrylamide gel electrophoresis
SEC	size exclusion chromatography
SUMO	small ubiquitin related modifier
TEP	transparent exopolymer particles
T-CEP	Tris-(2-carboxyethyl)phosphine
TBDT	TonB-dependent transporter
TGS	Tris-glycine-SDS
Tris	tris(hydroxymethyl)aminomethane
UL	ulvan lyase
Xyl	D-xylose

List of figures

List of tables

Background

Algal polysaccharides

Marine phytoplankton converts ~ 45 gigatons of carbon dioxide per year, contributing to half of the global photosynthetic carbon fixation (Falkowski *et al*., 1998). In contrast to microalgae, the impact of macroalgae is often not considered since they make less contribution to primary production and respiratory (Duarte *et al*., 2005). However, they have important ecological functions such as nutrient source (e.g. Neumann *et al*., 2015), release external organic metabolites (Khailov & Burlakova, 1969), serve as habitats for diverse organisms (e.g. Kirkman & Kendrick, 1997), are important carbon burials, and influence the sedimentation of organic material (Duarte *et al*., 2005). Both micro- and macroalgae are fast-growing, often exceeding terrestrial plants and do not require fertilization due to currents and water movements (Kraan, 2012). Many algal species do not grow continuously, but in temporary blooms (Teeling *et al*., 2016) limited by nutrients, grazing predators and viral infections (Valiela *et al*., 1997). Algae produce substantial quantities of reduced carbon compounds such as polysaccharides, lipids and proteins, which can subsequently trigger blooms of planktonic bacteria with a successions of distinct bacterial clades over time (Teeling *et al*., 2012; Teeling *et al*., 2016).

Marine algal consist of up to 70 % of polysaccharides which physically support the thallus of macroalgae, have storage properties (Kraan, 2012) or are part of extracellular transparent exopolymer particles (TEP) (Teeling *et al*., 2016). Cellulose and hemicellulose are the major cell wall polysaccharides with 2 – 10 % and 9 % of algal dry weight, respectively. However, the overall composition of polysaccharides is seasonal and species-specific, with green algae mainly consisting of sulphuric acid polysaccharides, sulphated galactans and xylans, whereas brown algae are rich in alginic acid, fucoidan, laminarin and seagrass and red algae are mainly composed of agars, carrageenans, xylans, floridean starch, sulphated galactan and porphyrin (Kraan, 2012). Due to their variety of biological and chemical properties, algal polysaccharides have become attractive candidates for food, cosmetic and agriculture industries as stabilizers, thickeners and emulsifiers, but also in medicine and pharmacy as potential anti-carcinogens, due to of prebiotic and anti-bacterial properties (Kraan, 2012). The present study focuses on two macroalgal polysaccharides, ulvan and alginate, and how these substrates are utilized by marine, bacterial polysaccharide lyases.

Background

Ulvan is the main cell wall polysaccharide of the algae order Ulvales from the globally distributed green algae (Chlorophyta) contributing up to 29 % of the algae dry weight (Lahaye & Robic, 2007) with an average molecular weight of 189 – 8200 kDa (Lahaye, 1998). There are two types of ulvan in nature – water-soluble and insoluble cellulose-like material (Kraan, 2012). It has a high structural versatility, but mainly consists of rhamnose, uronic acids, and D-xylose (Xyl). Ulvan is an anionic polysaccharide sulphated at C3 of rhamnose and / or C2 of xylose. The degree of sulfation varies, with a maximum of 30 %. Ulvan is composed of repeating disaccharides of D-glucuronic acid (GlcUA) and L-iduronic acid (IdoUA) linked to 3-sulfated rhamnose (R3S). These building blocks are termed ulvanobiuronic acid A or B, respectively. There are also lower amounts of disaccharides of RS3 linked to Xyl (Lahaye & Robic, 2007). In comparison with polysaccharides derived from brown and red algae such as alginate, polysaccharides of green algae are less exploited (Kopel *et al*., 2016). Ulvan is an attractive candidate for detailed studies but due to its biological and physicothermal properties (Lahaye & Robic, 2007).

Alginate is the main cell wall component of brown algae (Phaeophyceae) and can contribute > 45 % to the dry weight (Mabeau & Kloareg, 1987). Alginate is an unbranched, binary copolymer firstly discovered in the 1880s (Kraan, 2012) and available in the acid and salt form. It is composed of uronic acids ß-D-mannuronate (M) and its C5-epimer α-L-guluronate (G) occurring in 1,4-linked blocks of either polyguluronate (polyG), polymannuronate (polyM), or alternating polyguluronate and polymannuronate (polyGM). The number and the ratio of M and G in the blocks depend on the species and affect the mechanical strength and flexibility of the algae. Alginate is an anionic polysaccharide containing one carboxylic acid per sugar monomer (Draget *et al*., 2005). Besides brown seaweed, alginate is also synthesized by two heterotrophic bacterial families, the *Azotobacteriaceae* and the *Pseudomonadaceae*. In contrast to algal alginate, bacterial alginate is often substituted with O-acetyl groups at the C2 and / or C3 of D-mannuronate which effects the biochemical properties of alginate such as the binding of selective ions (Wong *et al*., 2000). Alginate is widely used due to its biochemical properties including the ability to retain water, gelling due to selective binding of multivalent cations such as Ca^{2+} and Mg^{2+}, stabilizing, viscosifying properties (Draget *et al*., 2005) and as hydrocolloid (Kraan, 2012). In the marine environment, gel particles are three-dimensional networks of biopolymers imbedded in seawater, formed from dissolved organic matter (DOM) or polymer chains released by phytoplankton or bacteria. Marine gels are varying in composition, size and formation time. Micro- and nanogels are thought to gain size by continued annealing and collision forming macrogels such as TEP which is important regarding

sedimentation processes in the oceans (Verdugo *et al*., 2004). Previously, alginate gel particles have been shown to serve as nutrient source and microhabitat for bacteria (Mitulla *et al*., 2016). Hence, marine gels are significant regarding the transition of DOM to particulate organic matter (POM), carbon cycling and the microbial loop of the marine food web (Verdugo *et al*., 2004).

Polysaccharide lyases of marine bacteria

Polysaccharide-degrading bacteria specialize on glycans resulting in a pronounced niche partitioning with respect to algal polysaccharide degradation during and after algal blooms (Teeling *et al*., 2012; Teeling *et al*., 2016). In this study we investigated the degradation of anionic algal polysaccharides, focusing on alginate lyases from *Alteromonas macleodii* 83-1 and ulvan lyases *Formosa agariphila* KM3901^{T}. Proteins involved in carbohydrate degradation are sugar transporter, transcriptional regulators, and carbohydrate-active enzymes (CAZymes) including polysaccharide lyases (PL), glycoside hydrolases (GH), carbohydrate esterases, and glycosyl transferases (Lombard *et al*., 2014). In Bacteroidetes, CAZymes are frequently organized in large operon like structures (Thomas *et al*., 2011), termed polysaccharide utilization loci (PUL) (Sonnenburg *et al*., 2010).

Polysaccharide lyases (EC 4.2.2.-) are enzymes cleaving polysaccharide chains containing uronic acids via β-elimination resulting in an unsaturated hexenuronic acid residue and a new reducing end. PLs are classified in 26 families based on similarities of their amino acid sequence intending to reflect their structural features and often substrate specificity. Since there is a variety of known fold types, it is likely that PLs evolved more than once during evolution (Garron & Cygler, 2010; Lombard *et al*., 2010; Lombard *et al*., 2014).

PLs involved in ulvan degradation are classified as ulvan lyases of families PL24 and PL25 produced by bacteria from the orders Flavobacteriales and Alteromonadales, such as *Nonlabens ulvanivorans* (Collen *et al*., 2011; Kopel *et al*., 2014), *Pseudoalteromonas* sp. PLSV (Kopel *et al*., 2014b; Ulaganathan *et al*., 2017) and *Alteromonas* spp. (Kopel *et al*., 2016; Kopel *et al*., 2014c). Ulvan lyases cleave the ß-(1→4) glycosidic bond between the building blocks ulvanobiuronic acid A or B resulting in the formation of a reducing end on one fragment and an unsaturated ring (Δ, 4-deoxy-L-*threo*-hex-4-enopyranosiduronic acid) on the non-reducing end of the second fragment (Figure 1). Bacterial model organisms are a valuable resource for the detailed characterization of polysaccharide utilization by CAZymes.

Formosa agariphila KMM 3901^T is a Gram-negative, aerobic, and motile bacterium (Ivanova *et al*., 2004) originally isolated from Troitsa Bay, Gulf of Peter the Great, East Sea from the green alga *Acrosiphonia sonderi* (Nedashkovskaya *et al*., 2006). Genome analysis revealed that *F. agariphila* KMM3901^T exhibits an algae-associated lifestyle, having many putative genes for the degradation of algal polysaccharides in at least 13 PULs, consisting of 45 sulfatases, 13 PLs, 88 GHs, SusD-like proteins, transporter proteins (mainly TBDTs and ABCs), transcriptional regulators and other proteins (Mann *et al*., 2013). One of these PULs contains genes essential for the degradation of sulphated marine algal polysaccharides, including GH105 and ulvan lyase homologs which have been previously found active on ulvan (Figure 2). This suggested that this PUL may be involved in the metabolism of ulvan.

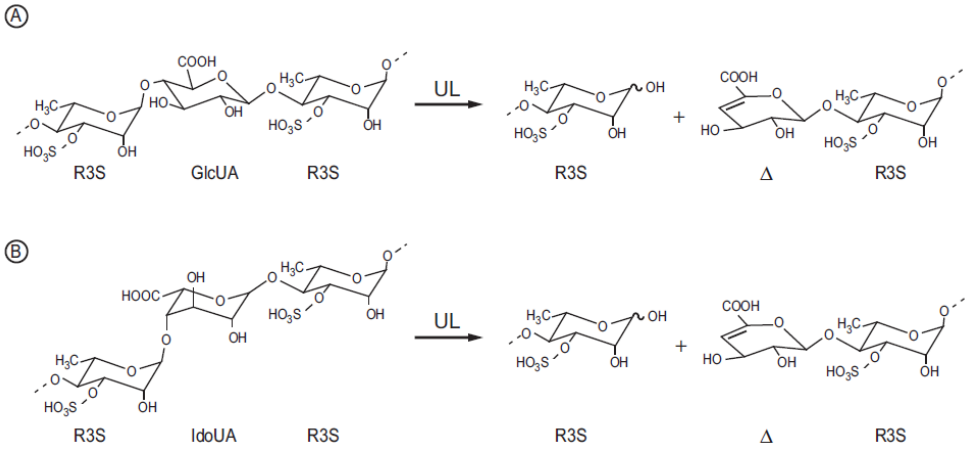

Figure 1. Degradation of ulvan by *Nonlabens ulvanivorans*. *Nonlabens ulvanivorans* cleaves the glycoside bond between the building blocks rhamnose (R3S) and (A) D-glucuronic acid (GlcUA) or (B) L-iduronic acid (IdoUA) via β-elimination resulting in the formation of an unsaturated ring (Δ, 4-deoxy-L-*threo*-hex-4-enopyranosiduronic acid) on the non-reducing end of the second fragment and a reducing end on one fragment (Kopel *et al*., 2016).

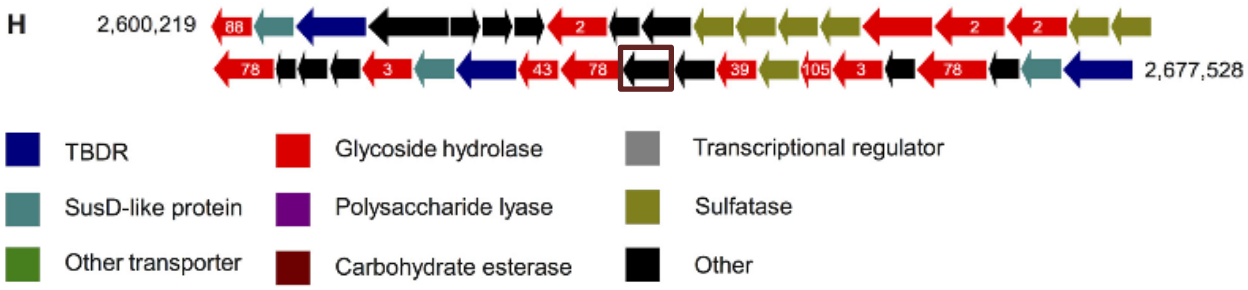

Figure 2. Putative ulvan utilization locus from *Formosa agariphila* KMM3901^T (in modification of Mann *et al.*, 2013). The numbers at the sides of the PUL indicate the position within the genome whereas the numbers in the arrows indicate the CAZyme family of the genes. The ulvan lyase characterized in this study is marked by a dark red box.

Marine heterotrophic bacterial lineages known for alginate degradation are Bacteroidetes and Proteobacteria (Thomas *et al*., 2012; Neumann *et al*., 2015). In-depth phylogenetic analysis has shown that the ancestral origin of alginolytic operons was probably a marine flavobacterium. Via independent lateral gene transfer (LGT), alginolytic operons were transferred to marine Proteobacteria (Alpha- and Gammaproteobacteria) and Japanese gut *Bacteroides* as a result of algae-based dietary (Thomas *et al*., 2012). Alginate lyases (Aly) are typically extracellular or periplasmic (Wong *et al*., 2000), classified into the PL families 5-7, 14, 15, 17 and 18 (Lombard *et al.*, 2014). They cleave the glycosidic bond resulting in the oligomers L-guluronate or D-mannuronate and a nonreducing end with a 4-deoxy-L-erythro-hex-4 en pyranosyl uronate residue (Figure 3). Although most enzymes are characterized to have an endoactive specificity (Wong *et al*., 2000), there are also reports of exoactive enzymes for the complete degradation (Badur *et al*., 2015; Lee & Mooney, 2013).

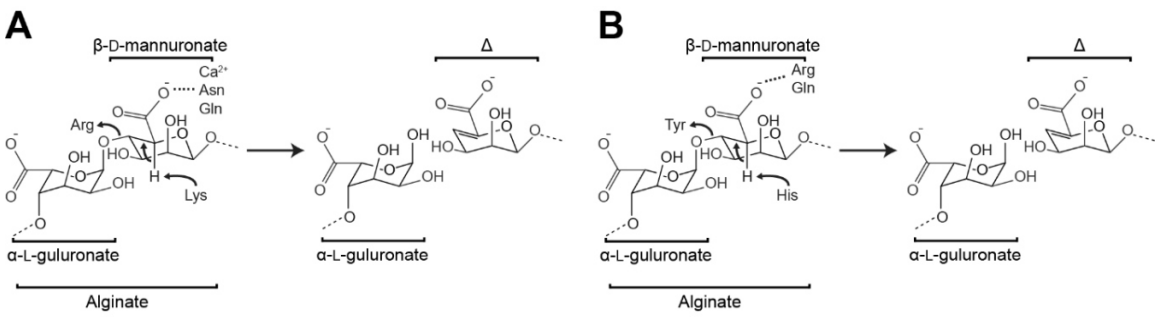

Figure 3. Degradation of alginate by *Vibrio splendidus*. *Vibrio splendidus* degrades alginate into the uronic acids α-L-guluronate and β-D-mannuronate by β-elimination using (A) PL6 and (B) PL7 (unpublished data Plutz *et a*l., 2016).

Alteromonas macleodii is a Gram-negative, copiotrophic r-strategist which is globally distributed in temperate surface oceans and occurs at all depths of the Mediterranean Sea (Ivars-martinez *et al*., 2008). *A. macleodii* was firstly described by Baumann *et al*. in 1972. Since then, several studies investigated its physiological adaptation to the marine environment. *A. macleodii* is capable of utilizing easily accessible substrates such as glucose (Allers *et al.*, 2007), and recent studies supplied evidence for the degradation of complex polymers by showing its hydrolytic capabilities on the algal polysaccharides alginate and laminarin (Neumann *et al*., 2015; Wietz *et al*., 2015). Moreover, strain 83-1 was reported to rapidly colonize and degrade alginate particles (Mitulla *et al*., 2016). Neumann *et al*. (2015) proposed a putative alginolytic system for *Alteromonas macleodii* strain 83-1, similar organized like PULs in Bacteroidetes species, but missing a pair of SusC and SusD homologs. Its alginolytic system is located in a 24 kp genomic island, which harbors five alginate lyases (two PL6, two PL7, and one PL17) as well as adjacent cupin-domain, sugar permease, sugar kinase and isobutyrate dehydrogenase genes (Figure 4). The core of the alginolytic system is highly conserved among several *A. macleodii* strains, while strains from the sister clade *A. mediterranea* only possess a single PL6 in a specific, much smaller genomic island. Differences in the architecture of alginolytic system were also reported for Vibrionaceae. *V. splendidus* 12BL01 harbors four different PL families with distinct molecular functions. Alys PL6 and PL7 were identified to initiate the extracellular lysis of the polymer, while families PL15 and PL17 complete the degradation into monomers that can be further catabolized. The presence and absence of PL families in closely related species results in different ecotypes adapted to ecological niches (Hehemann *et al*., 2016). A similar alginate degrading pathway might also be present in *A. macleodii* 83-1.

The high abundance of *Alteromonas macleodii* in bacterial blooms when organic nutrients are present (Allers *et al*., 2008; McCarren *et al*., 2010), its hydrolytic capacity, as well as its ability to colonize and degrade gel particles suggesting that it has an ecological relevance in the marine environment, thus being an attractive model organism for alginate degradation.

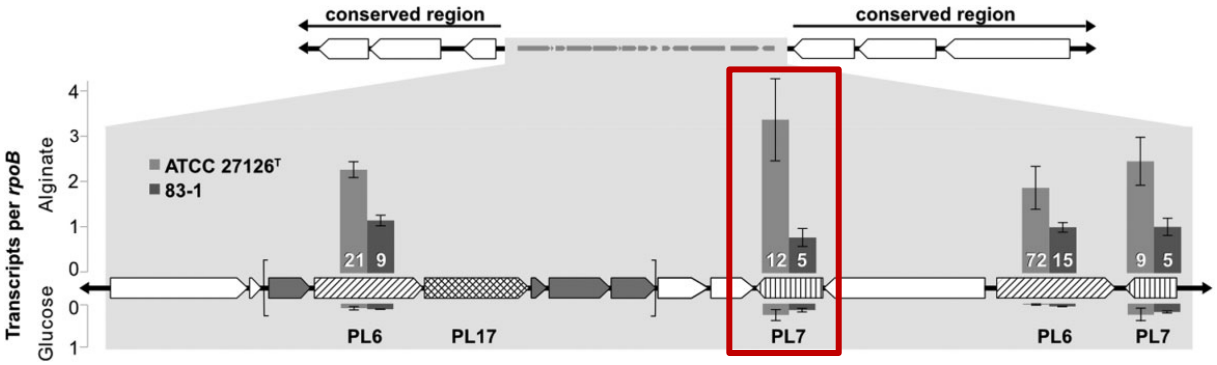

Figure 4. Alginolytic system within a genomic island from *Alteromonas macleodii* 83-1. Genetic organization of a putative PUL for alginate utilization where the up- and downstream boundaries are conserved among all *A. macleodii* strains. The core of the PUL is indicated by square brackets including alginate lyases PL6, PL17 and adjacent cupin-domain, sugar permease, sugar kinase and isobutyrate dehydrogenase genes (gray). Bars represent the relative expression of alginate lyases from strain 83-1 and ATCC 27126^T compared with *rpoB*, with numbers designating *n*-fold induction with alginate in comparison to glucose (Neumann *et al*., 2015). Alginate lyase PL7-1, which presents the focus of this thesis, is marked with a red box.

Carbohydrate binding modules

Carbohydrate binding modules (CBMs) are defined as contiguous amino acid sequences with discrete folds within the modular structures of CAZYmes and cellulosomal scaffolding proteins with carbohydrate-binding activity. Previously, CBMS were classified as cellulose-binding domains (CBDs) due to the initial discovery of several modules within GHs binding to cellulose (Tomme *et al.*, 1996). However, CBDs were reclassified since more and more modules in CAZymes were found that bind to carbohydrates other than cellulose. CBMs consist of 30 to 200 amino acids and can be located at both termini of a protein (Shoseyov *et al*., 2006). These modules can have ligand specificity of poly- and oligosaccharides because the carbohydrate-recognition site mirrors the solution confirmation of the targeted substrate and thereby minimizes the energetic costs upon binding. CBMs do not possess catalytic activity, but have a proximity effect as well as targeting and disruptive functions (Boraston *et al.*, 2004). At present, CBMs are divided into 81 families (Lombard *et al*., 2014) based on amino acid similarities (Tomme *et al*., 1996), the fold or on structural and functional similarities such as surface-binding, glycan-chain-binding, small-sugar-binding (Boraston *et al.*, 2004).

Overall, CBMs are thought to play a pivotal role in polysaccharide-degrading enzymes (Boraston *et al*., 2004), but they might be attractive candidates in future applications such as probes to detect specific polysaccharides.

Aim of the study

This study investigated marine bacterial PLs capable of degrading the anionic algal polysaccharides alginate and ulvan, respectively. A particular focus was given to *(i)* an alginolytic system in *Alteromonas macleodii* 83-1 and *(ii)* a putative polysaccharide utilization locus for ulvan in *Formosa agariphila* KMM3901^T.

The alginolytic system in *Alteromonas macleodii* 83-1 was studied by producing its five Alys as recombinant proteins, which were expressed in *E. coli*, and purified via chromatography in order to investigate enzyme activity and kinetics. In addition, phylogenetic analysis was done as well as protein crystallization to solve the enzyme structure of PL7-1. This project is part of the work of Dr. Wietz who is doing culture-based and genomic studies on *Alteromonas macleodii* 83-1.

The analysis of a polysaccharide utilization locus for ulvan in *Formosa agariphila* KMM3901^T is part of collaboration between the MPI Bremen and the University of Greifswald. Our colleagues from Greifswald are currently working on enzyme kinetics and activity, whereas we contributed the structural analysis of an undescribed ulvan lyase. Our work included protein purification and analytical chromatography, determination of thermal stability, and X-ray crystallography.

The present study provides detailed insights into the biochemistry, evolution and functionality of PLs from *F. agariphila* and *A. macleodii* with focus on PL7-1 (alginate), as well as PL24 and PL25 (ulvan). Studying the utilization pathways of marine heterotrophic bacteria capable of degrading reduced carbon compounds such as algal polysaccharides contributes to the understanding of processes that considerably impact marine food web dynamics and carbon cycling in the oceans.

Chapter 1: Structural and functional analysis of an alginate lyase family PL7 from *Alteromonas macleodii* 83-1

Nadine Gerlach[1], Craig Robb[2,3], Matthias Wietz[1], Jan-Hendrik Hehemann[2,3]

[1] Institute for Chemistry and Biology of the Marine Environment (ICBM), University of Oldenburg, Germany

[2] Max Planck Institute for Marine Microbiology, Bremen, Germany

[3] Center for Marine Environmental Sciences (MARUM), University of Bremen, Germany

Abstract

Alginate is a linear anionic heteropolysaccharide which can contribute up to 45 % of the dry weight of brown macroalgae, and thus is an important nutrient source for marine heterotrophic bacteria. Bacterial utilization of polysaccharide is crucial for the marine carbon cycling, but still little is known about the enzymatic machinery and degradation mechanisms of bacterial key degraders. Alginate lyases are carbohydrate active enzymes (CAZymes) which cleave the glycosidic bond of uronic acids ß-D-mannuronate (M) and its C5-epimer α-L-guluronate (G) by ß-elimination. Here, we investigated the alginate lyase PL7-1 from *Alteromonas macleodii* 83-1, a globally distributed marine bacterium capable of degrading alginate and other complex polysaccharides. PL7-1 was identified as a monomeric protein of 50 kDa and very likely endoactive on G-, M-, as well as GM-enriched algal alginate, whereas no utilization of acetylated bacterial alginate was observed. PL7-1 was most active at 23 °C with a pH optimum of 8 - 9, and thermal stability until 37 °C. 3D crystal structure modeling indicated a carbohydrate binding module of family 32 at the N-terminus and a β-jelly roll fold of the catalytic domain consisting of two α-helices and 14 β-strands arranged as two antiparallel β-sheets.

Key words: *Alteromonas*, alginate lyase, PL7, endoactivity, CBM32

Introduction

The remineralization of algal biomass by heterotrophic bacteria is an important step in the marine carbon cycle. Macroalgae release substantial amount of organic matter (OM) per year (Khailov & Burlakova, 1969), and are rich in polysaccharides, contributing up to 70 % of the algal dry weight depending on seasonal variations and algal species. Polysaccharides physically support the thallus, have storage properties (Kraan, 2012) or are part of extracellular transparent exopolymer particles (TEP) (Teeling *et al*., 2016). Alginate is the main cell wall component of brown algae (Phaeophyceae) such as *Fucus spiralis* in coastal or *Sargassum* in oceanic regions, contributing up to 45 % to the algal dry weight (Mabeau & Kloareg, 1987). Alginate is an unbranched, binary copolymer composed of the uronic acids ß-D-mannuronate (M) and its C5-epimer α-L-guluronate (G), occurring in 1,4-linked blocks of either polyguluronate (polyG), polymannuronate (polyM), or alternating polyguluronate-polymannuronate (polyGM). The number and ratio of M and G in the blocks depend on algal species and affect its mechanical strength and flexibility. Alginate is an anionic polysaccharide containing one carboxylic acid at each monomeric unit (Draget *et al*., 2005). The biological degradation of alginate is largely done by bacteria using extracellular or periplasmic alginate lyases (Alys) (Wong *et al*., 2000). Alys are carbohydrate-active enzymes (CAZymes) that cleave the glycosidic bond between uronic acid containing polysaccharides by ß-elimination resulting in the oligomers L-guluronate or D-mannuronate and a nonreducing end with a 4-deoxy-L-erythro-hex-4ene pyranosyluronate residue. Although most Alys characterized to date have an endoactive specificity (Wong *et al*., 2000), there are reports of exoactive Alys for the complete degradation (Badur *et al*., 2015; Lee & Mooney, 2013). According to their structures, known Alys are classified into seven polysaccharide lyase (PL) families: 5-7, 14, 15, 17 and 18 (Lombard *et al.*, 2014; Lombard *et al*., 2010; Garron & Cygler, 2010). Marine bacterial lineages known for alginate degradation are Bacteroidetes and Proteobacteria (Thomas *et al*., 2012; Neumann *et al*., 2015) with an ancestral origin form marine Flavobacteria (Thomas *et al*., 2012). In Bacteroidetes, CAZymes are often arranged in polysaccharide utilization loci (PUL), operon-like genomic clusters allowing the concerted degradation of polysaccharides (Sonnenburg *et al*., 2010). Despite the insights afforded by these studies and biochemical characterization of Alys from marine bacteria (e.g. Badur *et al*., 2015; Iwamoto *et al*., 2001), many specifics about the enzymatic machinery and degradation mechanisms of bacterial alginate degraders remain unknown to date. For a comprehensive understanding of bacterial alginate degradation, enzymatic, genomic and phylogenetic studies of so far undescribed Alys

represent a promising approach. Here, we performed the structural and functional analyses of Alys from an alginolytic system *from A. macleodii* 83-1. *A. macleodii* is a Gram-negative, heterotrophic Gammaproteobacterium. It is a copiotrophic r-strategist, which is globally distributed in temperate and tropically surface oceans and occurs at all depths of the Mediterranean Sea (Ivars-martinez *et al*., 2008). Besides its ability to utilize easily accessible substrates such as glucose (Allers *et al.*, 2007), recent studies showed considerable hydrolytic capabilities on the algal polysaccharides alginate and laminarin (Neumann *et al*., 2015; Wietz *et al*., 2015). Moreover, strain 83-1 was reported to rapidly colonize and degrade alginate particles *in situ* (Mitulla *et al*., 2016). Neumann *et al*. (2015) revealed that these activities relate to a putative alginolytic system (AS) within a 24 kb genomic island that has a similar organization to PUL in Bacteroidetes species, however missing key transporter and transcriptional regular genes that make up the definition of the genetic clusters (Terrapon *et al*., 2015). The AS of strain 83-1 and closely related *A. macleodii* strains harbors five alginate lyases belonging to families PL6 (2 genes), PL7 (2 genes), and PL17 (1 gene) plus adjacent cupin-domain, sugar permease, sugar kinase and isobutyrate dehydrogenase genes.

The high prevalence of *Alteromonas macleodii* in bacterial blooms at high nutrient concentrations (Allers *et al*., 2008; McCarren *et al*., 2010), its distinct CAZyme repertoire, as well as its ability to utilize gel particles suggest an ecological relevance in natural systems. Hence, a comprehensive understanding of its CAZyme machinery is of great interest. Using our model organism *Alteromonas macleodii* 83-1, the present study investigated structure and function of alginate lyase PL7 to provide additional insight in the biochemistry and phylogeny of the only partially characterized PL7 family. Our results on enzyme size, activity and structure contribute to the understanding of bacterial polysaccharide degradation in the oceans, a process with ecological relevance in the marine carbon cycle.

Material and methods

Bacterial strain. *Alteromonas macleodii* 83-1, isolated from a Mauritanian upwelling surface seawater amended with 0.001 % sodium alginate, has been analyzed for CAZymes in an earlier study (Neumann *et al*., 2015). Aly sequences from *A. macleodii* 83-1 (Table S1) were used to design primers (Table S2) for specific amplification and subsequent cloning.

Construction of recombinant plasmid for overexpression. All five alginate lyases PL7-1, PL7-2, PL6-1, PL6-2, and PL17 were constructed as recombinant plasmids for overexpression, but we focused on detailed characterization of PL7-1. Aly PL7-1 (aa 23 - 469) was PCR-amplified (Table S3) using genomic DNA of *A. macleodii* 83-1, forward primer with a *Nhe*I restriction site (5'-gcg gca gcc ata tgg cta gct cca caa cct cgc aaa cgc ctt tac-3') and reverse primer with a *Xho*I restriction site (5'-tgg tgg tgg tgg tgc tcg agg tta cca tgt tca ttc tca att gaa t-3'). The PCR product was cloned into the expression plasmids pet28a(+) (69864, Merck Millipore), pet GFP (29659, Addgene), and pet SUMO (29663, Addgene) with a single 6-His-Tag at the N-terminus and transformed into *Escherichia coli* NEB5α according to the manufacturer's instructions (EE510S, Gibson Assembly© Cloning Kit, New England Biolabs). For overexpression, purified plasmid DNA containing Alys was transformed into *Escherichia coli* BL21(DE3) according to the manufacturer's instructions (C2527H, New England Biolabs). Transformed cells were grown on lysogeny broth (LB) agar plates with 50 µg/ml kanamycin (Sigma Aldrich) at 37 °C overnight.

Protein expression and purification. *Escherichia coli* BL21(DE3) was grown in 5 l Erlenmeyer flasks with 1 l of ZYP5052 auto-induction medium (Studier, 2005) for four days at 20 °C and 150 rpm. Bacterial cultures were harvested at 4900 *g* and 4 °C for 15 minutes. The cell pellet was subjected to chemical lysis by resuspending in 20 ml buffer (25 % sucrose, and 50 mM Tris pH 8), adding 30 mg of lysozyme (~ 7000 U/mg, Sigma Aldrich), and incubating at room temperature (~ 25 °C) for 10 minutes while stirring. 40 ml of deoxycholate solution (20 mM Tris pH 8, 1 % w/v deoxycholate, 100 mM NaCl, 1 % w/v Triton X-100), $MgSO_4$ (5 mM final concentration) and 100 µl of 10 mg ml^{-1} DNase I (≥ 400 Kunitz mg^{-1}, Sigma Aldrich) was added. The mixture was incubated at room temperature (~ 25 °C) until it was no longer viscous and centrifuged at 30966 *g* and 4 °C for 45 minutes.

Soluble proteins were purified done via immobilized metal affinity chromatography (IMAC) and size exclusion chromatography (SEC). IMAC was performed in ÄKTA™ start chromatography system (29-0220-94, GE Healthcare Life Sciences) with a 5 ml cobalt column (HiTrap™ Talon crude, 28953766, GE Healthcare Life Sciences). The supernatant from the chemical lysis was applied to the column equilibrated in binding buffer (20 mM Tris pH 8, 500 mM NaCl) at a flow rate of 5 ml min^{-1}. The column was washed with 40 ml binding buffer followed by elution with a linear gradient of 0 – 100 % buffer (20 mM Tris pH 8, 0.5 M NaCl, 0.5 M imidazole) over 25 ml. SEC was performed for concentrated IMAC fractions in

NGC™ Chromatography System (Biorad) using a HiPrep 16/60 Sephacryl™ S-200 HR column (17116601, GE Healthcare Life Sciences) and 20 mM Tris pH 8 elution buffer.

Purity of IMAC and SEC fractions was verified via sodium dodecyl sulphate polyacrylamide gel electrophoresis (SDS-PAGE) for soluble proteins (Laemmli, 1970). The 1 mm polyacrylamide gel was run at constant 200 V for 40 minutes in 1x Tris-Glycine-SDS (TGS) buffer (Biorad). Purified protein fractions were concentrated in a stirred ultrafiltration unit (Amicon) using 50 psi nitrogen and a 10 kDa membrane (Biomax). The concentration was determined by measuring the absorbance at 280 nm (BioSpectrophotometer basic, Eppendorf) using the calculated molar extinction coefficient of 0.599.

Refolding of alginate lyase from inclusion bodies. Due to the insufficient amount of soluble protein, we attempted to refold all five Alys from inclusion bodies. Inclusion bodies are insoluble, miss-folded proteins formed when the spatio-temporal control of its expression in *E. coli* is lost (Rosano & Ceccarelli, 2014). Since only PL7-1 was expressed in inclusion bodies, we focused on a detailed characterization of PL7-1. The refolding from inclusion bodies was done in a modification of Qi *et al*. (2015). The bacterial cell pellet of the chemical lysis was washed at least three times with washing buffer (20 mM Tris pH 8, 0.3 M NaCl, 1 mM EDTA, 1 % Triton X-100, 1 M urea) until the pellet turned almost colorless. The pellet was resuspended in extraction buffer (20 mM Tris pH 8, 2 M urea) and frozen overnight at – 20 °C. The solution was thawed at room temperature and centrifuged at 30966 *g* and 4 °C for 15 minutes. The supernatant was diluted with extraction buffer to a final protein concentration of 0.5 to 1 mg ml^{-1}. The diluted protein solution was dialyzed in 0.5 M NaCl, 1 mM $CaCl_2$, 20 mM Tris pH 8 at 4 °C overnight while stirring within a dialysis membrane (1 kDa molecular-porous membrane tubing, Spectra/Por). After dialysis, the protein solution was concentrated with a 10 kDa membrane (Biomax) and purified via IMAC and subsequently SEC.

Phylogenetic analysis. A NCBI BLASTp of PL7-1 from *A. macleodii* 83-1 was performed to determine the 50 closest relatives with a query cover of > 50 %. Sequences were aligned using MUSCLE (Edgar, 2004). In MEGA 7.0 (Kumar *et al*., 2016) the best phylogenetic model was determined to calculate a maximum likelihood tree with 1000 bootstraps replicates (Felsenstein, 1985) and the WAG+G+I model (Whelan & Goldman, 2001). Carbohy-

drate esterase from *Actinoalloteichus hymeniacidonis* (AOS63257.1) was used as an outgroup.

Enzymatic assays.

Substrate preparation. Alginate block fractions were generated by acid hydrolysis in modification of Haug *et al*. (1966). 5 % low viscosity alginate from brown algae (A1112, Sigma Aldrich) was hydrolyzed in 0.3 M HCl at 90 °C for 20 min. Hydrolysis was interrupted by neutralization with 5 M NaOH, followed by centrifugation to separate the fractions containing insoluble mannuronate- and guluronate-enriched alginate (M- & G-block) as well as mixed-linked alginate (MG-block). The MG-block was further hydrolyzed at 70 °C. The pellet containing the M- and G-enriched alginate was resuspended in water. Adjusting the pH to 3 led to precipitation of the G-enriched alginate, whereas the M-block-enriched alginate remained soluble. The pellet was resuspended in water, while the pH of the supernatant was adjusted to 1.3 to precipitate the M-enriched alginate. All fractions were neutralized to pH 7 prior freeze-drying (ScanVac CoolSafe, Labogene).

Enzyme activity. Activity of the refolded PL7-1 was determined via the increasing absorbance of 232 nm which represents the production of unsaturated uronic acids over time using a FLUOstar Omega microplate reader (BMG Labtech GmbH). The influence of pH, sodium chloride concentration, temperature as well as cations were tested using 0.1 % low viscosity alginate from brown algae (A1112, Sigma Aldrich) and 1 µl of enzyme (~ 0.4 mg/ml) in a total reaction volume of 300 µl. The influence of pH was tested first in order to provide the optimum conditions for the following reactions. Buffers containing Tris (Tris-HCl, Bis-Tris-propane) could not be evaluated due to a high absorbance at 232 nm of the buffer itself. Substrate specificity was investigated using native algal alginate and its enriched fractions of uronic acids as well as bacterial alginate (PS104, Dextra Laboratories). Enzymatic parameters were determined at 25 °C using 50 mM HEPES pH 9, 1 mM $CaCl_2$, and low viscosity algal alginate

Dynamic light scattering (DLS). Thermal stability of PL7-1 was determined via DLS. Triplicates of 30 µl of SEC-purified sample were transferred into a microtiter plate (Aurora), centrifuged at 4500 *g* and 4 °C for 10 min to remove air bubbles and analyzed in a DynaPro plate reader-II (Wyatt Technology). Thermal stability was monitored using a temperature gradient

of 25 – 80 °C with an increase of 0.1 °C min^{-1} and 5 acquisitions per sample measured for 5 seconds each.

Cleavage mechanisms of the enzyme. Analytical chromatography was performed to determine the cleavage mechanism of PL7-1. 0.1 % of algal alginate was incubated at 37 °C in 50 mM HEPES pH 9, 1 mM $CaCl_2$, 10 µM enzyme and aliquots at different time points were taken. High pressure liquid chromatography (HPLC) was carried out in Dionex ICS-5000+SP (3005177, Thermo Fischer) using a Dionex CarboPac™ PA 100 column (043055 Thermo Fischer) at 25 °C. Alginate degradation products were eluted using a linear gradient from 0 – 100 % of 0.1 M NaOH, 1 M $NaO_2C_2H_3$ at 1 ml min^{-1} for 20 min.

Structural analysis. PL7-1 was structurally analyzed via dynamic light scattering (DLS), analytical size exclusion chromatography (SEC), protein crystallization, as well as crystal structure prediction based on a protein model.

Dynamic light scattering was performed to determine protein size and polydispersity of the SEC-purified protein fractions. Triplicates of 30 µl protein sample were transferred into a microtiter plate (Aurora), centrifuged at 4500 *g* and 4 °C for 10 min to remove of air bubbles, and analyzed in a DynaPro plate reader-II (Wyatt Technology). Standard DLS analysis was performed at 25 °C with 10 acquisitions per sample and a measuring time of 5 seconds per acquisition.

Analytical size exclusion chromatography was performed to determine the molecular size of PL7-1 using pooled and concentrated SEC fractions containing protein with low polydispersity. SEC was carried out in NGC™ Chromatography System (Bio Rad) using a high resolution column ENrich™ SEC 650 10 x 300 (Bio Rad) and 1 ml/min flow rate with 20 mM Tris pH 8, 250 mM NaCl. The absorbance at 280 nm of 60 µl Gel Filtration Standard (1511901, Bio Rad) and protein sample was measured.

Protein crystallization and X-ray crystallography. In order to crystallize the protein, two sparse matrix screens (MCSG-1 and MCSG-2 (McPherson & Cudney, 2006)) and one grid screen (MD1-36 PACT premier™ HT-96 (Newman *et al*., 2005) were tested to find conditions for protein crystallization. All screens were set up in 96-well sitting drop trials at 20 °C. Conditions which showed crystallized protein were repeated and optimized with slight modifications to the original recipe. The optimization of the conditions was set up in 24-well hang-

ing drop crystal trials using vapor diffusion method at 20 °C. Three different dilutions (1:2, 2:1 and 1:1) of protein to crystallization solution were tested for each condition with a total volume of 3 µl and 500 µl Motherliqor. Protein crystals were flash-frozen to cryo-temperatures using liquid nitrogen to reduce X-ray radiation damage. Prior freezing, crystals were soaked in 25 % glycerol in the mother liquor to prevent the formation of ice crystals. Data collection was done at the European Molecular Biology Laboratory (EMBL, Hamburg) at beam line P13.

3D structure modelling. Structural homologues of PL7-1 were obtained from NCBI BLASTp in Protein Data Bank (PDB) (Berman *et al*., 2000) and the carbohydrate-active enzyme database (CAZy) (Lombard *et al*., 2014). Protein structure prediction of the alginate lyase PL7-1 of *A. macleodii* 83-1 was visualized in PyMOL (Version 1.2r3pre, Schrödinger, LLC) based on the closest homologue *Klebsiella pneumoniae* (PDB code: 4OXZ, Howell *et al*., unpublished data) calculated in Phyre2 (Kelly *et al*., 2015). For comparison, the protein structure of PL7-2 was modeled based on the closest homologue *Zobellia galactanivorans* (PDB code: 4BE3, Thomas *et al*., 2013).

In order to identify conserved residues in crystallized PL7 homologues, a protein alignment was done in MEGA 7.02 (Kumar *et al*., 2016) using MUSCLE (Edgar, 2004) and further processed in ESPript 3.0 (Robert & Gouet, 2014). Additionally, a maximum likelihood for PL7-1 tree was constructed based on the WAG+G (Whelan & Goldman, 2001) model using all sites as well as a MUSCLE protein alignment (Edgar, 2004) calculated in MEGA 7.02 (Kumar *et al*., 2016).

Results and discussion

Protein expression and purification of Alys. All five alginate lyases (PL6-1, PL6-2, PL17, Pl7-1, PL7-2) were cloned into pet28a(+) and transformed into *E. coli* BL21(DE3). Purification via IMAC and subsequent SDS-PAGE of IMAC fractions resulted in an insufficient and impure expression of soluble proteins for protein crystallography. Therefore, the Gibson assembly cloning with *E. coli* NBE5α was performed before the transformation into *E. coli* BL21(DE3) which also did not result in sufficient expression (Figure 5A). Protein refolding from inclusion bodies did only increase the amount of soluble protein for PL7-1 (Fig-

ure 5C-D). In addition, ligation independent cloning (LIC) vectors GFP and SUMO were tested. *In tandem* expression of fusion partners with the desired protein have been reported to enhance the expression of soluble protein (Rosano & Ceccarelli, 2014). Only PL7-1 fused to GFP was expressed at an observable level but still too low for crystallography. The other could not be detected by SDS-PAGE despite showing peaks in the IMAC chromatogram.

Structure modeling of PL7-1 indicated a carbohydrate binding module (CBM) of family 32 at the N-terminus. CBM was also cloned into pet28a(+) and transformed into *E. coli* NBE5α for overexpression. Similar to PL7-1, CBM32 showed a very low amount of soluble proteins after purification via IMAC and subsequent SDS-PAGE, whereas refolding yielded in a higher amount of soluble protein (Figure S1). SEC analysis showed that the protein eluted at the void volume, suggesting that the CBM occurred as aggregated protein. We did not observe soluble protein suitable for crystallization. The presence of a cysteine in CBM32 c might have led to aberrant covalent disulfide bonds between protein monomers. The reducing agent Tris-(2-carboxyethyl)phosphine (T-CEP) was added to the concentrated protein prior to SEC in an effort to improve this results. However, this purification as well as ion exchange chromatography (IEX) showed no peak, potentially due to irreversible binding of the CBM32 to the column.

In the following, PL7-1 (starting at the CBM) was cloned using pet28a(+), transformed into *E. coli* NBE5α and overexpressed with *E. coli* BL21(DE3). Using isopropyl β-D-1-thiogalactopyranoside (IPTG) instead of ZYP5052 as auto-induction medium also did not enhance the expression of soluble PL7-1 (Figure 5B). At least four liters of culture were necessary to result in about 4 mg ml^{-1} refolded and purified protein needed for protein crystallization.

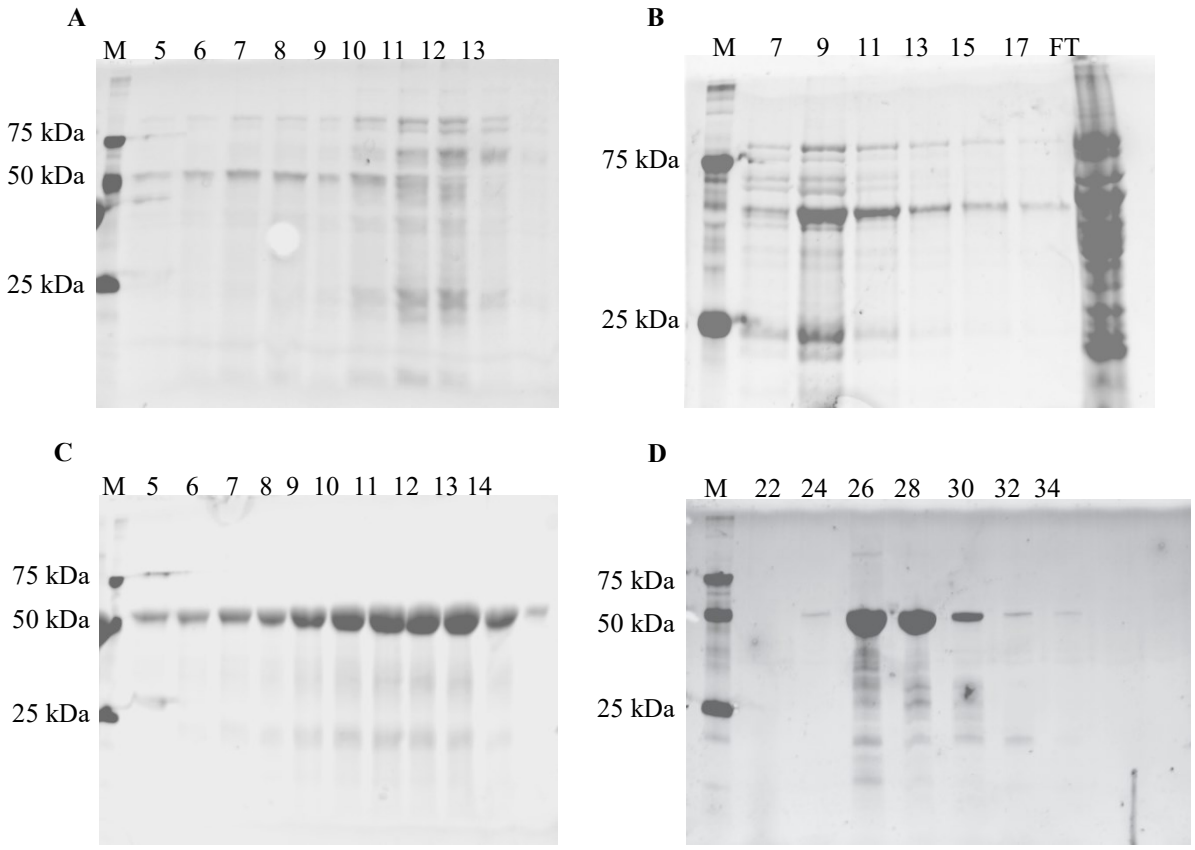

Figure 5. Purified alginate lyase PL7-1 from *Alteromonas macleodii* 83-1. (A) Soluble protein purified via IMAC after ZYP5052 auto-induction, (B) soluble protein purified via IMAC after ITPG induction, (C) refolded protein purified via IMAC and (D) subsequent SEC after ZYP5052 auto-induction. 10 µl protein of each purified protein fraction were analyzed with SDS-PAGE. FT: flow through of chromatography, M: protein marker.

Protein size of PL7-1. The molecular mass of PL7-1 was determined to be ~50 kDa by SDS-PAGE (Figure 5) which fits the calculated value of 49.7 kDa based on the amino acid sequence. Alys differ in size, but seem to fall into three classes according to their molecular mass: 20-35, ~40, and ~ 60 kDa (Wong *et al*., 2000). DLS and the elution time during SEC suggested that PL7-1 either aggregated during purification or that the protein consisted of a dimeric structure. Hence, concentrated SEC fractions were analyzed using a high-resolution column as well as protein standards for calibration (Figure S1), showing one protein peak with the expected molecular size of 50 kDa for the refolded PL7-1 (Figure 6). Therefore, we assume a monomeric protein structure for the refolded PL7-1 which requires confirmation by X-ray crystallography.

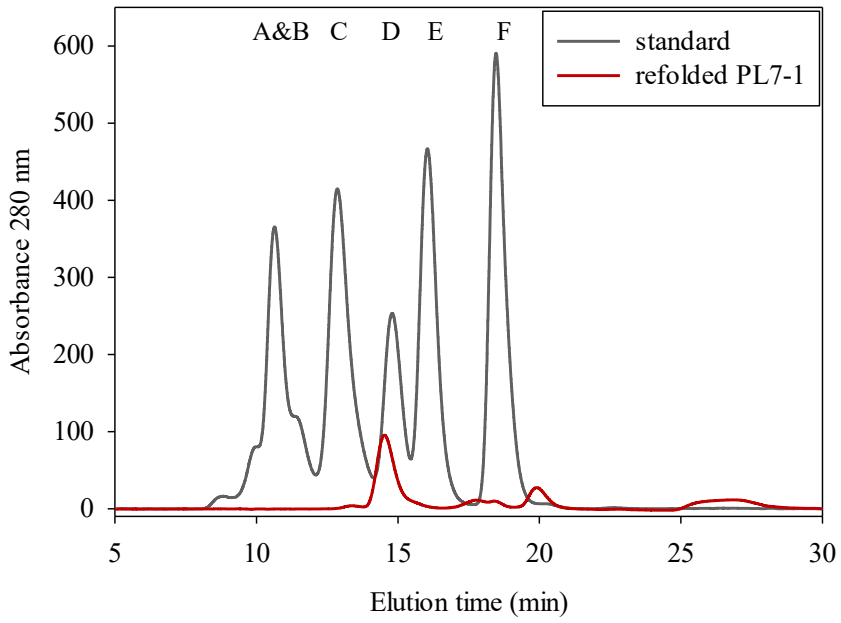

Figure 6. Analytical SEC chromatogram of refolded PL7-1 from *Alteromonas macleodii* 83-1. Shown is the absorbance at 280 nm of 60 µl Gel Filtration Standards (1511901, Bio Rad) as well as 60 µl of 4 mg ml^{-1} refolded PL7-1 against time. SEC was performed in NGC™ Chromatography System (Biorad) using an ENrich™ SEC 650 10 x 300 Column (Bio Rad) and 20 mM Tris pH 8, 0.25 M NaCl at 1 ml min^{-1} flow rate. The gel filtration standard consisted of A: Protein aggregates, B: Thyroglobulin (670 kDa), C: γ-globulin (158 kDa), D: Ovalbumin (44 kDa), E: Myoglobin (17 kDa), F: Vitamin B_{12} (1.35 kDa). The calibration curve (Figure S2) to determine the molecular weight is given as supplementary information.

Phylogeny of PL7-1 and homologous enzymes. Phylogenetic analysis of PL7-1 and 50 bacterial homologs showed two main clusters relating to Gammaproteobacteria and Bacteroidetes. Bacteroidetes sequences only originated from Flavobacteria, mainly *Tamlana* sp.. Within the Gammaproteobacteria, three orders were identified – (i) Vibrionales, only represented by *Vibrio* sp., (ii) Chromatiales, only represented by *Rheinheimera baltica*, and (iii) ten genera belonging to Alteromonadales. The most dominant species were alginate lyases from *Vibrio* sp. as well as nucleotide binding proteins of *Microbulbifer* sp. and *Alteromonas* sp.. Alginate lyase PL7-1 of *Alteromonas macleodii* 83-1 clustered together with *Alteromonas macleodii* strains (Figure 7). PL7 homologues exclusively found in marine Gammaproteobacteria and marine Flavobacteria indicate considerably sequence conservation and gene transfer between taxa (Thomas *et al*., 2012; Neumann *et al*., 2015).

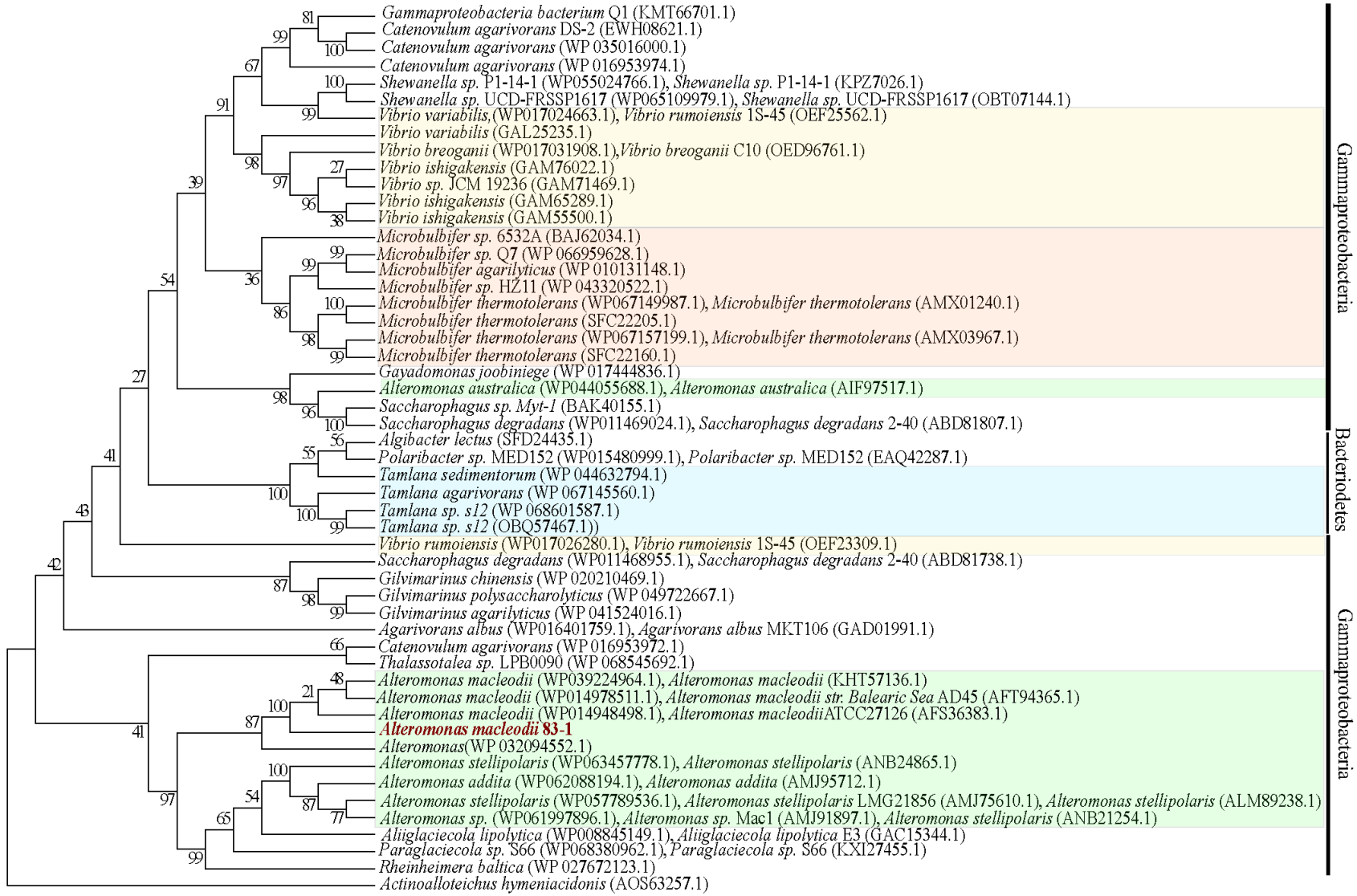

Figure 7. Phylogenetic tree of PL7-1 from *Alteromonas macleodii* 83-1 and homologues enzymes. The indicated values at each branch derive from 1000 bootstrap replications. PL7-1 from *A. macleodii* 83-1 is highlighted in red. *Alteromonas* sp. are color-colored green, *Vibrio* sp. in yellow, *Microbulbifer* sp. in orange, and *Tamlana* sp. in blue. Carbohydrate esterase from *Actinoalloteichus hymeniacidonis* (AOS63257.1) was used as an out-group.

Protein blast in PDB for closest homologues of PL7-1 showed crystallized Aly PL7 (PDB codes: 4OXZ, 4BE3, 2JD9, 3G1C) in four bacterial strains. In CAZy, four more PL7 structures were found, with *Sphingomonas* sp. A1 being the only lyase co-crystallized alginate. Overall, most species belonged to Proteobacteria, except for *Zobellia galactanivorans* being a member of Bacteroidetes, *Corynebacterium* sp. belonging to Actinobacteria as well as *Eubacterium eligens* belonging to Firmicutes. However, low bootstrap values indicated variety among PL7 homologues rather than highly conserved enzymes (Figure 8).

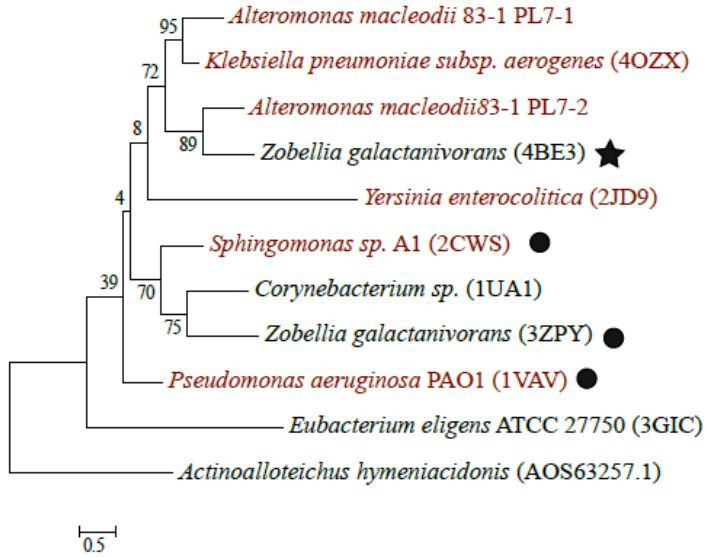

Figure 8. Phylogenetic tree of alginate lyase PL7-1 and crystallized homologues. The indicated values at each branch derive from 1000 bootstrap replications. Proteobacteria are colored in red. Carbohydrate esterase from *Actinoalloteichus hymeniacidonis* (AOS63257.1) was used as an out-group. Endoactive enzymes are marked with a dot, whereas exoactive enzymes are marked with a star.

Influence of physicochemical parameters on enzyme activity of PL7-1.

pH - No enzyme activity was observed with citric acid pH 4 and 5 as well as dibasic potassium phosphate buffer pH 4. Highest enzyme activity was measured with HEPES buffer at pH 9.0, followed by pH 8.0 with dibasic potassium phosphate buffer and MOPS pH 8.0 (Figure 9A). This is consistent with reported activities for alginate lyases with a pH optima from 7 to 8.5 (Iwamoto *et al*., 2001; Miyake *et al*., 2003; Yamasaki *et al*., 2004; Thomas *et al*., 2013; Badur *et al*., 2015) based on the buffer, resembling the pH of natural seawater (Chester & Jickells, 2012).

Temperature – Enzyme activity was observed from 20 to 37 °C, with highest activity at ~ 23 °C. Very little to almost no activity was measured above 37 °C (Figure 9C). This observation was underlined by thermal protein stability ranging from 25 to ~ 37 °C (Figure 9D). Above 37 °C, the hydrodynamic radius of the protein strongly increased due to unfolding and further denaturation. Enzyme activities for Alys from Gram-negative marine bacteria have been reported in a similar range but with varying optima at 25, 30, 45, or 50 °C (Wong *et al*., 2000). The temperature optimum for a endoactive alginate lyase from *Vibrio splendidus* 12B01 and *Alteromonas* sp. strain 272 were reported at 20 and 20 - 25 °C, respectively (Badur *et al*., 2015; Iwamoto *et al*., 2001). Thermal stability and highest enzyme activity might indicate physiological adaption to the environment, since brown seaweeds thrive best in waters up to 20 °C (Kraan, 2012) and *A. macleodii* mainly occurs in temperate waters (Ivars-martinez *et al*., 2008).

Cations - Previous studies reported that divalent cations are essential cofactors for polysaccharide lyases as they decrease the surface density of the substrate charge leading to less ionic interactions between enzyme and the alginate (Wong *et al*., 2000). Especially calcium has been reported to play a significant role by maintaining the binding site in the correct confirmation and direct co-ordination with the carbohydrate (Boraston *et al.*, 2004). Therefore, we tested the influence of 1 mM cations. The addition of $ZnCl_2$, $CoCl_2$, $Ni(II)Cl_2$, EDTA, and $Cu(II)SO_4$decreased enzyme activity markedly. The inhibition of enzyme activity by divalent metal ions was also observed for Aly PL7 from *Sphingomonas* sp. A1 (Miyake *et al*., 2003) and *Alteromonas* sp. strain 272 (Iwamoto *et al*., 2001). $CaCl_2$, $MgCl_2$, $Mn(II)Cl_2$, $MgSO_4$, and $MnSO_4$ did not have a significant effect on alginate degradation of the refolded alginate lyase in comparison to no cations (H_2O as control) (Figure 9F), indicating that PL7-1 may not require divalent cations for full enzyme activation. Similar observations have also been reported

for alginate lyases from other Gram-negative bacteria such as *Pseudomonas syringae* (Preston *et al*., 2000) and *Sphingomonas* sp. A1 (Hisano *et al*., 1993). Nevertheless, this observation must be confirmed by using buffers and protein free of metal ions (e.g. using Chelex100) since ETDA acting as a scavenger of metal ions did lead to activity loss of the enzyme.

Salt – Two buffer systems, HEPES pH 9.0 and dibasic potassium phophate pH 8.0, were used to investigate the impact of NaCl on enzyme activity. In enzymatic assays using HEPES, a stronger effect on enzyme activity was measured for saliniy where a moderate amount of salt was optimal (Figure 9B). Highest enzyme activity was observed using 50 mM HEPES pH 9.0 and 0.3 M NaCl with a decrease above and below this value. On the other hand, the phosphate buffer system at at lower pH of 8.0 was relatively insensitive to salinity. At concentrations above 0.1 M NaCl, the enzyme did not significantlly respond to further increasing NaCl. Activity of alginate lyases for marine bacteria have been reported at 0.2 – 1 M NaCl (Brown & Preston, 1991; Thomas *et al*., 2013; Tseng *et al*., 1992), suggesting that salt concentration of ≥ 0.2 M NaCl are required for the activation of alginate lyases (Tseng *et al*., 1992). Kitamikado *et al*. (1992) also reported the activation of bacterial alginate lyases in the presence of metal ions (Ca^{2+}, Na^{+}, and Mg^{2+}) and sodium chloride concentration of 0.3 – 1 M. The authors suggested that the enzyme activation due to high NaCl may be caused by removal of bound water from sodium alginate molecules or by the effects of charge in forming the alginate-enzyme complex. Overall, our data suggest that alginate lyase PL7-1 requires NaCl, possibly for shielding the strongly negative charge of alginate. However, adding natural salts such as NaCl to phosphate buffers has been reported to have a decreasing effect on the pH (Robinson, 1929), which might explain lower activity comparing both buffer systems. To our knowledge, similar investigation has not been done for HEPES buffer so far. To confirm that high concentrations of sodium chloride do not affect pH, future experiments should consider checking, and if necessary, adjusting pH after adding salts.

Substrate specificity – Substrate specificity was tested using bacterial and algal alginate as well as algal alginate enriched in GM-, G-, and M-blocks. Refolded PL7-1 was active on algal alginate but without any specificity in the different fractions (Figure 9E). Most alginate lyases have been reported to prefer M-enriched alginate (EC 4.2.2.3), and only a few G-enriched alginate (EC 4.2.2.11) (Wong *et al*., 2000). An important aspect is that many protocols for producing alginate enriched in G-, M-, or GM-blocks often do not result in alginate fractions devoid of the other homo- or heteropolymer. Nevertheless, multiple substrate specificity has

been observed in some crude lyase extracts (Wong *et al*., 2000) as well as for *Alteromonas* sp. H-4 (Sawabe *et al*., 1997).

Phylogenetic analysis showed a close relatedness of both Alys of PL7 from *A. macleodii* 83-1 to PLs from pathogens *Pseudomonas aeruginosa*, *Klebsiella pneumonia*, *Yersinia enterocolitica* and *Eubacterium eligens* (Figure 8). They are known for synthesizing alginate inter alia in biofilms and causing mainly lung diseases in humans (Wong *et al*., 2000). These relationships suggested that *A. macleodii* 83-1 might also be able to degrade bacterially synthesized alginate which is acetylated at the C2 and / or C3 position of the D-mannuronate in various degrees (Rehm & Valla, 1997). However, enzymatic assays did not show utilization of bacterial alginate (Figure 9E).

Mode of action – HPLC revealed increasing oligosaccharide peaks over time, whereas the peak for high molecular weight matter decreased (Figure S3). The finding of oligosaccharide peaks, plus a tiny peak with the same elution time of mannuronic acid indicated that PL7-1 is probably endoactive, generating oligosaccharides which we were unable to identify or quantify yet. Enzyme homologues of PL7-1 from *Zobellia galactanivorans* (PDB code: 3ZPY), *Pseudomonas aeruginosa* PAO1 (PDB code: 1VAV) and *Sphingomonas* sp. A1 (PDB code: 2CWS) have also been described as endoactive (Thomas *et al*., 2013; Yamasaki *et al.*, 2004; Yamasaki *et al*., 2005) comparable to the majority of alginate lyases (Wong *et al*., 2000). Like *Alteromonas macleodii* 83-1, *Zobellia galactanivorans* also possesses two Alys PL7 with different mode of action (Thomas *et al*., 2013). Sequence alignments revealed that the exoactive PL7 from *Zobellia galactanivorans* showed greater similarity to PL7-2 than to PL7-1. This indicated that a similar mechanism of alginate utilization with one endo- and one exoactive version of PL7 might also be present in *A. macleodii* 83-1.

Kinetics – Kinetic parameters for PL7-1 were determined as K_M 0.03 ± 0.01 % of algal alginate with a V_{max} of 0.00023 ± 1.9E-05 % alginate s^{-1} (Figure S4). Enzyme activity of PL7-1 was comparably low to other PL7 from marine bacteria (Badur *et al*., 2015; Farrell & Tipton, 2012; Thomas *et al*., 2013), potentially due to the process of refolding and purification.

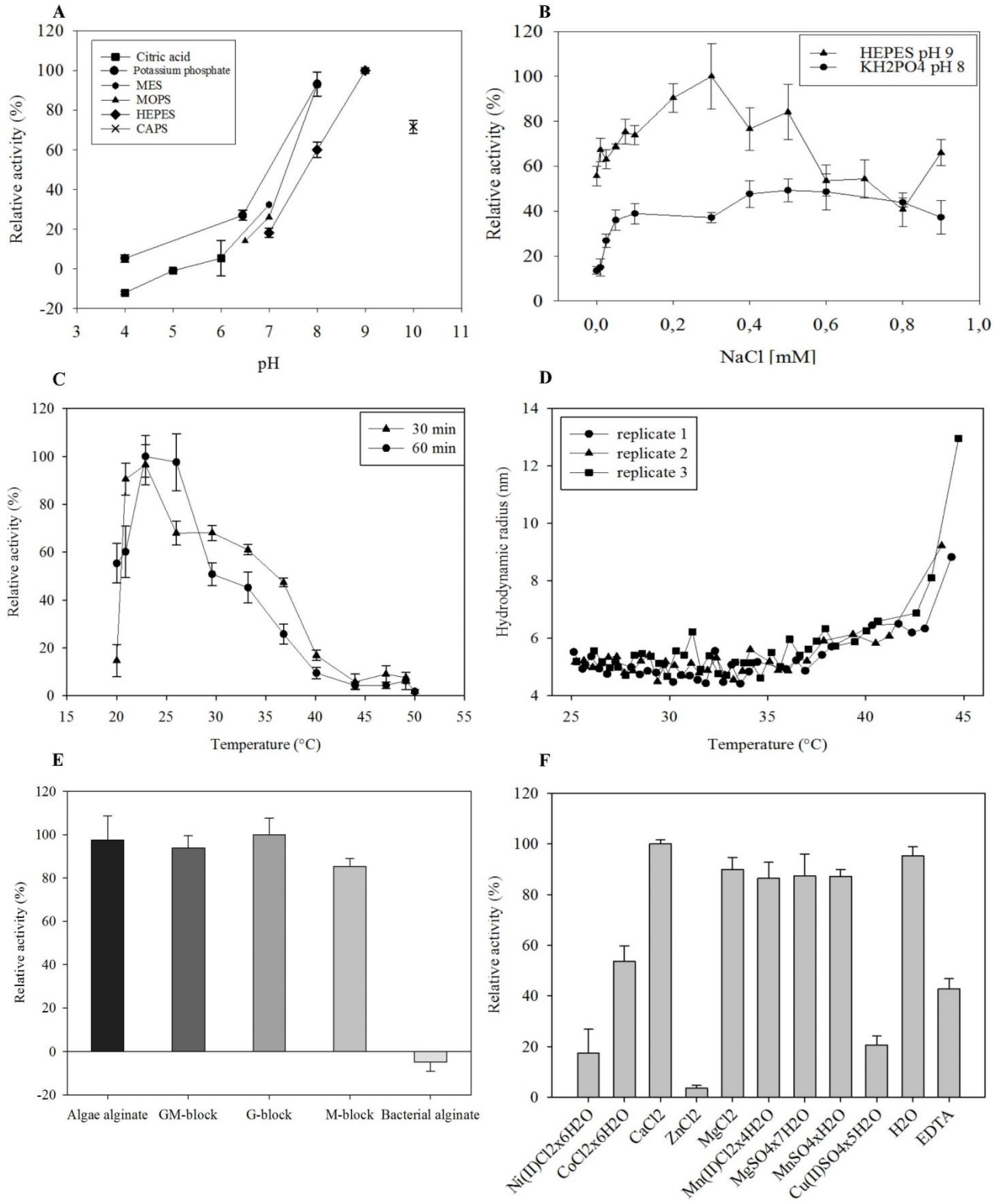

Figure 9. Enzyme activity of refolded alginate lyase PL7-1 from *Alteromonas macleodii* 83-1. The influence of (A) pH, (B) sodium chloride concentration, (C, D) temperature and cations (F) on enzyme activity were tested as well as (E) substrate specificity. Error bars indicate the standard deviation of replicates.

Crystallized PL7-1 and preliminary diffraction analysis. In total, 5 conditions in two sparse matrices and one grid screens contained small needle-like protein crystals. All conditions included ≥ 20 % PEG and buffer with a pH of 6 – 7. Three conditions were chosen to optimize enzyme crystals to obtain limited protein precipitation as well as big and untwined crystals. So far, crystals of each condition could be reproduced. The best protein crystallization was observed with 4 mg/ml protein in 20 mM Tris pH 8 and PEG 1500 followed by PEG 3350 and 6000. Protein crystals of 0.13 M Bis-Tris-propane pH 7, 10 and 14 % PEG 1500 were analyzed using X-ray crystallography. Both crystals diffracted without any indication of ice or salt crystals interference. One crystal diffracted at ~ 4 Å, but the data collection was not completed since the protein melted. Data processing of the limited data set was not successful.

3D structural analysis of PL7. Since crystal structure determination via X-ray crystallography is currently ongoing. In the meantime, we performed 3D structure modeling for both PL7-1 and the nearby paralog PL7-2 using the available structure PL7 from *Zobellia galactanivorans* (PDB code: 4BE3, Thomas *et al*., 2013) and from *Klebsiella pneumoniae* (PDB code: 4OXZ, Howell *et al*., unpublished data) with 50 % and 40 % sequence identity, respectively. The N-terminal domain of PL7-1 was also modeled using CBM32 from *Yersinia enterocolitica* (PDB code: 2JDA, Abbott *et al*., 2007) with 26 % sequence identity, which has been shown to bind poly-galacturonic acid from land plants (Abbott *et al*., 2007).

Overall topology - Structure modeling of PL7-1 indicated a carbohydrate binding module (CBM) of family 32 at the N-terminus containing one α-helix and seven β-strands arranged in two anti-parallel β-sheets, whereas the catalytic domain compromises two α-helices and two antiparallel β-sheets composed of 14 β-strands (Figure 10). PL7-1 superimposes well with its closest structural homologues *Klebsiella pneumoniae* (PDB code: 4OXZ) and *Zobellia galactanivorans* (PDB code: 4BE3).

Catalytic domain – PL7 alginate lyases are known to have a β-jelly roll fold (Lombard *et al*., 2014; Yamasaki *et al*., 2005; Yamasaki *et al*., 2004; Osawa *et al*., 2005; Thomas *et al*., 2013). Multiple sequence alignments of *A. macleodii* 83-1 Aly PL7 and crystallized PL7 homologues displayed conserved regions in four β-sheets (Figure 13). PL7-1_β20/ PL7-2_β14 (≙ β17 of *K. pneumoniae*) and PL7-1_β14/ PL7-2_β7 (≙ β9 of *K. pneumoniae*) were located in the middle, whereas PL7-1_β8/ PL7-2_β1 (≙ β1 of *K. pneumoniae*) and PL7-1_β12/ PL7-2_β5 (≙ β5 of *K. pneumoniae*) were at the right edge of the active site cleft.

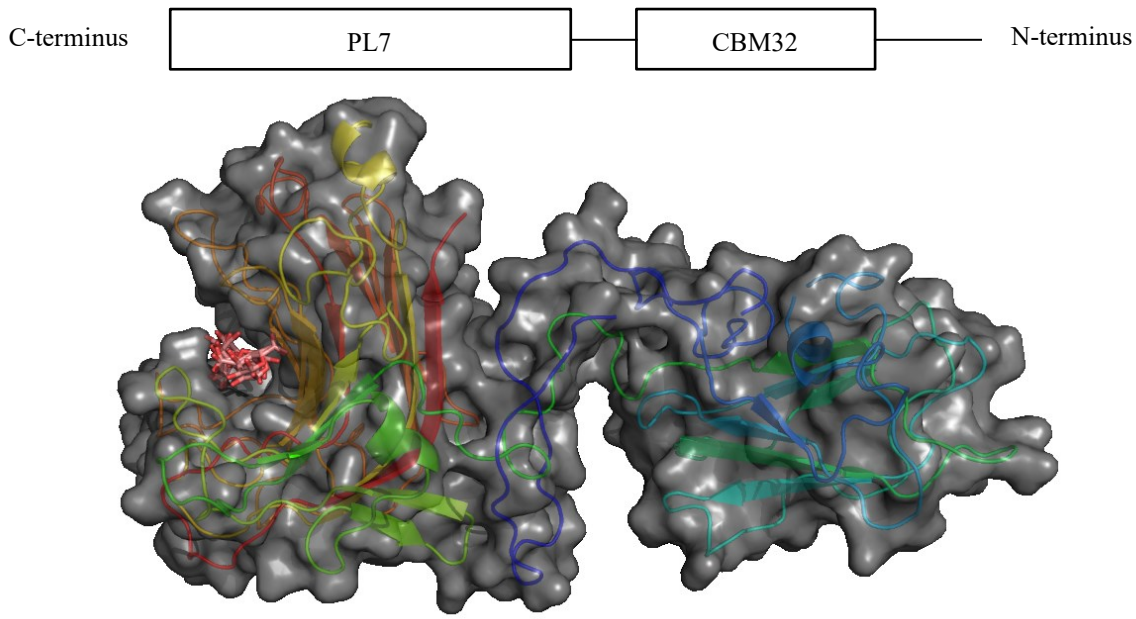

Figure 10. Crystal structure model of PL7-1 from *Alteromonas macleodii* 83-1. Surface crystal structure as well as secondary structure modeling of PL7-1 with a CBM32 at the N-terminus. β-D-4-deoxy-ManpA-(1-4)-α-L-GulpA-(1-4)-β-D-ManpA-(1-4)-α-GulpA of crystal structure in complex of *Sphingomonas* sp. A1 (PDB code: 2ZAA, Ogura *et al*., unpublished data) was superimposed to the surface representation in red color.

β20 was characterized by a highly conserved 9-amino-acid-block YFKAGVY*Q, where * is a variable residue (Figure 11, 12). This striking feature has, among others, also been found for alginate lyases from the marine bacteria ATCC433367 (Malissard *et al*., 1993) and *Alteromonas* sp. H-4 (Sawabe *et al*., 1997) as well as for an extracellular pectate lyase in *E. chrysanthemi* (Keen & Tamaki, 1986) as YSYPVSAQ in the C-terminus region. Alginate and pectate / pectin lyases share several features such as β-elimination, the recognition of substrates of a similar structure and primary sequence similarity, indicating that they probably share a similar core structural fold. Since this conserved region was predicted in the cleft of the active site of PL7-1 despite having differing substrate specificity, it is likely not related to substrate recognition, but rather to maintaining a stable 3D-conformation (Wong *et al*., 2000). Nevertheless, this conserved region as well as VIIGQIH in β14, R*ELREML in β12 and LQ*W*LSIP in β8 were mainly characterized by hydrophobic amino acids (especially aromatic amino acids) such as leucine, tryptophan and methionine as well as residues with planar polar side chains (especially amino acids with charged side chains) such as arginine, glutamic acid, glutamine (Figure 11, 12). These residues have been suggested to be substrate-binding molecules (Wong *et al*., 2000).

Putative catalytic residues in alginate lyases PL7 were identified as H104+Y193+Y199 in *P. aeruginosa* (PDB: 1VAV, Yamasaki *et al*., 2004), Q189+H191+Y284 in *Sphingomonas* sp. A1 (PDB code: 2CWS, Yamasaki *et al*., 2005), Y195+H119+Q117+R72 in *Corynebacterium* sp. (PDB code: 1UAI, Osawa *et al*., 2005) and Q321+H323+Y420 in *Zobellia galactanivorans* (PDB code: 3ZPY, Thomas *et al*., 2013). Osawa *et al*. (2005) assumed that Q117+Y195 interact near the reaction site of alginate to maintain proper orientation of the substrate, R72 interacts with alginate due to the formation of salt bridges with the carboxyl groups at the C5 and H119 acts as a base to deprotonate. Sequence and structural analysis of *Sphingomonas* sp. A1 revealed similarities of putative catalytic residues in alginate lyase of families PL5 and PL7. Mutational analysis showed that H192+Y246 of PL5 are crucial for the catalytic reaction of the enzyme (Mikami *et al*., 2002), which superimpose well with the catalytic residues of PL7 (Yamasaki *et al*., 2005). Moreover, multiple alignment showed that all five putative catalytic residues (R, Q, H, 2xY) superimposed well in all species including PL7-1 and PL7-2 from *A. macleodii* 83-1 (Table 1) located in β5, β9 and β17 (Figure 11, 12). This result indicates that the family PL7 has a highly conserved cluster of catalytic residues despite substrate specificity.

Superimposing the substrate β-D-4-deoxy-ManpA-(1-4)-α-L-GulpA-(1-4)-β-D-ManpA-(1-4)-α-GulpA of crystal structure in complex of *Sphingomonas* sp. A1 (PDB code: 2ZAA, Ogura *et al*., unpublished data) into the active site cleft of the models of PL7-1 and PL7-2 revealed additional space along the cleft for longer substrates. Additional aromatic residues towards the glycone side of the active side cleft of both alginate lyases were found (Figure 11, 12), which could be involved in alginate recognition. Comparisons of structure models of PL7-1 with PL7-2 revealed that the catalytic domain of PL7-1 is smaller due to missing a loop at the left site of the active site. This loop is characterized by Y290, which together with F325 likely closes the right edge of the active site (Figure 11). The blocking of the active site by these aromatic residues indicates an exoactive mode of PL7-2, comparable to observations in *Zobellia galactanivorans* (Thomas *et al*., 2013).

Overall, the results of 3D structure modeling, HPLC, and phylogeny provide evidence in support of a hypothetical model of alginate degradation in *A. macleodii* 83-1. PL7-1 is most likely endoactive, initiating the degradation of alginate into oligosaccharides, which might be further utilized by other enzymes. Similar architecture of alginolytic system were found in both *Zobellia galactanivorans* (Thomas *et al*., 2013) and *Vibrio splendidus* (Hehemann *et al*., 2016). *Zobellia galactanivorans* possess two alginate lyases PL7, one endoactive with a wide-open active cleft, whereas the active side of the exoactive one is smaller and rather closed.

Vibrio splendidus harbors several PL families with distinct molecular functions. Alginate lyases PL6 and PL7 initiate the extracellular lysis of the polymer, and families PL15 and PL17 complete the degradation into monomers that can be further catabolized. A similar utilization pathway of alginate might also be presence in *A. macleodii* 83-1.

Table 1. Putative catalytic residues in conserved regions of the active site cleft of Aly PL7. Shown are the putative catalytic residues of crystallized alginate lyases PL7 (PDB codes: 1UAI, 3ZPY, 1VAV, 2CWS). Residues which were not assumed to be catalytic by the corresponding authors but found in conserved regions due to multiple sequence alignment are indicated in brackets.

Enzyme (PDB code)	Putative catalytic residues				
1UAI	R72	Q117	H119	(Y189)	Y195
3ZPY	(R275)	Q321	H323	(Y414)	Y420
1VAV	(R64)	(Q102)	H104	Y193	Y199
2CWS	(R67)	Q189	H191	(Y278)	Y284
PL7-1	R267	Q336	H338	Y446	Y452
PL7-2	R106	Q175	H177	Y302	Y308

Characteristics and function of CBM32 –. The putative CBM32 o consists of ~ 200 residues with a theoretical molecular weight of ~ 21 kDa, which is consistent by SDS-PAGE (Figure S4). To date, structures of CBM32s have only been solved for pathogenic bacteria (exception: *Micromonospora viridifaciens*), mainly *Clostridium perfringens* (Lombard *et al*., 2014). CBM family 32 is characterized by the most dominant fold, the β-sandwich fold with at least one bound metal ion and the ligand-recognition site located at the edge. CBM32 is common in bacterial toxins or enzymes that attack eukaryotic cells surfaces and in matrix glycans, having a great potential for ligand diversity (Boraston *et al.*, 2004). Multiple sequence alignment of crystallized CBM32s showed no highly conserved regions (Figure S5) indicating a high variation of the primary structure. Phylogenetic analysis of CBM32 by Abbott *et al*. (2008) also showed a significant amino acid variation at all levels, with the peculiarity that the extent of this protein variation is roughly the same within and between species, as well as within and between enzyme groups. Superimposition of CBM32 model from PL7-1 with its closest related homologues from *Y. enterocolitica* (PDB code: 2JDA) and *C. perfringens* (PDB code: 4TXW) revealed that they share a rather similar fold (Figure S6).

Key residues for sugar binding and recognition of CBM32 have been mainly identified as charged and aromatic residues: W125, R69, K65, R37 in *Y. enterocolitica*, F757, N695, R690, W661, H658 in GH84 from *C. perfringens* (Abbott *et al*., 2007), R110, H79, F170, W82 in sialidase from *C. perfringens* (PDB code: 2V72, Boraston *et al*., 2007), H1671, N1707, R1702, Y1674 (W661 in GH84), Y1774 (F757 in GH84), D1769 (D749 in GH84) in GH31 from *C. perfringens* (PDB code: 4LPL, Grondin *et al*., 2017), W948 in EndoD from *S. pneumoniae* (PDB code: 2XQX, Abbott & Boraston, 2011) and E14, R31, E36/Y36, E61, Y119/Y120 in chitosanase/glucanase from *Paenibacillus* sp. IK-5 (PDB code: 4ZY9, Shinya *et al*., 2016). Basic amino acids (R, H, K) are thought to interact with negatively charged sugars (Abbott *et al*., 2007), by stabilizing the binding via hydrogen bonds (Grondin *et al*., 2017). The relatedness of CBMs from *Alteromonas macleodii* 83-1 and *Y. enterocolitica* may relate to similar binding specificities, since CBM32 from *Y. enterocolitica* binds polygalacturonic acid chains, a central component of pectin. Additionally, R37 in *Y. enterocolitica* is conserved among all crystallized CBM32s as well as in *Alteromonas macleodii* 83-1, indicating its relevance for the sugar binding. A CBM32 containing Aly PL7 is also present in *Zobellia galactanivorans* (PDB code: 3ZPY), which was described to be endoactive on G-rich alginate (Thomas *et al*., 2013).

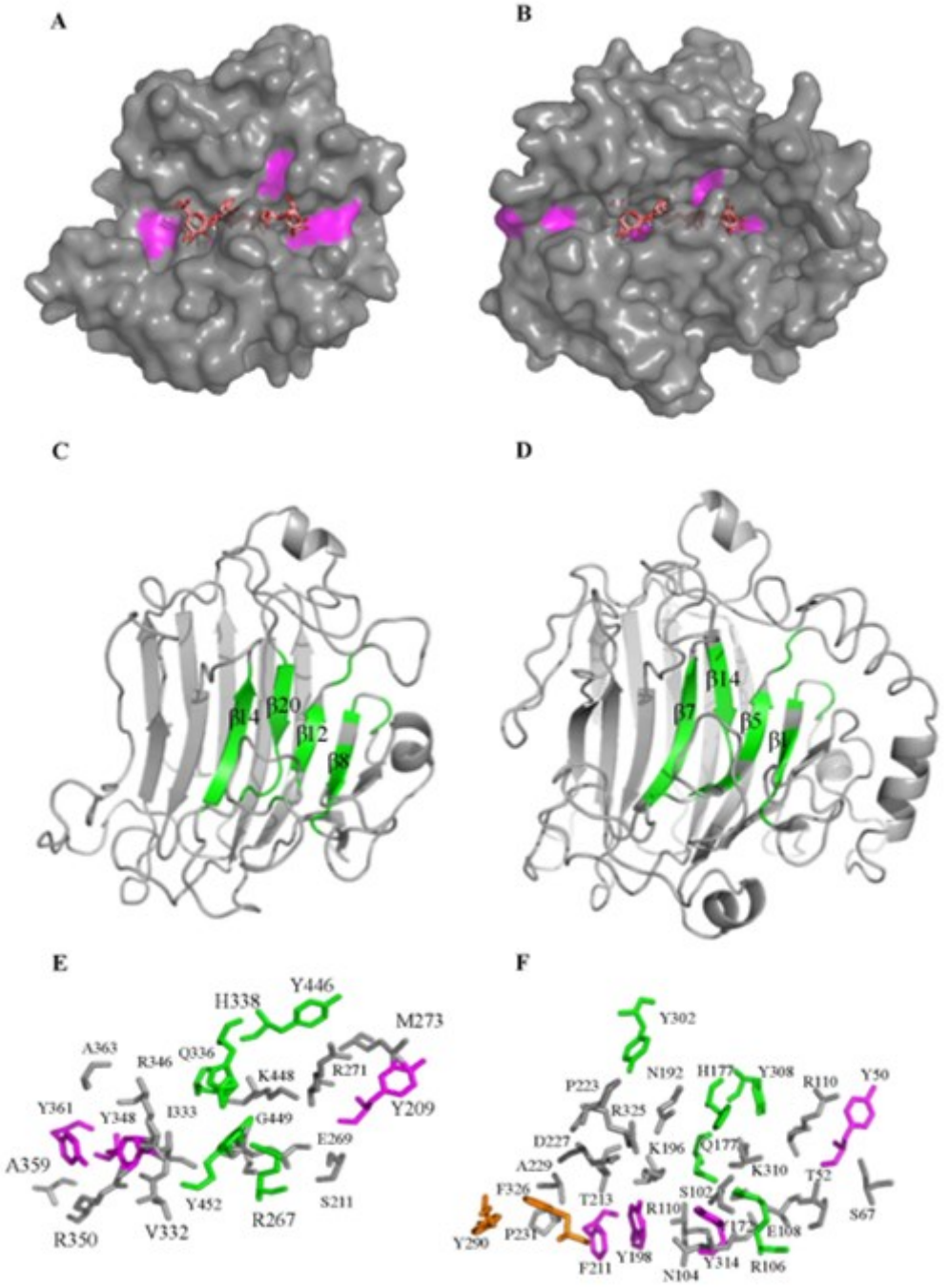

Figure 11. Crystal structure representation of PL7-1 and PL7-2 models from *Alteromonas macleodii* 83-1. Shown is the (A, B) surface and the (C-F) secondary structure including residues in the active site cleft of PL7-1 and PL7-2 from *A. macleodii* 83-1, respectively. β-D-4-deoxy-ManpA-(1-4)-α-L-GulpA-(1-4)-β-D-ManpA-(1-4)-α-GulpA of crystal structure in complex of *Sphingomonas* sp. A1 (PDB code: 2ZAA, Ogura *et al*., unpublished data) was superimposed to the surface representation. Pink color represents aromatic residues in the active site potentially be involved in the degradation of longer substrates. Green color indicates conserved regions among PL7 including putative catalytically residues. Orange highlighted residues of PL7-2 might be responsible for closing the active site cleft.

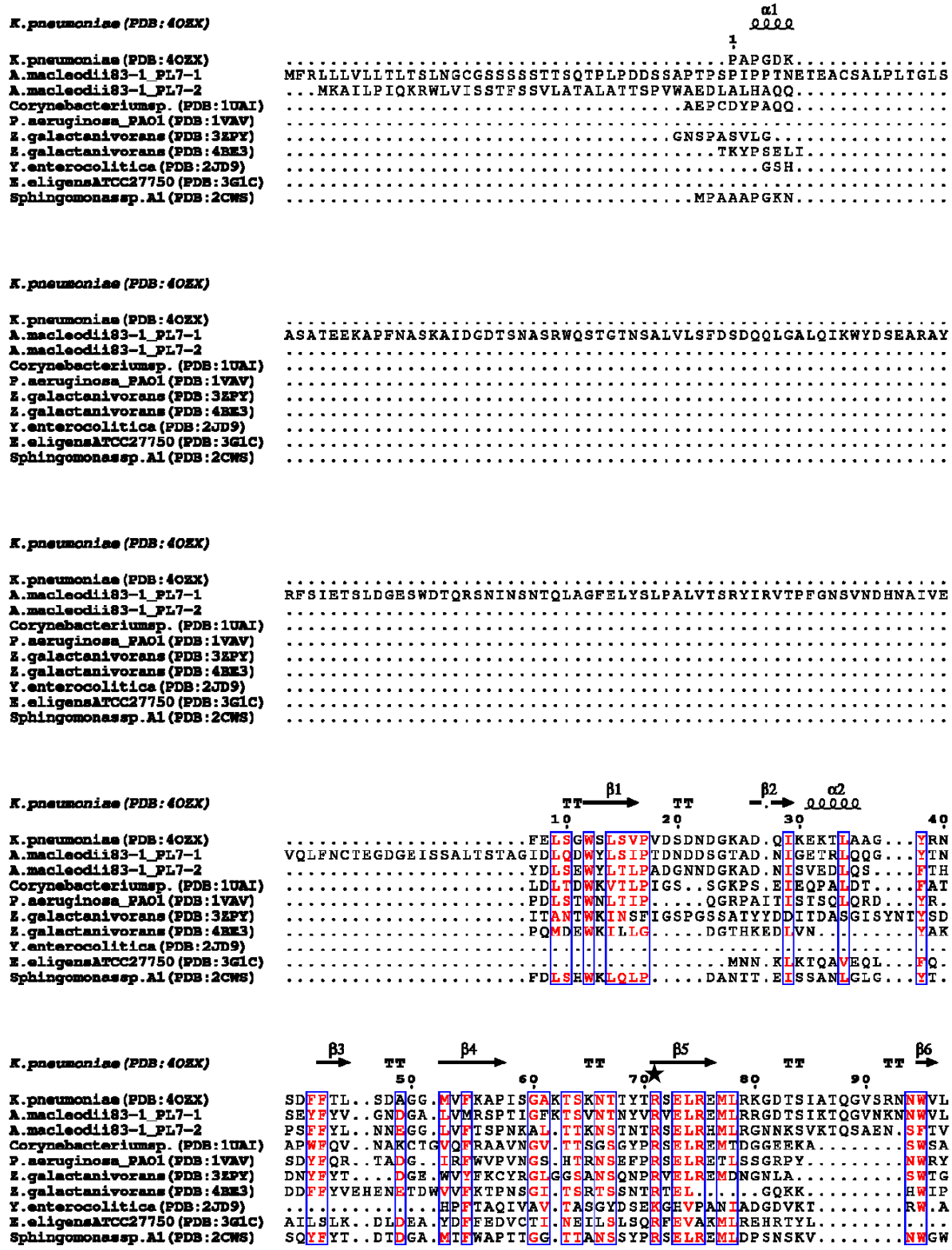

Figure 12. Structure-based alignment of *Alteromonas macleodii* 83-1 PL7 and its crystallized homologues. Multiple protein alignment of Aly PL7 as well as a secondary structure prediction of the closest homologue of *Klebsiella pneumoniae* (PDB code: 4OXZ, Howell *et al*., unpublished data). Conserved residues in the homologues are colored in red and putative catalytic residues are indicated by a star.

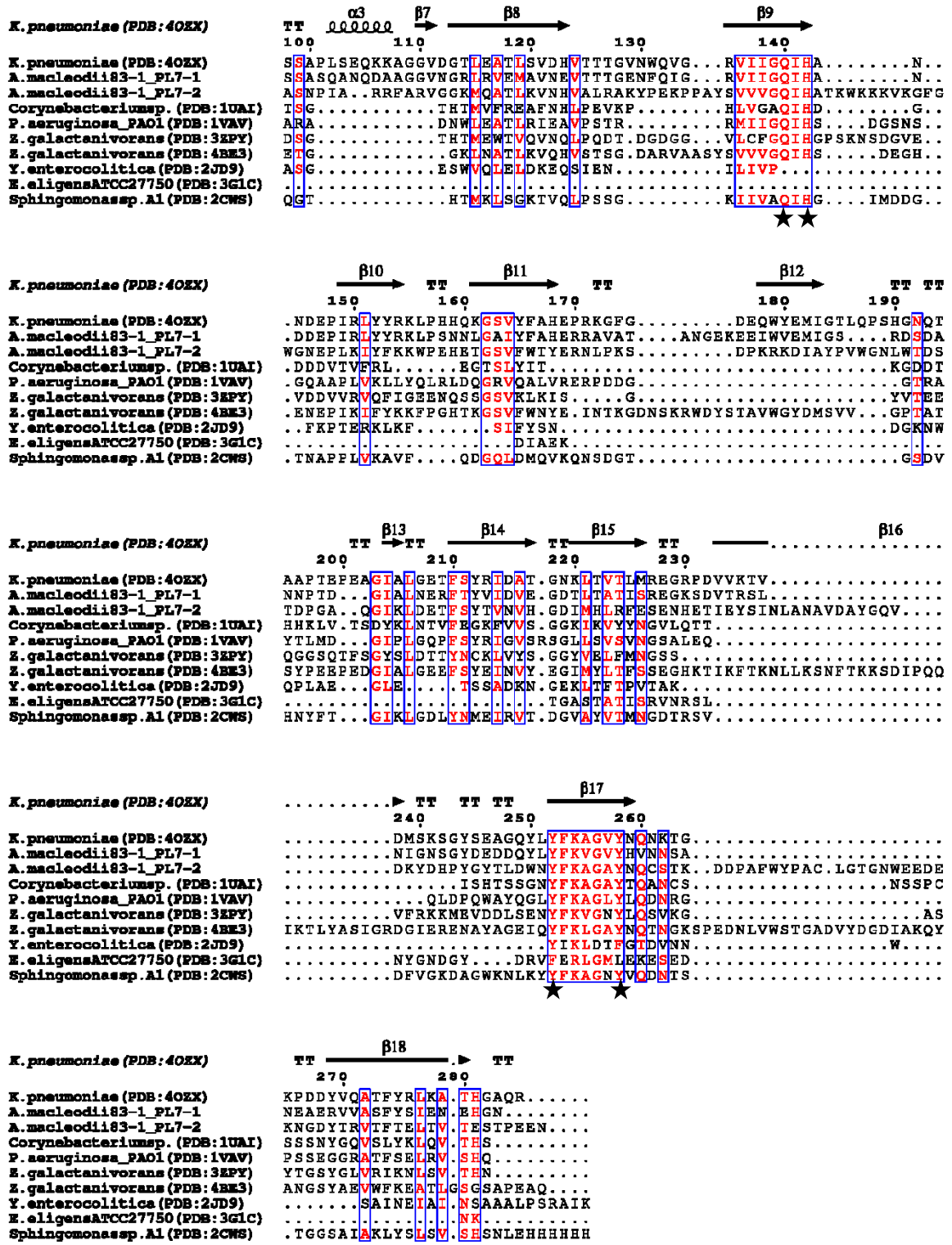

Figure 12. Continued.

Chapter 2: Crystal structure of the ulvan lyase from *Formosa agariphila* KMM3901^T

Nadine Gerlach[1], Craig S. Robb[2,3], Lukas Reisky[4], Uwe T. Bornscheuer[4], Jan-Hendrik Hehemann[2,3]

[1] Institute for Chemistry and Biology of the Marine Environment (ICBM), University of Oldenburg, Germany

[2] Max Planck Institute for Marine Microbiology, Bremen, Germany

[3] Center for Marine Environmental Sciences (MARUM), University of Bremen, Germany

[4] Institute of Biochemistry, University Greifswald, Germany

Abstract

Marine algae consist of up to 70 % of polysaccharides serving a cell wall structure and storage compounds. During and after algal blooms, polysaccharides are released into the marine food web and catabolized by heterotrophic bacteria. So far, many bacterial key enzymes used to depolymerize and metabolize algal polysaccharides remain uncharacterized. Here, we investigated the structure of a novel ulvan lyase from *Formosa agariphila* KMM3901^T. *F. agariphila* is a Gram-negative, motile, and facultative anaerobic Flavobacteriia belonging to the Bacteroidetes phylum and capable of degrading several marine polysaccharides including ulvan from marine green algae. The ulvan lyase was produced as recombinant enzyme in *E. coli* BL21 and purified by immobilized metal affinity chromatography and size exclusion chromatography. Analytical chromatography revealed a dimeric enzyme structure most likely composed of a catalytic and a binding domain according to phylogenetic analysis. The purified protein was subjected to different crystallization screens to obtain crystals for X-ray crystallography. Several conditions supported the formation of enzyme crystals, which will be used to solve the enzyme structure in further investigation.

Key words: *Formosa*, ulvan lyase, crystal structure, X-ray crystallography, CBM

Introduction

Marine algae produce substantial quantities of reduced carbon compounds such as polysaccharides, lipids and proteins by fixing inorganic carbon. Especially during and after algal blooms these compounds are release into the marine food web and further catabolized by heterotrophic bacteria. Marine macroalgae consist of up to 70 % of polysaccharides, which are mainly used for cell wall structure and storage (Kraan, 2012). Ulvan is the main cell wall polysaccharide of the algae order Ulvales belonging to the globally distributed green algae (Chlorophyta). Ulvan is a water-soluble, anionic polysaccharide contributing up to 29 % of algal dry weight and therefore serves as an important food and energy source for marine heterotrophic bacteria. It mainly consists of 3-sulfated rhamnose (R3S), D-glucuronic acid (GlcUA), L-iduronic acid (IdoUA), and D-xylose (Xyl). The degree of sulfation varies, with a maximum of 30 %. Ulvan is composed of repeating disaccharides of GlcUA or IdoUA linked to RS3. These building blocks are termed ulvanobiuronic acid A or B, respectively. There are also disaccharides of RS3 linked to Xyl found in lower amounts (Lahaye & Robic, 2007). In comparison with polysaccharides derived from brown and red algae such as alginate, polysaccharides of green algae are less exploited (Kopel *et al*., 2016). Due to ulvan's biological and physicothermal properties, it is an attractive candidate for the chemical, pharmaceutical, and agricultural industries (Lahaye & Robic, 2007).

Bacteria known for degrading ulvan belong to the orders Flavobacteriales and Alteromonadales, such as *Nonlabens ulvanivorans* (Collen *et al*., 2011; Kopel *et al*., 2014), *Pseudoalteromonas* sp. PLSV (Kopel *et al*., 2014b; Ulaganathan *et al*., 2017) and *Alteromonas* sp. (Kopel *et al*., 2016; Kopel *et al*., 2014c). Ulvan-degrading carbohydrate-active enzymes (CAZymes) include ulvan lyases of families PL24 and PL25 as well as one ulvan hydrolase of family GH105. Ulvan lyases cleave the ß-(1→4) glycosidic bond between the building blocks resulting in in the formation of a reducing end on one fragment and an unsaturated ring (Δ, 4-deoxy-L-*threo*-hex-4-enopyranosiduronic acid) on the non-reducing end of the second fragment. GH105 possess an unsaturated β-glucuronyl activity (Lombard *et al*., 2014). Together with further enzymes such as sulfatases, rhamnosidases and xylosidases, these enzymes lead to complete degradation of ulvan (Kopel *et al*., 2016; Ulaganathan *et al*., 2017).

In this study we investigated the structure of a novel ulvan lyase from *Formosa agariphila* KMM3901^T, Flavobacteriia, Bacteroidetes. *Formosa agariphila* is Gram-negative, heterotrophic, aerobic, and motile (Ivanova *et al*., 2004). Strain KMM 3901^T was originally isolated

in Troitsa Bay, Gulf of Peter the Great, East Sea from the green alga *Acrosiphonia sonderi* (Nedashkovskaya *et al*., 2006). Genome analysis revealed that *F. agariphila* KMM3901^T exhibits an algae-associated life style with many putative genes for the degradation of algal polysaccharides. As in many Bacteroidetes species, these CAZymes are organized in large operon or regulation like structures (Thomas *et al*., 2011), termed polysaccharide utilization loci (PUL) (Sonnenburg *et al*., 2010). Mann and colleagues (2013) have identified at least 13 PULs in *Formosa agariphila* KMM3901^T, compromising a total of 45 sulfatases, 13 polysaccharide lyases (PLs), 88 glycoside hydrolases (GHs), SusD-like proteins, transporter proteins (mainly TBDTs and ABCs), transcriptional regulators, and other proteins. One of these PULs contains genes essential for the degradation of sulphated marine algal polysaccharides, harboring enzyme homologs of genes previously found active on ulvan from green algae including GH105 and ulvan lyase.

Here, we perform structural analysis of the novel ulvan lyase produced as recombinant enzyme in *E. coli BL21* and purified by immobilized metal affinity chromatography followed by size exclusion chromatography. The purified enzyme was tested in different crystallization screens. Several conditions supported enzyme crystals which will be used to solve the enzyme structure in further investigation. Based on initial phylogenetic and electrophoretic analyses, we propose that the dimeric enzyme structure consisting of two domains based on phylogenetic analysis and gel electrophoresis. These insights contribute to a better understanding of the function and evolution of ulvan degradation in *F. agariphila* KMM3901^T.

Material and methods

Microorganism and culture conditions. The ulvan lyase from *Formosa agariphila* KM3901^T was PCR-amplified with a *Nhe*I restriction site at the forward primer and a *Xho*I restriction site at the reverse primer prior cloning into the expression plasmid pet28a(+) (69864, Merck Millipore) with a single 6-His-Tag at the N-terminus (provided by Lukas Reisky). Recombinant purified plasmids were transformed into *Escherichia coli* BL21(DE3) according to the manufacturer's instructions (C2527H, New England Biolabs). Transformed cells were grown on lysogeny broth (LB) agar plates with 50 µg/ml kanamycin (Sigma Aldrich) at 37 °C overnight prior growing in 5 l Erlenmeyer flasks with 1 l of ZYP5052 autoinduction medium (Studier, 2005) for four days at 20 °C and 150 rpm. Bacterial cultures were

harvested at 4900 *g* and 4 °C for 15 minutes. For cell lysis, the pellet was resuspended in 20 ml buffer (25 % sucrose, 50 mM Tris pH 8), 30 mg of lysozyme (~ 7000 U mg^{-1}, Sigma Aldrich) was added and the mixture was incubated at room temperature (~ 25 °C) for 10 minutes while stirring. 40 ml of deoxycholate solution (20 mM Tris pH 8, 1 % w/v deoxycholate, 100 mM NaCl, 1 % w/v Triton X-100), $MgSO_4$ (5 mM final concentration) and 100 µl of 10 mg ml^{-1} DNase I (≥ 400 Kunitz mg^{-1}, Sigma Aldrich) were added. The mixture was incubated at room temperature (~ 25 °C) until it was no longer viscous and centrifuged at 30966 *g* and 4 °C for 45 minutes.

Protein purification. Immobilized metal affinity chromatography (IMAC) was carried out in ÄKTA™ start chromatography system (29-0220-94, GE Healthcare Life Sciences) with a 5 ml cobalt column (HiTrap™ Talon® crude, 28953766, GE Healthcare Life Sciences). The supernatant from chemical lysis was applied to the column equilibrated in binding buffer (20 mM Tris pH 8, 500 mM NaCl) at a flow rate of 5 ml min^{-1}. The column was subsequently washed with 40 ml binding buffer followed by elution with a linear gradient of 0 – 100 % elution buffer (20 mM Tris pH 8, 0.5 M NaCl, 0.5 M imidazole) over 25 ml. Size exclusion chromatography (SEC) was performed for concentrated IMAC fractions in NGC™ Chromatography System (Biorad) using a HiPrep 16/60 Sephacryl™ S-200 HR column (17116601, GE Healthcare Life Sciences) and 20 mM Tris pH 8 elution buffer.

IMAC and SEC fractions were verified for purity via sodium dodecyl sulphate polyacrylamide gel electrophoresis (SDS-PAGE) for soluble proteins according to the manufacturer's manual (Biorad). The 1 mm polyacrylamide gel was run at constant 200 V for 40 minutes in 1x Tris-Glycine-SDS (TGS) buffer. Purified protein fractions were concentrated in a stirred ultrafiltration unit (Amicon) using 50 psi nitrogen pressure and a 10 kDa membrane (Biomax®). The concentration was determined measuring the absorbance at 280 nm (BioSpectrophotometer basic, Eppendorf) using the calculated molar extinction coefficient of 0.69.

Thermal stability. Dynamic light scattering (DLS) was done to determine the thermal stability of the protein. Triplicates of 30 µl of SEC-purified protein were transferred into a microtiter plate (Aurora), centrifuged at 4500 *g* and 4 °C for 10 min to remove of air bubbles, and analyzed in a DynaPro plate reader-II (Wyatt Technology). Thermal stability was monitored using a temperature gradient of 25 – 80 °C with an increase of 0.1 °C min^{-1} and 5 acquisitions per sample each measured for 5 sec.

Analytical size exclusion chromatography. In order to determine the molecular size of the protein, analytical size exclusion chromatography (SEC) was performed using pooled and concentrated SEC fractions containing protein with low polydispersity. SEC was carried out in NGC™ Chromatography System (Bio Rad) using a high-resolution column ENrich™ SEC 650 10 x 300 (Bio Rad) and 1 ml/min flow rate with 20 mM Tris pH 8, 250 mM NaCl. The absorbance at 280 nm of 60 µl Gel Filtration Standard (1511901, Bio Rad) and protein sample was measured.

Protein crystallization and X-ray data collection. Two sparse matrix screens (MCSG-1 and MCSG-2 (McPherson & Cudney, 2006)) and two grid screens (MD1-30 HT Structure Screen (Jancarik & Kim, 1991; Wooh *et al*., 2003) and MD1-36 PACT premier™ HT-96 (Newman *et al*., 2005) were tested to find conditions which allow the protein to crystallize. All screens were set up in 96-well sitting drop trials at 20 °C. Conditions which showed crystallized protein were repeated and optimized with slight modifications to the original recipe. Optimization was performed using hanging drop vapor diffusion method at 20 °C. 24-well hanging drop crystal trials were set up containing 500 µl mother liquor and three different dilutions (1:2, 2:1 and 1:1) of protein and crystallization solution with a total volume of 3 µl. At this point in time, there was no crystallized ulvan lyase or homologues enzyme available. Therefore, molecular replacement was not an option to solve the enzyme structure. For this reason, native crystals were soaked in sodium iodide for different time intervals, to perform multiple isomorphous replacement to solve the enzyme structure. Moreover, we produced selenomethionine-substituted crystals according to the manufacturer's instructions (MD12-501&MD12-507, Molecular Dimensions) to perform anomalous X-ray scattering. Additionally, we tried to solve the enzyme structure in complex. Thus, native crystals were soaked with the substrate (tetrasaccharide) and crystals were co-crystallized (Hehemann *et al*., 2012) with 0.2 and 0.4 % (w(v) ulvan (digest of *Ulva armoricana* using UL and GH105 from *Formosa agariphila*).

Protein crystals were flash-frozen to cryo-temperatures using liquid nitrogen to reduce radiation damage caused by the high intensity of the X-rays at the synchrotron. Crystals were soaked in 25-30 % glycerol in the mother liquor to prevent the formation of ice crystals that

may interfere with the protein diffraction. Data collection was done at the European Molecular Biology Laboratory (EMBL, Hamburg) at beam line P13.

Phylogenetic analysis. Sequences of the 50 closest NCBI BLASTp relatives with a query cover of > 40 % were aligned using MUSCLE (Edgar, 2004). A maximum likelihood tree and the best phylogenetic model were calculated in MEGA 7.0 (Kumar *et al*., 2016) using the WAG+G (Whelan & Goldman, 2001) model and 1000 bootstraps replications (Felsenstein, 1985). Carbohydrate esterase from *Actinoalloteichus hymeniacidonis* (AOS63257.1) was used as an out-group. Multiple sequence alignment of ulvan lyase from *F. agariphila* KMM3901^T and its homologues obtained from the carbohydrate-active enzyme (CAZy) database (Lombard *et al*., 2014) was processed in ESPript 3.0 (Robert & Gouet, 2014) in order to identify conserved residues.

Results and discussion

Phylogeny of ulvan lyase and homologous enzymes. A NCBI BLASTp of the ulvan lyase from *F. agariphila* KMM3901^T showed an exclusive relatedness to Bacteroidetes species. In total, related enzymes were found in 16 genera mainly belonging to Flavobacteriaceae except for *Lewinella*, *Flammeovirga*, and *Labilibacter* (Figure 13). The related genes were annotated as hypothetical proteins, T9SS C-terminal target domain-containing protein and Por secretion system C-terminal sorting domain-containing protein. The Por secretion system (PorSS) or Type IX Secretion System T9SS is unique secretion system in Bacteroidetes to transport proteins across the outer membrane e.g. for gliding motility (McBride & Nakane, 2015; Sato *et al*., 2010). It is likely that the PorSS of polysaccharide-degrading enzymes is much more widespread in Bacteroidetes than thought, indicating the high relevance of polysaccharide utilization.

Phylogenetic analysis of ulvan lyase homologues revealed two clusters, one for family PL25 and one for family PL24 plus unclassified homologues. The long and short ulvan lyases of *Alteromonas* and *Pseudoalteromonas* spp. clustered together, respectively, strengthen the hypothesis that Alteromonadales species possess ulvan lyase of a different PL family than

Nonlabens ulvanivorans (Kopel *et al*., 2016). The highest similarities of ulvan lyase from *F. agariphila* KMM 3901^T was seen with *C. dokdonensis* and *N. ulvanivorans* PLR (Figure S8), the latter having 53 % sequence identity (E-value 1^{-171}) with *Nonlabens ulvanivorans* (WP_036579437.1). The long ulvan lyase is composed of a catalytic domain with a signal peptide at the N-terminus and a Por secretion system C-terminal sorting domain sequence (Collen *et al*., 2011) plus a binding domain (18 kDa) with high affinity and specificity for ulvan (Melcher *et al*., 2017). Therefore, the ulvan lyase from *F. agariphila* is likely characterized by similar enzyme architecture than *N. ulvanivorans* and belongs to the same PL family. At present, these are the first indication for carbohydrate binding modules (CBM) present in polysaccharide lyases specific for ulvan.

Protein size and thermal stability. SDS-PAGE of IMAC and subsequent SEC showed pure soluble protein with a molecular weight of ~ 40 kDa (Figure 14). DLS of SEC-purified protein revealed a hydrodynamic radius of ~ 5 nm as well as polydispersity values of ≥ 20 % (data not shown) indicating protein aggregation. The elution time during SEC purification as well as protein size determination via DLS measured a protein size of 145 - 165 kDa which is three to four times higher as the theoretical protein size. These observations led to the assumption that the ulvan lyase either aggregated during protein purification or that it might consist of a homotrimeric structure. Therefore, analytical SEC was performed and revealed a protein size of 106.6 kDa (Figure 15) indicating a dimeric structure.

Thermal protein stability was determined by the temperature with a strong increase of the measured protein radius. Thermal stability of the ulvan lyase from *F. agariphila* KMM3901^T was observed from 25 - 37 °C (Figure 16). Our results confirm similar observations obtained with different experiments by our collaborator Lukas Reisky at the University of Greifswald as well as Kopel *et al*. (2016) who reported enzyme inactivation for endoactive ulvan lyases from Alteromonadales at temperatures above 40 °C.

Figure 13. Phylogenetic tree of relatedness of the ulvan lyase from *Formosa agariphila* KMM3901T and other Bacteroidetes species. The indicated values at each branch derive from 1000 bootstrap replications. Species belonging to Flavobacteriia are shown on a grey background. Ulvan lyase from *F. agariphila* KMM3901^T is highlighted in red. Carbohydrate esterase from *Actinoalloteichus hymeniacidonis* (AOS63257.1) was used as an out-group.

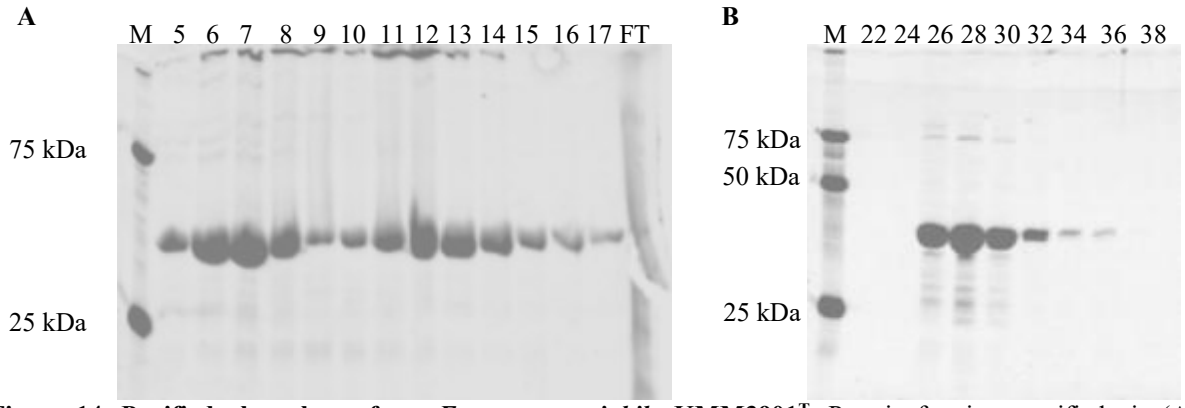

Figure 14. Purified ulvan lyase from *Formosa agariphila* KMM3901^T. Protein fractions purified via (A) IMAC and (B) IMAC and subsequent SEC. 10 µl protein of each fraction were analyzed with SDS-PAGE.

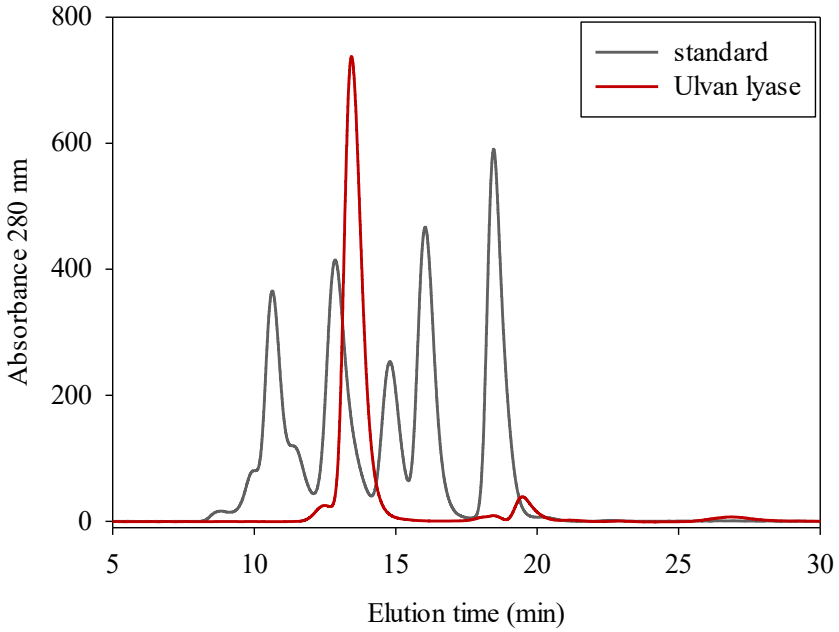

Figure 15. Analytical SEC chromatogram of ulvan lyase from *Formosa agariphila* KMM3901^T. Shown is the absorbance at 280 nm of 60 µl Gel Filtration Standards (1511901, Bio Rad) as well as 60 µl of 29 mg ml^{-1} ulvan lyase against the elution time. SEC was performed using NGC™ Chromatography System (Biorad) with an ENrich™ SEC 650 10 x 300 Column (Bio Rad) and 20 mM Tris pH 8, 0.25 M NaCl at 1 ml min^{-1} flow rate. The gel filtration standard consisted of A: Protein aggregates, B: Thyroglobulin (670 kDa), C: γ-globulin (158 kDa), D: Ovalbumin (44 kDa), E: Myoglobin (17 kDa), F: Vitamin B_{12} (1.35 kDa). The calibration curve (Figure S2) to determine the molecular weight is given as supplementary information.

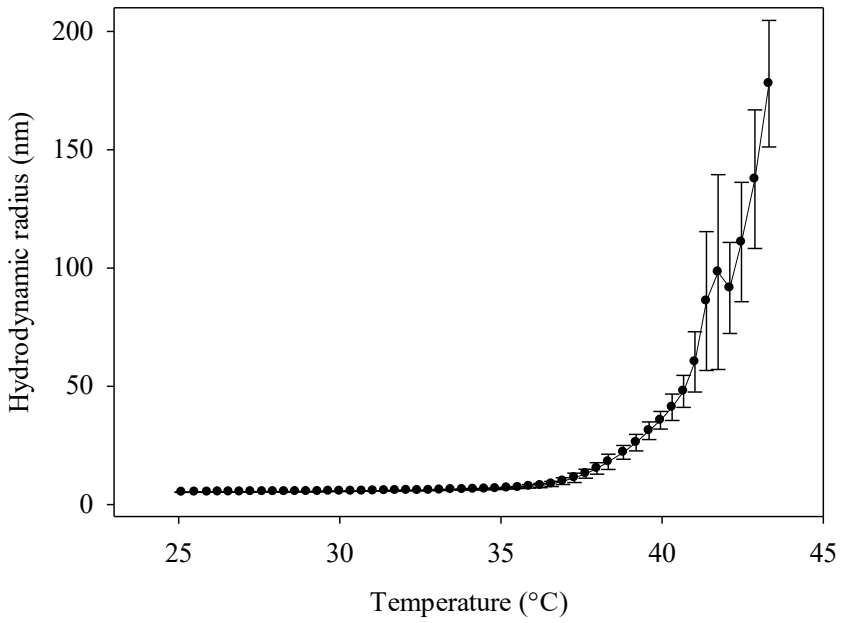

Figure 16. Thermal stability of the ulvan lyase from *Formosa agariphila* KMM3901^T. Thermal stability of the protein was indicated by a constant radius (nm). Triplicates of two different concentrations were measured from 25 – 45 °C. Protein melting increases above 35 °C, when the protein started to unfold and aggregate leading to increasing hydrodynamic radius of protein aggregates.

Determination of enzyme structure. In total, 11 conditions in two sparse matrix and two grid screens were found with small needle-like protein crystals. All conditions included 18 – 25 % PEG and buffer with a pH of 5 – 9. Three conditions were chosen to optimize enzyme crystals to obtain limited protein precipitation as well as big and untwined crystals. So far, crystals of each condition could be reproduced. SEC purification with NaCl-containing elution buffer resulted in increasing volume of the crystallization drops over time, probably due to different salt concentration of mother liquor and enzyme. Therefore, we repeated the SEC purification without sodium chloride in the elution buffer. The best protein crystallization was observed with 29 mg/ml protein in 20 mM Tris pH 8 and 17-19 % PEG 3350, 0.02 M monobasic potassium / dibasic sodium phosphate buffer (Figure S7). All crystals diffracted without any indication of ice or salt crystals interference (Table 2). While adding barium acetate to the mother liquor led to the formation of big crystal needles, the concentration was too low to be detected at the synchrotron. This was also the case for crystals soaked in sodium iodide. Selenomethionine-substituted protein crystallized slower than the native protein and crystals diffracted with a very low resolution, and co-crystallized proteins could not be analyzed yet. Nevertheless, we were able to collect data with a diffraction resolution of ~ 3Å from native

crystals (Table 3) as well as crystals soaked with the tetrasaccharide grown in 17-19 % PEG 3500, 0.02 M monobasic potassium / dibasic sodium phosphate buffer. Even though the structure of the ulvan lyase was not solved yet, our results are promising that further optimization of the crystallization conditions will resolve this problem.

Table 2. Crystallization and data collection of the ulvan lyase from *Formosa agariphila* KMM3901^T. Shown is the number of crystals per crystallization condition, the soaking as well as the data collection at the synchrotron.

# Crystals	Crystallization condition	Soak	Data collection
1	19 % PEG 3500, 0.02 M KH_2PO_4 pH 4 : Na_2HPO_4 pH 9 (1:4)	Sodium iodide 15 sec	Little to no diffraction
2	19 % PEG 3500, 0.02 M KH_2PO_4 pH 4 : Na_2HPO_4 pH 9 (1:4)	Sodium iodide 30 sec	Little to no diffraction
1	19 % PEG 3500, 0.02 M KH_2PO_4 pH 4 : Na_2HPO_4 pH 9 (1:4)	Sodium iodide 40 sec	Little to no diffraction
3	19 % PEG 3500, 0.02 M KH_2PO_4 pH 4 : Na_2HPO_4 pH 9 (1:4)	Native	Little to no diffraction
1	14 % PEG 1500, 0.11 M bis-Tris-propane pH 9	Native	Little to no diffraction
1	14 % PEG 1500, 0.1 M bis-Tris-propane pH 9	Native	Little to no diffraction
2	18 % PEG 3500, 0.02 M KH_2PO_4 pH 4 : Na_2HPO_4 pH 9 (1:4)	Native	Collected 3.26 Å, auto-processing failed
3	10 % PEG 3350, 0.02 M KH_2PO_4 pH 4 : Na_2HPO_4 pH 9 (1:4), 0.005 M barium acetate	Native	Data collected, no barium expected
3	10 % PEG 3350, 0.02 M KH_2PO_4 pH 4 : Na_2HPO_4 pH 9 (1:4), 0.007 M barium acetate	Native	Data collected, no barium expected
5	19 % PEG 3500, 0.02 M KH_2PO_4 pH 4 : Na_2HPO_4 pH 9 (1:4)	Tetrasaccharide	Little to no diffraction
5	17 % PEG 3500, 0.02 M KH_2PO_4 pH 4 : Na_2HPO_4 pH 9 (1:4)	Tetrasaccharide	Collected 3.1 Å
3	18 % PEG 3500, 0.02 M KH_2PO_4 pH 4 : Na_2HPO_4 pH 9 (1:4)	Tetrasaccharide	Collected 3.2 Å
4	Selenomethionine	Native	Little to no diffraction

Table 3. Data processing statistics for native ulvan lyase crystal. Space group 19 ($P2_12_12_1$), unit cell: a 87.98 Å, b 138.74 Å, c 169.80 Å; α 90.00°, β 90.00°, γ 90.00°.

	Overall	Inner shell	Outer shell
Low resolution limit (Å)	47.6	47.6	3.42
High resolution limit (Å)	3.26	10.81	3.26
R*merge* (within I+/I-)	0.339	0.061	1.086
R*merge* (all I+/I-)	0.369	0.065	1.197
R*meas* (within I+/I-)	0.407	0.073	1.307
R*pim* (all I+/I-)	0.404	0.072	1.309
R*pim* (within I+/I-)	0.223	0.04	0.719
R*merge* in top intensity bin	0.162	0.3	0.525
Total number of observations	0.09	-	-
Total number unique	199114	5464	26323
Mean((I)/sd(I))	5.6	16.1	1.6
Mean(I) half-set correlation CC(1/2)	0.953	0.997	0.579
Completeness (%)	99.3	98.9	99.9

Recently, the first structure of an endoactive ulvan lyase from *Pseudoalteromonas* sp. PLSV_3936 was solved (Ulaganathan *et al*., 2017). It is composed of two virtually identical molecules in an asymmetric unit, each molecule folding into a seven-bladed β-propeller. Due to the great overall similarity of the active site of the ulvan lyase and Alys PL15 the authors proposed a convergent evolution among polysaccharides towards a common active site architecture embedded in distinct folds. Basic and polar sidechains were identified at the sides of the deep crevice on top of the propeller fold, indicating the binding of negatively charged ulvan. Side-directed mutagenesis revealed H123, Y188, R204, H264 as putative active residues, probably involved in catalysis or substrate binding. Multiple sequence alignment of ulvan lyases *Croceitalea dokdonensis* DOKDO023, *Pseudoalteromonas* sp. PLSV, *Alteromonas* sp. LOR&LTR, *N. ulvanivorans* PLR and *F. agariphila* showed no greatly conserved regions, but fully conserved residues: G103, G120, W226, and Y260 in *F. agariphila* KMM3901^T. Three of these residues have been detected in slightly conserved regions as the following: TG*FR*L (102 – 108 aa), I*G**FNW*I (219 – 228 aa), RW*N**Y (254 – 260 aa). None of them refer to the conserved residues from *Pseudoalteromonas* sp. PLSV_3936, but H123 and Y188 were also slightly conserved as I95 and Y165 in *F. agariphila*, respectively (Figure S9). However, ulvan lyases from *Pseudoalteromonas* sp. PLSV_3936 and *F. agariphila* KMM3901^T are very unlike regarding primary and thus overall structure. Hence, molecular replacement is still not an option for phasing to. solve the enzyme structure.

Conclusion

In summary, the present study has performed molecular and biochemical analyses of two polysaccharide lyases from marine bacteria. PL7-1 was the only soluble expressed Alys in *E. coli* BL21(DE3) using expression vector pet28a(+) and GFP. Refolding PL7-1 from inclusion bodies was needed to gain a sufficient amount of protein concentration for crystallization. Moreover, induction with IPTG did not enhance the expression compared to ZYP5052 auto-induction medium. Therefore, we conclude that the expression system has to be further optimized for each alginate lyase to investigate the functional mechanisms of the alginolytic system in *Alteromonas macleodii* 83-1. Structural analysis of all alginate lyase will deliver more detailed information of its polysaccharide degrading capabilities. Based on HPLC results, phylogenetic analysis as well as 3D structure model prediction, we propose that PL7-1 is probably endoactive, whereas PL7-2 might be exoactive. Furthermore, PL7-1 was not able to act upon acetylated alginate, mainly produced by bacteria, but was active on algal alginate without any substrate specificity to M-, G-, or GM-enriched alginate.

For the ulvan lyase from *Formosa agariphila* KMM3901^T we propose a dimeric structure, consisting of a catalytic domain fused to a signal peptide at the N-terminus and a binding domain with a Por secretion signal at the C-terminus based on the great relatedness with *N. ulvanivorans*.

We were able to crystallize both the ulvan lyase from *Formosa agariphila* KMM3901^T as well as alginate lyase PL7-1 from *Alteromonas macleodii* 83-1. The two enzymes diffracted without any indication of salt or ice crystals. Although we were able to collect data with a resolution of > 3 Å, it was not possible to determine the accurate space group needed for solving the enzyme structures yet. Regardless, our results are promising that further optimization of the crystallization conditions will resolve this problem.

Outlook

This study provided first detailed insights in the function and structure of anionic algal polysaccharide-degrading polysaccharide lyases from the marine bacteria *Alteromonas macleodii* 83-1 and *Formosa agariphila* KMM3901^T. In order to gain a fully understanding of the functional mechanism of the alginolytic system from *Alteromonas macleodii* 83-1, the function and the structure of all five alginate lyases should be analyzed. Since we were only able to

express PL7-1 in a sufficient amount, optimization of the expression and purification system is needed. There are several aspects that must be considered when designing the ideal expression system.

Overexpression & purification of alginate lyases. Several studies investigated the optimization of protein expression and purification (e.g. Young *et al*., 2012; Rosano & Ceccarelli, 2014).

Protein expression and solubility – None of the five alginate lyases was soluble expressed in an amount sufficient for protein crystallization. There are several factors which have to be considered if in no or low expression of soluble protein is observed: including the choice of the appropriate expression vector, cultivation strain, induction mechanism such as ZYP5052 or IPTG and affinity tags. Particular focus should be given to increase the solubility of all five alginate lyases in future experiments. This can be achieved by testing protein constructs of different length, different affinity tags, or by positioning the His-tag at the C-terminus (Rosano & Ceccarelli, 2014). Even though we also tested fusion tags (GFP-His_6, SUMO-His_6) without any improvement, there are several more available which might enhance solubility (Young *et al*., 2012). Another reason for missing or low expression could be codon usage bias which occurs when there is a significantly different frequency of occurrence of synonymous codons in the foreign coding DNA from that of the host. The easiest strategy to counteract possible codon usage bias are to avoid foaming of the cultures and using codon bias-adjusted strains such as *E. coli* BL21(DE3)CodonPlus strain (Rosano & Ceccarelli, 2014).

Formation of inclusion bodies – Overexpression of proteins in *E. coli* often leads to the formation of water-insoluble aggregates of the targeted protein. A sufficient amount of soluble PL7-1 was only achieved after refolding from these so-called inclusion bodies. Obtaining soluble, active proteins from inclusion bodies is not successful for most proteins, and if so often results in a low protein concentration and / or loss of secondary structure (Qi *et al*., 2015). Hence, the recovery of proteins from inclusion bodies is not the optimal strategy considering structural analysis. To avoid the formation of protein aggregation, the production rate should be slowed down by decreasing the cultivation temperature below 20 °C leading to allow more time for proper protein folding. Supplementation of cofactors such as metal ions and co-expression with chaperons, which can aid the protein to fold and achieve the final confirmation or to disassemble unfolded proteins in inclusion bodies, have been shown to yield in a higher amount of soluble protein (Rosano & Ceccarelli, 2014).

Purification – In order to enhance the amount of (refolded) soluble protein needed for crystallography, the purification can be further optimized. This includes testing different affinity tags as His-tag or multiple affinity tags as well investigating the ideal elution conditions by using different buffers and / or increasing, for instance, the imidazole concentration in the binding buffer. Nevertheless, optimizing the purification system should be done in the case when the expression of the alginate lyases was or could not further be improved.

Overall, the number of options when designing an expression system is extremely high, which leads to multiple options for improvement. In order to save time and costs, small scale cultures are advantageous. If optimizing expression and purification of alginate lyases does not result in appropriate enzyme concentrations, especially for crystallization, further upscaling of the cultures and protein refolding is needed.

Endoactive PL7-1. Our results indicated that PL7-1 from *A. macleodii* 83-1 might be endoactive, whereas PL7-2 is probably exoactive. This hypothesis can be confirmed by solving the enzyme structure as well as by identification of the degradation products of algal alginate using e.g. nuclear magnetic resonance (NMR) or mass spectrometry (MS). Furthermore, growth experiments using purified degradation products on other heterotrophic bacteria occurring in the same or similar environment will lead to a better understanding on how bacteria utilize algal polysaccharides and DOM especially during algal blooms.

Functional analysis of CBM32. *A. macleodii* 83-1 has been reported to colonize and degrade alginate particles (Mitulla *et al*., 2016). 3D structure modeling revealed a putative CBM32 at the N-terminus of PL7-1. To gain fully understanding of the alginate utilization pathway in *A. macleodii* 83-1, it is particularly important to investigate the structural and functional features of the putative carbohydrate binding module. Besides X-ray crystallography, this should be done by using ligands that act as agonists or antagonists as well via side-directed mutagenesis (Boraston *et al*., 2004) of either key residues in the binding site or cloning PL7-1 without the CBM. Possible experiments studying CBM-carbohydrate recognition include affinity gel electrophoresis, UV difference experiments and isothermal titration calorimetry (Abbott *et al*., 2007). Additionally, the binding to artificially produced alginate beads could be tested. Therefore, the absorbance at 280 nm will be measured after incubating the CBM with alginate for a certain time. In comparison to the controls, the absorbance should decrease due to the binding to the substrate.

Domain structure of ulvan lyase. To characterize the structure and mode of action of the ulvan lyase from *Formosa agariphila* KMM3901^T, different constructs of the enzyme should be cloned and tested for substrate binding and specificity. This approach may confirm that the enzyme consists of two domains - a catalytic domain with a signal peptide at the N-terminus and a binding domain with a Por secretion signal at the C-terminus – comparable to the ulvan lyase from *N. ulvanivorans* (Kopel *et al*., 2016; Melcher *et al*., 2017). Additionally, catalytic residues should be identified since tested ulvan lyase homologues were not characterized by highly conserved regions.

Solving enzyme structure. Protein crystallization and X-ray crystallography are powerful tools to determine the enzyme's structure and function, i.e. mode of action. In order to solve the enzyme structure, protein crystallization needs to be further optimized, e.g. by testing more additive screens or co-crystallization with the substrate. Additional soaking with the substrate or phasing solutions might also increase the diffraction resolution.

Another powerful tool in protein crystallization is the streak seeding technique to separate the processes of nucleation and crystal growth. This technique avoids the paradox that optimal conditions for crystal nucleation and subsequent growth can differ substantially. The reason for that is that nucleation more likely occurs in a higher degree of supersaturation. But the higher the level of supersaturation, the faster the crystals' growth rate, often resulting in lower quality due to unstable nucleus formation or incorporation of defects. In the streak seeding technique, previously grown crystals are introduced into new crystallization drops containing protein where they function as seeds. Depending on the size of the crystal, seeding is divided into macro- and microseeding. Nevertheless, there are two important aspects that have to be considered - *(i)* it is essential to know and maintain the degree of supersaturation required for growing crystals while avoiding nucleating new ones and *(ii)* to carefully select the initial seed since its nature may influence the quality of the final crystal. Even though seeding can be time-consuming, laborious and result in difficulties to control the amount of transferred crystals, it also offers several advantageous: it can be performed in conjugation with other optimizations and fine-tuning, speeds up the growth of crystals if the nucleation is the very slow, and can facilitate the growth of similar, related proteins by using a different protein as initial nucleates. This cross-seeding approach has been especially successful for modified proteins. Protein modification can either be done by site-directed mutagenesis or chemically, including for instance selenomethionine-substitution, heavy atoms or substrates. These modifications can change the proteins' solubility, i.e. the degree of supersaturation required for crystalliza-

tion is different from the native form (Bergfors, 2003; Stura & Wilson, 1991). Since we were only able to grow very small crystals for alginate lyase PL7-1 as well as selenomethionine-substituted ulvan lyase within several days, the streak seeding technique seems to be promising approach to solve both enzyme structures.

Polysaccharide-degrading bacteria. The remineralization of algal biomass is an important step in the marine carbon cycle (Teeling *et al*., 2016), and the hydrolytic capacities of polysaccharide-degrading bacteria have ecological relevance for the marine environment. Moreover, they also impact organic matter sedimentation and the biological pump, since some polysaccharides such as alginate form marine gels that represent an important link between DOM and POM sinking to the ocean bottom (Verdugo *et al*., 2004). Studying the degradation mechanisms of abundant key degraders will contribute to our knowledge on the ecophysiology of marine bacteria, and thus to our understanding of the biogeochemical cycles in the oceans. Bacteroidetes and Proteobacteria species have become of big interest as model organisms because they possess PULs or PUL-like systems for specific glycans, respectively (e.g. Mann *et al*., 2013; Zhu *et al*., 2017, Neumann *et al*., 2015). What is still unknown is how these degrading machineries are organized, especially if different families of CAZymes are present. Here we ask whether the alginolytic system in *A. macleodii* 83-1 is similar to the one from *V. splendidus* 12BL01 (Hehemann *et al*., 2016). The presence and absence of PL families in related taxa can result in different ecophysiological types adapted to certain ecological niches (Hehemann *et al*., 2016). Future studies may address whether the architecture of the alginolytic system in *A. macleodii* 83-1, may be indicative of particular functions for each of the alginate lyases.

References

Abbott, D. W., & Boraston, A. (2011). Structural analysis of a putative family 32 carbohydrate-binding module from the *Streptococcus pneumoniae* enzyme EndoD. *Acta Crystallographica Section F: Structural Biology and Crystallization Communications*, *67*(4), 429–433. http://doi.org/10.1107/S1744309111001874

Abbott, D. W., Eirín-López, J. M., & Boraston, A. B. (2008). Insight into ligand diversity and novel biological roles for family 32 carbohydrate-binding modules. *Molecular Biology and Evolution*, *25*(1), 155–167. http://doi.org/10.1093/molbev/msm243

Abbott, D. W., Hrynuik, S., & Boraston, A. B. (2007). Identification and Characterization of a Novel Periplasmic Polygalacturonic Acid Binding Protein from *Yersinia enterolitica*. *Journal of Molecular Biology*, *367*(4), 1023–1033. http://doi.org/10.1016/j.jmb.2007.01.030

Allers, E., Gómez-Consarnau, L., Pinhassi, J., Gasol, J. M., Šimek, K., & Pernthaler, J. (2007). Response of Alteromonadaceae and Rhodobacteriaceae to glucose and phosphorus manipulation in marine mesocosms. *Environmental Microbiology*, *9*(10), 2417–2429. http://doi.org/10.1111/j.1462-2920.2007.01360.x

Allers, E., Niesner, C., Wild, C., & Pernthaler, J. (2008). Microbes enriched in seawater after addition of coral mucus. *Applied and Environmental Microbiology*, *74*(10), 3274–3278. http://doi.org/10.1128/AEM.01870-07

Badur, A. H., Jagtap, S. S., Yalamanchili, G., Lee, J., Zhao, H., & Rao, C. V. (2015). Alginate Lyases from Alginate-Degrading *Vibrio splendidus* 12B01 are andolytic. *Applied and Environmental Microbiology*, *81*(5), 1865–1873. http://doi.org/10.1128/AEM.03460-14

Baumann, L., Baumann, P., Mandel, M., & Allen, R. D. (1972). Taxonomy of aerobic marine eubacteria. *Journal of Bacteriology*, *110*(1), 402–429.

Bergfors, T. (2003). Seeds to crystals. *Journal of Structural Biology*, *142*(1), 66–76. http://doi.org/10.1016/S1047-8477(03)00039-X

Berman, H. M., Westbrook, J., Feng, Z., Gilliland, G., Bhat, T. N., Weissig, H., Shindyalov, I. N., Bourne, P. E. (2000). The protein data bank. *Nucleic Acids Research*, *28*(1), 235–242. http://doi.org/10.1093/nar/28.1.235

Boraston, A. B., Bolam, D. N., Gilbert, H. J., & Davies, G. J. (2004). Carbohydrate-binding modules : fine-tuning polysaccharide recognition. *Biochemical Journal*, *781*, 769–781.

Boraston, A. B., Ficko-blean, E., Healey, M. (2007). Carbohydrate Recognition by a Large Sialidase Toxin from. *Biochemistry*, *46*, 11352–11360.

Brown, B. J., & Preston, J. F. (1991). l-Guluronan-specific alginate lyase from a marine bacterium associated with Sargassum. *Carbohydrate Research*, *211*(1), 91–102. http://doi.org/10.1016/0008-6215(91)84148-8

Chester, R., Jickells, T. (2012). Marine Geochemistry. *Blackwell Publishing.* ISBN 978-1-118-34907-6.

Collen, P. N., Sassi, J. F., Rogniaux, H., Marfaing, H., & Helbert, W. (2011). Ulvan lyases isolated from the flavobacteria *Persicivirga ulvanivorans* Are the first members of a new polysaccharide lyase family. *Journal of Biological Chemistry*, *286*(49), 42063–42071. http://doi.org/10.1074/jbc.M111.271825

Draget, K., Smidsrød, O., & Skjåk-Bræk, G. (2005). Alginates from algae. *Biopolymers,* 1-30. http://doi.org/10.1002/3527600035.bpol6008

Duarte, C. M., Middelburg, J. J., & Caraco, N. (2005). Major role of marine vegetation on the oceanic carbon cycle. *Biogeosciences*, *2*, 1–8. http://doi.org/10.5194/bgd-1-659-2004

Edgar, R. C. (2004). MUSCLE: Multiple sequence alignment with high accuracy and high throughput. *Nucleic Acids Research*, *32*(5), 1792–1797. http://doi.org/10.1093/nar/gkh340

Falkowski, P. G., Barber, R. T., & Smetacek, V. (1998). Biogeochemical controls and feedbacks on ocean primary production. *Science*, *281*(1998), 200–206. http://doi.org/10.1126/science.281.5374.200

Farrell, E. K., & Tipton, P. A. (2012). Functional Characterization of AlgL, an Alginate Lyase from *Pseudomonas aeruginosa*. *Biochemistry*, *51*(51), 10259–10266. http://doi.org/10.1021/bi301425r.Functional

Felsenstein, J. (1985). Confidence Limits on Phylogenies : An Approach Using the Bootstrap. *Evolution*, *39*(4), 783–791.

Garron, M., & Cygler, M. (2010). Structural and mechanistic classification of uronic acid-

containing polysaccharide lyases. *Glycobiology*, *20*(12), 1547–1573. http://doi.org/10.1093/glycob/cwq122

Grondin, J. M., Duan, D., Kirlin, A. C., Abe, K. T., Chitayat, S., Spencer, H. L., Spencer, C., Campigotto, A., Houliston, S., Arrowsmith, C. H., Allingham, J. S., Boratson, A. B. & Smith, S. P. (2017). Diverse modes of galacto-specific carbohydrate recognition by a family 31 glycoside hydrolase from *Clostridium perfringens*. *Plos One*, *12*(2), e0171606. http://doi.org/10.1371/journal.pone.0171606

Haug, A., Larsen, B., & Smidsrød, O. (1966). A Study of the Consitution of Alginic Acid by Partial Acid Hydrolysis. *Acta Chemica Scandinavica*, *20*, 183–190.

Hehemann, J.-H., Arevalo, P., Datta, M. S., Yu, X., Corzett, C. H., Henschel, A., Preheim, S. P., Timberlake, S., Alm, E. J. & Polz, M. F. (2016). Adaptive radiation by waves of gene transfer leads to fine-scale resource partitioning in marine microbes. *Nature Communications*, *7*, 12860. http://doi.org/10.1038/ncomms12860

Hehemann, J.-H., Kelly, A. G., Pudlo, N. A., Martens, E. C., & Boraston, A. B. (2012). Bacteria of the human gut microbiome catabolize red seaweed glycans with carbohydrate-active enzyme updates from extrinsic microbes. *Proceedings of the National Academy of Sciences of the United States of America*, *109*(48), 19786–91. http://doi.org/10.1073/pnas.1211002109

Hisano, T., Yamaguchi, H., Yonemoto, Y., Sakaguchi, K., Yamashita, T., Abe, S., Kimura, A. & Murata, K. (1993). Bacterial alginate lyase inactive on alginate biosynthesized by *Pseudomonas aeruginosa*. *Journal of Fermentation and Bioengineering*, *75*(3), 220–222. http://doi.org/10.1016/0922-338X(93)90120-W

Ivanova, E. P., Alexeeva, Y. V., Flavier, S., Wright, J. P., Zhukova, N. V., Gorshkova, N. M., Mikhalilov, V. J., Nicolau, N. V. & Christen, R. (2004). Formosa algae gen. nov., sp. nov., a novel member of the family Flavobacteriaceae. *International Journal of Systematic and Evolutionary Microbiology*, *54*(3), 705–711. http://doi.org/10.1099/ijs.0.02763-0

Ivars-martinez, E., Auria, G. D., Mira, A., Ferriera, S., Johnson, J., Friedman, R., & Rodriguez-valera, F. (2008). Comparative genomics of two ecotypes of the marine planktonic copiotroph *Alteromonas macleodii* suggests alternative lifestyles associated with different kinds of particulate organic matter. *The ISME Journal*, *2*, 1194–1212.

http://doi.org/10.1038/ismej.2008.74

Iwamoto, Y., Araki, R., Iriyama, K., Oda, T., Fukuda, H., Hayashida, S., & Muramatsu, T. (2001). Purification and characterization of bifunctional alginate lyase from *Alteromonas* sp. strain no. 272 and its action on saturated oligomeric substrates. *Bioscience, Biotechnology, and Biochemistry*, *65*(1), 133–42. http://doi.org/10.1271/bbb.65.133

Jancarik, J., & Kim, S. H. (1991). Sparse matrix sampling. A screening method for crystallization of proteins. *Journal of Applied Crystallography*, *24*(pt 4), 409–411. http://doi.org/10.1107/S0021889891004430

Keen, N. T., & Tamaki, S. (1986). Structure of two pectate lyase genes from *Erwinia chrysanthemi* EC16 and their high level expression in Escherichia coli. *J. Bacteriol.*, *168*(2), 595–606.

Kelly, L. A., Mezulis, S., Yates, C., Wass, M., & Sternberg, M. (2015). The Phyre2 web portal for protein modelling, prediction, and analysis. *Nature Protocols*, *10*(6), 845–858. http://doi.org/10.1038/nprot.2015-053

Khailov, K. M., & Burlakova, Z. P. (1969). Organic By Marine and Distribution of Their Total Organic Production To Inshore Communities. *Limnology and Oceanopraphy*, *14*(4), 521–527. Retrieved from 10.4319/lo.1969.14.4.0521

Kirkman, H., & Kendrick, G. A. (1997). Ecological significance and commercial harvesting of drifting and beach-cast macro-algae and seagrasses in Australia: A review. *Journal of Applied Phycology*, *9*(4), 311–326. http://doi.org/10.1023/A:1007965506873

Kitamikado, M., Tseng, C. H., Yamaguchi, K., & Nakamura, T. (1992). Two types of bacterial alginate lyases. *Applied and Environmental Microbiology*, *58*(8), 2474–2478.

Kopel, M., Helbert, W., Belnik, Y., Buravenkov, V., Herman, A., & Banin, E. (2016). New family of ulvan lyases identified in three isolates from the alteromonadales order. *Journal of Biological Chemistry*, *291*(11), 5871–5878. http://doi.org/10.1074/jbc.M115.673947

Kopel, M., Helbert, W., Henrissat, B., Doniger, T., & Banin, E. (2014a). Draft Genome Sequence of Nonlabens ulvanivorans, an Ulvan-Degrading Bacterium. *Genome Announcements*, *2*(4), 3–4. http://doi.org/10.1128/genomeA.00793-14.Copyright

Kopel, M., Helbert, W., Henrissat, B., Doniger, T., & Banin, E. (2014b). Draft Genome Sequence of *Pseudoalteromonas* sp. Strain PLSV, an Ulvan-Degrading Bacterium. *Genome Announcements*, *2*(6), 4–6. http://doi.org/10.1128/genomeA.01257-14

Kopel, M., Helbert, W., Henrissat, B., Doniger, T., & Banin, E. (2014c). Draft genome sequences of two ulvan-degrading isolates, strains LTR and LOR , that belong to the *Alteromonas* genus. *Genome Announcements*, *2*(5), 13–15. http://doi.org/10.1128/genomeA.01081-14

Kraan, S. (2012). Algal polysaccharides, novel applications and outlook. *Carbohydrates - Comprehensive Studies on Glycobiology and Glycotechnology*, 489–532. http://doi.org/10.5772/51572

Kumar, S., Stecher, G., & Tamura, K. (2016). MEGA7: Molecular Evolutionary Genetics Analysis version 7.0 for bigger datasets. *Molecular Biology and Evolution*, *33*(7), msw054. http://doi.org/10.1093/molbev/msw054

Laemmli, U. K. (1970): (1970). Cleavage of Structural Proteins during Assembly of Head of Bacteriophage-T4. *Nature*, *227*. http://doi.org/10.1038/227680a0

Lahaye, M. (1998). NMR spectroscopic characterisation of oligosaccharides from two Ulva rigida ulvan samples (Ulvales, Chlorophyta) degraded by a lyase. *Carbohydrate Research*, *314*(1–2), 1–12. http://doi.org/10.1016/S0008-6215(98)00293-6

Lahaye, M., & Robic, A. (2007). Structure and function properties of Ulvan, a polysaccharide from green seaweeds. *Biomacromolecules*, *8*(6), 1765–1774. http://doi.org/10.1021/bm061185q

Lee, K. Y., & Mooney, D. J. (2013). Alginate : properties and biomedical applications. *Prog Polym Sci*, *37*(1), 106–126. http://doi.org/10.1016/j.progpolymsci.2011.06.003.

Lombard, V., Bernard, T., Rancurel, C., Brumer, H., Coutinho, P. M., & Henrissat, B. (2010). A hierarchical classification of polysaccharide lyases for glycogenomics. *Biochemical Journal*, *432*, 437–444. http://doi.org/10.1042/BJ20101185

Lombard, V., Golaconda Ramulu, H., Drula, E., Coutinho, P. M., & Henrissat, B. (2014). The carbohydrate-active enzymes database (CAZy) in 2013. *Nucleic Acids Research*, *42*(D1), 490–495. http://doi.org/10.1093/nar/gkt1178

Lombard, V., Ramulu, H. G., Drula, E., Coutinho, P. M., & Henrissat, B. (2014). The carbohydrate-active enzymes database (CAZy) in 2013. *Nucleic Acids Research*, *42*, 490–495. http://doi.org/10.1093/nar/gkt1178

Mabeau, S., & Kloareg, B. (1987). Isolation and Analysis of the Cell Walls of Brown Algae : *Fucus spiralis* , *F . ceranoides* , *F . vesiculosus* , *F . serratus*, *Bifurcaria bifurcata* and *Laminaria digitata*. *Journal of Experimental Botany*, *38*(194), 1573–1580.

Malissard, M., Duez, C., Micheline, G., & Vacheron, M. (1993). Sequence of a gene encoding a (poly ManA) alginate lyase active on *Pseudomonas aeruginosa* alginate. *FEMS Microbiology Letters*, *110*, 101–106.

Mann, A. J., Hahnke, R. L., Huang, S., Werner, J., Xing, P., Barbeyron, T., Huettel, B., Stüber K., Reinhardt, R., Harder, J., Glöckner, F. O. Amann, R. & Teeling, H. (2013). The genome of the alga-associated marine flavobacterium *Formosa agariphila* KMM 3901T reveals a broad potential for degradation of algal polysaccharides. *Applied and Environmental Microbiology*, *79*(21), 6813–6822. http://doi.org/10.1128/AEM.01937-13

McBride, M. J., & Nakane, D. (2015). Flavobacterium gliding motility and the type IX secretion system. *Current Opinion in Microbiology*, *28*, 72–77. http://doi.org/10.1016/j.mib.2015.07.016

McCarren, J., Becker, J. W., Repeta, D. J., Shi, Y., Young, C. R., Malmstrom, R. R., Chisholm, S. W. & DeLong, E. F. (2010). Microbial community transcriptomes reveal microbes and metabolic pathways associated with dissolved organic matter turnover in the sea. *Proceedings of the National Academy of Sciences of the United States of America*, *107*(38), 16420–7. http://doi.org/10.1073/pnas.1010732107

McPherson, A., & Cudney, B. (2006). Searching for silver bullets: An alternative strategy for crystallizing macromolecules. *Journal of Structural Biology*, *156*(3), 387–406. http://doi.org/10.1016/j.jsb.2006.09.006

Melcher, R. L. J., Neumann, M., Fuenzalida Werner, J. P., Gröhn, F., & Moerschbacher, B. M. (2017). Revised domain structure of ulvan lyase and characterization of the first ulvan binding domain. *Scientific Reports*, *7*, 1–9. http://doi.org/10.1038/srep44115

Mikami, B., Suzuki, S., Yoon, H.-J., Miyake, O., Hashimoto, W., & Murata, K. (2002). X-Ray Structural Analysis of Alginate Lyase a1-Iii Mutants/Substrate Complexes:

Activation of a Catalytic Tyrosine Residue By a Flexible Lid Loop. *Acta Crystallographica*, *58*.

Mitulla, M., Dinasquet, J., Guillemette, R., Simon, M., Azam, F., & Wietz, M. (2016). Response of bacterial communities from California coastal waters to alginate particles and an alginolytic *Alteromonas macleodii* strain. *Environmental Microbiology*, (April). http://doi.org/10.1111/1462-2920.13314

Miyake, O., Hashimoto, W., & Murata, K. (2003). An exotype alginate lyase in *Sphingomonas* sp. A1: Overexpression in *Escherichia coli*, purification, and characterization of alginate lyase IV (A1-IV). *Protein Expression and Purification*, *29*(1), 33–41. http://doi.org/10.1016/S1046-5928(03)00018-4

Nedashkovskaya, O. I., Kim, S. B., Vancanneyt, M., Snauwaert, C., Lysenko, A. M., Rohde, M., Frolova, G. M., Zhukova, N. V., Mikhailov, V. V., Bae, K. S., Oh, H. W. & Swings, J. (2006). *Formosa agariphila sp*. nov., a budding bacterium of the family Flavobacteriaceae isolated from marine environments, and emended description of the genus *Formosa*. *International Journal of Systematic and Evolutionary Microbiology*, *56*(1), 161–167. http://doi.org/10.1099/ijs.0.63875-0

Neumann, A. M., Balmonte, J. P., Berger, M., Giebel, H., Arnosti, C., Voget, S., Simon, M, Brinkhoff, T. & Wietz, M. (2015). Different utilization of alginate and other algal polysaccharides by marine *Alteromonas macleodii* ecotypes. *Environmental Microbiology*, *17*(10), 3857–3868. http://doi.org/10.1111/1462-2920.12862

Newman, J., Egan, D., Walter, T. S., Meged, R., Berry, I., Jelloul, M. Ben, Sussman, J. L., Stuart, D. I. & Perrakis, A. (2005). Towards rationalization of crystallization screening for small- To medium-sized academic laboratories: The PACT/JCSG+ strategy. *Acta Crystallographica Section D: Biological Crystallography*, *61*(10), 1426–1431. http://doi.org/10.1107/S0907444905024984

Osawa, T., Matsubara, Y., Muramatsu, T., Kimura, M., & Kakuta, Y. (2005). Crystal structure of the alginate (Poly α-L-guluronate) lyase from *Corynebacterium* sp. at 1.2 Å resolution. *Journal of Molecular Biology*, *345*(5), 1111–1118. http://doi.org/10.1016/j.jmb.2004.10.081

Preston, L. A., Wong, T. Y., Bender, C. L., & Schiller, N. L. (2000). Characterization of alginate lyase from *Pseudomonas syringae pv. syringae*. *Journal of Bacteriology*,

182(21), 6268–6271. http://doi.org/10.1128/JB.182.21.6268-6271.2000

Qi, X., Sun, Y., & Xiong, S. (2015). A single freeze-thawing cycle for highly efficient solubilization of inclusion body proteins and its refolding into bioactive form. *Microbial Cell Fractories*, 1–12. http://doi.org/10.1186/s12934-015-0208-6

Rehm, B. H. A., & Valla, S. (1997). Bacterial alginates: Biosynthesis and applications. *Applied Microbiology and Biotechnology*, *48*(3), 281–288. http://doi.org/10.1007/s002530051051

Robert, X., & Gouet, P. (2014). Deciphering key features in protein structures with the new ENDscript server. *Nucleic Acids Research*, *42*(W1), 320–324. http://doi.org/10.1093/nar/gku316

Robinson, H. W. (1929). The Influence of Neutral Salts on the pH of Phosphate Buffer Mixtures. *The Journal of Biological Chemistry*, *82*, 775–802.

Rosano, G. L., & Ceccarelli, E. A. (2014). Recombinant protein expression in *Escherichia coli*: Advances and challenges. *Frontiers in Microbiology*, *5*(APR), 1–17. http://doi.org/10.3389/fmicb.2014.00172

Sato, K., Naito, M., Yukitake, H., Hirakawa, H., Shoji, M., McBride, M. J., Rhodes, R. G. & Nakayama, K. (2010). A protein secretion system linked to bacteroidete gliding motility and pathogenesis. *Proc Natl Acad Sci U S A*, *107*(1), 276–281. http://doi.org/10.1073/pnas.0912010107

Sawabe, T., Ohtsuka, M., & Ezura, Y. (1997). Novel alginate lyases from marine bacterium *Alteromonas* sp. strain H-4. *Carbohydrate Research*, *304*(1), 69–76. http://doi.org/10.1016/S0008-6215(97)00194-8

Shinya, S., Nishimura, S., Kitaoku, Y., Numata, T., Kimoto, H., Kusaoke, H., Ohnuma, T. & Fukamizo, T. (2016). Mechanism of chitosan recognition by CBM32 carbohydrate-binding modules from a *Paenibacillus* sp. IK-5 chitosanase/glucanase. *Biochemical Journal*, *473*(8), 1085–1095. http://doi.org/10.1042/BCJ20160045

Shoseyov, O., Shani, Z., & Levy, I. (2006). Carbohydrate Binding Modules: Biochemical Properties and Novel Applications. *Microbiology and Molecular Biology Reviews*, *70*(2), 283–295. http://doi.org/10.1128/MMBR.00028-05

Sonnenburg, E. D., Zheng, H., Joglekar, P., Higginbottom, S., Firbank, S. J., Bolam, D. N., & Sonnenburg, J. L. (2010). Specifity of polysaachride use in intenstinal Bacteroides species determins diet-induced microbiota alterations. *Cell*, *141*(2), 1241–1252. http://doi.org/10.1016/j.pestbp.2011.02.012.Investigations

Studier, F. W. (2005). Protein production by auto-induction in high-density shaking cultures. *Elsevier Protein Expression and Purification*, *41*, 207–234. http://doi.org/10.1016/j.pep.2005.01.016

Stura, E. A., & Wilson, I. A. (1991). Applications of the streak seeding technique in protein crystallization. *Journal of Crystal Growth*, *110*(1–2), 270–282. http://doi.org/10.1016/0022-0248(91)90896-D

Teeling, H., Fuchs, B. M., Becher, D., Klockow, C., Gardebrecht, A., Bennke, C. M., Kassabgy, M., Huang, S., Mann, A. J., Waldmann, J., Weber, M., Klindworth, A., Otto, A., Lange, J., Bernhardt, J., Reinsch, C., Hecker, M., Peplies, J., Bockelmann, F. D., Callies, U., Gerdts, G., Wichels, A., Wiltshire, K. H., Glöckner, F. O., Schwerder, T. & Amann, R. (2012). Substrate-Controlled Succession of Marine Bacterioplankton Populations Induced by a Phytoplankton Bloom. *Science Reports*, *336*, 608–611.

Teeling, H., Fuchs, B. M., Bennke, C. M., Krüger, K., Chafee, M., Kappelmann, L., Reintjes, G., Waldmann, J., Quast, C., Glöckner, F. O., Lucas, J., Wichels, A., Gerdts, G., Witshire, K. H. & Amann, R. I. (2016). Recurring patterns in bacterioplankton dynamics during coastal spring algae blooms. *eLife*, *5*(APRIL2016), 1–31. http://doi.org/10.7554/eLife.11888

Terrapon, N., Lombard, V., Gilbert, H. J., & Henrissat, B. (2015). Automatic prediction of polysaccharide utilization loci in Bacteroidetes species. *Bioinformatics*, *31*(5), 647–655. http://doi.org/10.1093/bioinformatics/btu716

Thomas, F., Barbeyron, T., Tonon, T., Génicot, S., Czjzek, M., & Michel, G. (2012). Characterization of the first alginolytic operons in a marine bacterium: from their emergence in marine Flavobacteria to their independent transfers to marine Proteobacteria and human Bacteroides. *Environmental Microbiology*, *14*(9), 2379–2394. http://doi.org/10.1111/j.1462-2920.2012.02751.x

Thomas, F., Hehemann, J. H., Rebuffet, E., Czjzek, M., & Michel, G. (2011). Environmental and gut Bacteroidetes: The food connection. *Frontiers in Microbiology*, *2*(MAY), 1–16.

http://doi.org/10.3389/fmicb.2011.00093

Thomas, F., Lundqvist, L. C. E., Jam, M., Jeudy, A., Barbeyron, T., Sandström, C., Michel, G. & Czjzek, M. (2013). Comparative characterization of two marine alginate lyases from *Zobellia galactanivorans* reveals distinct modes of action and exquisite adaptation to their natural substrate. *Journal of Biological Chemistry*, *288*(32), 23021–23037. http://doi.org/10.1074/jbc.M113.467217

Tomme, P., Warren, R. A. J., Miller, R. C., Kilburn, D. G., & Gilkes, N. R. (1996). Cellulose-Binding Domains : Classification and Properties. *American Chemical Society*, *Chapter 10*, 142–163.

Tseng, C.-H., Yamaguchi, K., & Kitamikado, M. (1992). Isolation and some properties of alginate lyase from a marine bacterium *Vibrio* sp. AL-128. *Nippon Suisan Gakkaishi*, *58*(3), 533–538.

Ulaganathan, T., Boniecki, M. T., Foran, E., Buravenkov, V., Mizrachi, N., Banin, E., Helbert, W. & Cygler, M. (2017). New ulvan-degrading polysaccharide lyase family: structure and catalytic mechanism suggests convergent evolution of active site architecture. *ACS Chemical Biology*, acschembio.7b00126. http://doi.org/10.1021/acschembio.7b00126

Valiela, I., Mcclelland, J., Hauxwell, J., Behr, P. J., Hersh, D., & Foreman, K. (1997). Macroalgal blooms in shallow estuaries: Controls and ecophysiological and ecosystem consequences. *Limnology and Oceanography*, *42,* 5 Part 2, 1105–1118. http://doi.org/10.4319/lo.1997.42.5_part_2.1105

Verdugo, P., Alldredge, A. L., Azam, F., Kirchman, D. L., Passow, U., & Santschi, P. H. (2004). The oceanic gel phase : a bridge in the DOM – POM continuum, *92*, 67–85. http://doi.org/10.1016/j.marchem.2004.06.017

Whelan, S., & Goldman, N. (2001). A general empirical model of protein evolution derived from multiple protein families using a maximum-likelihood approach. *Molecular Biology and Evolution*, *18*(5), 691–699. http://doi.org/10.1093/oxfordjournals.molbev.a003851

Wietz, M., Wemheuer, B., Simon, H., Giebel, H., Seibt, M. A., Daniel, R., Brinkhoff, T. & Simon, M. (2015). Bacterial community dynamics during polysaccharide degradation at

contrasting sites in the Southern and Atlantic Oceans. *Environmental Microbiology*, *17*(10), 3822–3831. http://doi.org/10.1111/1462-2920.12842

Wong, T. Y., Preston, L. A., & Schiller, N. L. (2000). ALGINATE LYASE: review of major sources and enzyme characteristics, structure-function analysis, biological roles, and applications. *Annual Review of Microbiology*, *54*, 289–340. http://doi.org/10.1146/annurev.micro.54.1.289

Wooh, J. W., Kidd, R. D., Martin, J. L., & Kobe, B. (2003). Comparison of three commercial sparse-matrix crystallization screens. *Acta Crystallographica - Section D Biological Crystallography*, *59*(4), 769–772. http://doi.org/10.1107/S0907444903002919

Yamasaki, M., Moriwaki, S., Miyake, O., Hashimoto, W., Murata, K., & Mikami, B. (2004). Structure and function of a hypothetical *Pseudomonas aeruginosa* protein PA1167 classified into family PL-7: A novel alginate lyase with a β-sandwich fold. *Journal of Biological Chemistry*, *279*(30), 31863–31872. http://doi.org/10.1074/jbc.M402466200

Yamasaki, M., Ogura, K., Hashimoto, W., Mikami, B., & Murata, K. (2005). A structural basis for depolymerization of alginate by polysaccharide lyase family-7. *Journal of Molecular Biology*, *352*(1), 11–21. http://doi.org/10.1016/j.jmb.2005.06.075

Young, C. L., Britton, Z. T., & Robinson, A. S. (2012). Recombinant protein expression and purification: A comprehensive review of affinity tags and microbial applications. *Biotechnology Journal*, *7*(5), 620–634. http://doi.org/10.1002/biot.201100155

Zhu, Y., Thomas, F., Larocque, R., Li, N., Duffieux, D., Cladière, L., Souchaud, F., Michel, G. & McBride, M. J. (2017). Genetic analyses unravel the crucial role of a horizontally acquired alginate lyase for brown algal biomass degradation by *Zobellia galactanivorans*. *Environmental Microbiology*, (February). http://doi.org/10.1111/1462-2920.13699

Supplementary information

Table S1. Nucleotide sequences of (A) alginate lyases from *Alteromonas macleodii* 83-1 and (B) ulvan lyase from *Formosa agariphila* KMM3901^T.

A)

AL	Nucleotide sequence 5' → 3'
PL7-1	ATGTTTCGCTTATTGCTTGTTTTACTAACGCTTACTTCGCTAAATGGCTGTGGCTCTTCTTCA TCGTCCACAACCTCGCAAACGCCTTTACCAGACGATAGCTCTGCGCCAACACCGTCTCCCA TTCCCCCAACAAATGAGACGGAAGCATGTAGCGCGTTACCATTAACAGGGTTAAGCGCAT CGGCGACTGAAGAAAAAGCGCCTTTTAATGCATCTAAAGCTATCGACGGCGATACCTCTA ACGCCTCTCGTTGGCAATCAACAGGCACTAATTCTGCGCTCGTGCTTTCATTTGATAGCGA CCAACAACTAGGTGCTCTTCAAATTAAGTGGTATGACAGCGAAGCTCGCGCTTATCGCTTT TCTATTGAAACCTCACTAGATGGTGAAAGCTGGGATACACAGCGATCAAATATCAACTCAA ATACACAGCTTGCGGGTTTCGAGCTTTATTCATTACCAGCGCTTGTAACGTCTCGCTATATA CGTGTTACCCCGTTTGGAAACTCTGTTAATGACCATAACGCAATAGTTGAGGTTCAGTTATT CAATTGCACTGAAGGCGACGGTGAAATTTCATCTGCACTTACTTCAACTGCGGGTATCGAT TTACAAGACTGGTATTTAAGCATTCCAACAGACAATGATGACTCAGGCACGGCTGATAAC ATAGGCGAAACTAGGCTTCAGCAGGGGTATACCAACTCCGAATATTTCTATGTAGGTAACG ATGGCGCGTTAGTGATGCGCTCTCCTACAATCGGTTTTAAAACCTCTGTAAACACCAATTA TGTTCGCGTTGAGTTACGTGAAATGTTGCGACGCGGCGATACCAGTATTAAGACCCAAGG CGTTAATAAAAACAACTGGGTACTCTCCTCCGCCTCTCAGGCAAATCAAGATGCTGCAGGC GGCGTGAATGGTCGTTTACGGGTTGAGATGGCGGTAAACGAAGTTACCACTACAGGCGAG AATTTCCAAATAGGCCGCGTGATCATAGGTCAAATACATGCTAACGATGACGAGCCAATA CGCCTGTACTACCGCAAGTTGCCTAGTAATAACTTAGGCGCTATTTACTTTGCCCACGAGC GCAGAGCAGTGGCAACAGCGAATGGCGAGAAAGAAGAAATATGGGTAGAAATGATCGG CTCGCGAGACAGTGATGCAAACAACCCCACTGATGGCATAGCACTTAATGAGCGTTTTACC TACGTTATTGACGTTGAAGGTGACACGCTCACCGCAACGATTTCAAGAGAAGGAAAGTCT GACGTCACCCGTTCTTTAAATATTGGGAATAGTGGTTATGATGAAGATGATCAATATCTGT ATTTCAAGGTAGGTGTATATCACGTTAACAATTCTGCAAATGAAGCAGAGCGTGTAGTTGC CAGCTTTTATTCAATTGAGAATGAACATGGTAACTAG
PL7-2	ATGAAAGCAATTTTGCCAATCCAAAAGCGCTGGCTTGTTATCTCTAGTACATTCTCTAGTGT ACTCGCCACTGCATTAGCAACCACAAGTCCAGTATGGGCGGAAGACCTCGCGCTGCATGC ACAACAGTATGATTTAAGTGAGTGGTATTTAACGTTACCTGCAGACGGTAACAACGATGG AAAAGCTGACAACATTTCTGTTGAAGACCTTCAATCTTTTACGCATCCTTCGTTTTTCTATT TGAATAACGAAGGTGGATTGGTGTTCACCAGCCCTAACAAAGCATTAACTACAAAGAACT CTACAAATACGCGAAGCGAACTGCGCCACATGCTGCGTGGCAACAATAAGTCAGTTAAAA CACAGTCAGCAGAAAATAGCTTTACCGTTGCCAGTAACCCCATAGCGCGACGCTTTGCCCG TGTGGGTGGAAAAATGCAGGCCACATTGAAAGTGAATCATGTAGCGCTAAGAGCTAAGTA TCCCGAGAAACCACCAGCATATTCTGTGGTTGTAGGCCAAATTCACGCAACTAAATGGAAA AAGAAAGTAAAAGGCTTTGGCTGGGGCAATGAACCGCTAAAAATATATTTTAAAAAATG GCCTGAACACGAAACCGGCTCGGTATTTTGGACCTATGAGCGAAACCTTCCTAAAAGCGA CCCAAAACGCAAAGACATTGCCTATCCTGTTTGGGGTAACCTGTGGACTGACAGTACCGA CCCTGGCGCTCAAGGCATTAAGCTTGATGAGACGTTCAGCTACACCGTGAACGTTCATGGC GATATCATGCACCTTAGGTTCGAGTCAGAAAATCATGAAACCATTGAGTATTCCATTAACC TTGCCAATGCCGTTGATGCGTATGGACAGGTAGATAAATACGATCACCCCTACGGTTATAC CCTTGATTGGAACTACTTCAAAGCTGGCGCTTATAACCAGTGCAGCACAAAAGACGACCCC GCATTCTGGTATCCGGCCTGTTTAGGCACGGGTAATTGGGAAGAAGATGAAAAAAATGGT GACTACACGCGAGTAACCTTTACTGAACTTACGGTGACAGAAAGTACACCAGAAGAGAAC TAG

PL17	ATGATTAAAAACCTCTGTTCCCTACAACAAAAATCTGCGCTTTTACTTTTCATTTTTTGTTC GCTTTCTTTTTCTTCTCTTGCCGCTCACCCTAACTTGGTGATCACGCAAGACGACGTTGTAA AAATGCGCAACGCCATAATGCAAGAAGGGCGTTTCCAAGATGCTTATTTGCAAGTTAAAC AAGAGGTAGATTTGCATTTAGCAATGCCAAACGTTGTTCCTGTGCCAAAAGACGGCGGCG GTGGTTACACTCACGAACGTCATAAAAAGAACTATCAGCTTATGTATAACGCTGGCGTGGT GTACCAAATTAGTGATAACGAAAAGTATGCGAATTATGTAAAAAATCTCTTGTTAGATTAT GCCGCACTTTATCCTACATTAGGGTTGCACCCACAGCGTAAAGTGAACGCCCAAAACCCTG GTGTTTTCTTCTGGCAAAGCCTAAATGAAGCCGTATGGCTTGTGAATACTATTCAAGCTTAC GACTTGATATACAACGCGCTTGATGAAGAAGAGCGAAGCGTAATTGAGAACCAACTGTTG CGTCCTGTCGCGTTGTTCTTATCAGAGGGTCAACCGTCTACGTTTAATAAAGTACACAACC ACGGAACGTGGGCTACCGCTGGCGTAGGTATGGCAGGGTATGTGTTAAACGAACCAGAAT GGGTTGAAAAAGCACTTTACGACCTAGAAAAGTCAGGCAAAGGTGGTTTTTTAAAACAGC TCGATACGCTATTTTCCCCTCAAGGCTACTATAACGAAGGGCCGTACTACCAACGCTACGC GCTAATGCCGTTCGTTACGTTCGCTAAAGCAATTGAAAATAATGAGCCTCAACGCAATATT TTCGACCACCGCGATAAGGTTTTGCTTAAAGCAATAAATACCACCATTCAGCTTAGCTACA ATGGATTGTTCTTCCCAATCAATGACGCAATTAAAAGCAAAGGCATAGATACTATTGAGTT AGTGTATGGTGTTGCTGTGGCGTATCAGCAAACAAAAGATAAAGGCTTACTGGATATTGC CAAGCAGCAAGGGCGAATTGTACTCACAGGCGATGGTGTTGACGTAGCGAAGGCGCTGG ATGAGAACAAAGCAACGCCTTATATTTTCGAATCGATGGCCTTGGGTGACGGTAAAGATG GCGATGAAGGTGCATTAGTAATTATGCGCACTGAAGAACCTCAGGGTGAAACAGTGTTAT TTAAACCTGCAGCCCAAGGTTTAGGACATGGGCATTTCGATAAACTAACATGGCAGCTTTA CGATAAAGGCAGTGAGATTGTAACCGACTATGGTGCGGCACGATTCTTAAATGTAGAAGC CAAATTTGGTGGTCGTTACCTTCCAGAAAATAATAGCTATGCCAAACAAACCGTTGCGCAC AATACGGTAGTGGTTGATGAGCAAAGTCATTTCTCTTTTAACTTGGAAAAGGCGAATGCGA ATGCGCCTACGCTACACTTCTTTGAAAATAACGAGCACGGTACAGTTGCTCGCGCCAGCAT CGAAACTGCCTATGACGATGTTGTACTTGATAGAACGATAGCGCTGCTTTCTTTACCTACCT TAAATAAGCGCATTGTTGTTGATGTGTTTGATGTATCTAGTGACAAGCCGCACACCTACGA TTTACCACTGCATTATAGCGGTCATTTAATTGATACTAACTTTGAATATCAGGGTTATACCA ATACGTTATCTGCACTAGGAAGCGTAAGTGGATATCAGCACTTGTGGCTAAGGGCGAAGG GTATTCCGAAAGCTGATATAGCTAGAGTGACTTGGCTAAATAGTAACGGCCGTTTCTATTC ACAACACAGCGTTGCAAAAGGCAACGAAACCTTTCTATTTACCCAGCTAGGTGCCGGTGA CCCAAATTTCAATCTTCGCAACGAGAGCAGCGTGATACGCAGGGTAGAAGGTAAGGCGCA TCACCAATTCGTTTCCGTTCTAGAGCCTCACGGTGAATACAACCCTAGTAAGGAATATACC TTGGGTGCAGAAAGCATTATTACATCAGTTCAGACAGTAAAAAACGACACATTGCTTTTAC TTGTAATAAAAGCAGCTGAACAGCAGTTTCTAATAGCCATAAATACCACAGACGGTAGCG AGTCGACCGAGTCTGTTTCTTTTGATTTTGATAAAAACCGTTACACGCTTTCAAGCCGTTTC GCTGTGTATGCGCTGTAA
PL6-1	ATGCAAGTGCAATTTATTAAGTGGCTAGCTGTGTTTATTGTTATTAGCGCTATGTCGTCAAA CGCGGGCGCTAAACAATATAACGTTAGCTCACCAGATGAATACAACGCAATAGCATCGTC TCTTAAGGCGGGTGACGACGAATTTTACAAAATGGTGTTTATCGAGACTTTGAAATTTTAC TAGTAGGGCAGGGTAGCGCTGAAAAGCCCATTACGCTGACTGCGCAAACTAAAGGTAAG GTTATTCTGTCTGGTCGTTCTAACTTAAAGTTAGCTGGGCAGTATTTAGAAGTATCGGGTTT GGTATTCAAAGACGGATATACCCCTAGCAGCGCTGTTATCGCGTTTAGGAAAGATGCACAA ACGCCAGCTAATTATTCACGAGTAAGTGAAGTAGTCATTGATGAGTACAGTAATCCGGACC GCCAAGAATCAGATTATTGGGTTGCACTTTATGGTAAGCACAACCGGTTTGACCATAACCA CCTGACGGGTAAGCGTAACAAGGGGGTTACTGTCGCTGTTCGGCTTAACGGCGAGGCACA TCAAGAGAACCATCACAGTATCGATCACAACTACTTCGGTTATCGCCCTGTATTCGGTTCA AATGGAGGAGAGACGTTAAGGATAGGTACAAGTCATTACTCACTGAGTAATTCGAATACT CAGGTTATCAATAACATATTCGAACAAACTAATGGCGAAGTTGAAATTATTTCTGTTAAGT CTGGTGAGAACCTGCTGAAAGGAAACGTTTTTCTATCCGCTAAAGGCACCCTAACCCTTAG ACACGGTAATAATAATCGCGTTGAAGATAATGTGTTTTTAGGCAATGGCGTGGACCATACC GGTGGAATTCGCGTTATCAATGAAGGCCAAGTGATAACCAATAACTACTTGGAGGGGCTA ACGGGCTATCGCTTTGGTAGTGGCTTTACGGTTATGAATGGTGTGCCTGACTCGCCTATCA

	ATCGTTATCATCAGGTTAATAACGCGCAAATCACAAATAACTCATTCATTAACGTGTCACA TATCCAACTTGGTGCTGGAAGCGATGAAGAGAGAAGCGCGACACCTATAAATTCATTGTTT GCCAATAACCTTATTTACAATGCTTCGCTAAACCAACCTTTTACATTATTTGATGATGTGAG CGGCATTACATTCGCTAACAATGTCGCTAATACCAAAATGATAAAAGAACTTAGCGAAGG CTTTACTACTGCATCGCTACCCCTTGTTAAGGGTGAGAATGGGCTTAACGTCGCTAAGCTA AACGAGCCTGAGGTAAAAGGCGCAGAAACAAAAGATGTTGGTGTTGCTTCTAACATGAAC GTCGTATCAAAAAGTGACGTCGGCGTAAGCTGGTATCCCAAAATAGTACCTGAAGTGAAC TTCGCTGCAGGTAAAACAATTAGCGTAAGTGCCGATGCTGCTGAACTTATGACAGCACTTG AAAATGCCAGTGACGGAGATGTTATTACAATGGCACCTGGCACTATCGTTGTGCCCAGTGT TCTTATTATCGATAAGACAGTAACGGTAACCGCACAGACTCCCAAAGCTACAACACTGTCG TTCGAACGCTCCGCCTTGTTCGAAATACATGACAATGGAAATTTGAAGCTTGAAGGTTTGG TGCTTTCAGGGAAAGACAGCCCAGACGCTTTTGGCAATAGCGTTGTAAGAACGAAAAAGT GGGGCATGCTTCACAACTATGTTTTGAACGTAGAAAACTGTGATATCGAGCGTCTCGATAT CAACCACTCTTTTAACTTCTTTACGTCTGGCAAAGGCGCGTTTGCCGATGACATATCACTCT CGAAAAATAGTTTTAACGGCATTACGGGCCATGTTTTAAGTCTTGATAAAGAGATAGAGG ACTACGGTATTTATAACGCTGAGTATGTCAGCATAACCAACAACACGTTTAGCAACATAAG TGGTAGCGTTGTAAATCTCTACCGAGGCGGTACCGATGAAAGTACCTTTGGACCGCACTTA GACATGCAGGGCAACGTGTTAACTAACGTAGGCAGTGGTAAACGCAACAAACAAAGTGC CAGCGTTTATCTTCATGGCGTGCAAGTTTCAACGCTAAAAAATAACAACTTTAATGAGTCT GAGCCTGTTGTGGTTAATCACACCGTTGGTGAGCCAATTACCGCAATAACAAACAATACGT TCCTAAATACACCTATGCCAATGATTAAAGAGCTGTTTGCACCTGGTCCGCACACTGCGGT ATTGAATGACAATGTTTCCACGAAAGCGAACAAGAGGTAA
PL6-2	ATGAAAAAAATAAGTATTTTAACGCTTAGCGCCTTAAGCCTAGGGCTTGCGGGTTGCGGTG GTGATGATGGTGCTACAAACCAGCCTGGTGCCTTATCTCTTTCTGGAACGGCTAAGGAAGG AGAGACGTTAACTGCATCAGTCAGTGACCCTGACGGTATTGATCAAAACACAGTGGTGTT TACATGGTTTGCAGATGGTACACCAATAGCAGATGCAACCGATGCTTCTTACACGCTTACG GTAAATGAAGCTGGTACACGTATTCGTGTAGCGGTTACGTACGTCGACCTGGGCAACACGC GTGAAGGTTTTACTACAGAAGAAACCGAGGTGGTAGAAGCGTTGCCTGTTAACTTTGAGG GTGTTATTACCATTTCAGGCTCTACAACGGTAGGGCAAACGTTAACGGCAGACATAACAG ACGATAATGGTTTGTCTGGCACCGTAACTTACAGCTGGGCCTCAGACGGCGATGTTATCGA AGGAGCTGTATCTAATTCGCTTGAGCTTGTTGAGGCTTACGAAGGAACTGCCATTACGGCT ATGGCTTCATATGTTGACGATAGTGGATTTGACGAATCAATTACCTCTGAGCCTACTGAAG CTATTGCACCAGTGCCGGCTGATAATGTAACGGGCTCGCTTGACGACCCTATTACTGGTGA GCTAACAGTAGGTGCCACGCTTACTGCACCTACCCCTGTTGATGCCAATGGCGTTTCAGGT GAAATTAGTTACCAGTGGCAGTCGCGTAACGTTGGTGAAGATTTATCTACAGCGGTCAATA TCGATGGTGCAACAGAAGCAACATTAGTCGTAACAGACGCAGACTTAGGCAAAGTGCTTT CAATTAACGTATCTTACACAGATGATGCGAACTATGAAGAAGACCTTTCGAAAAGTGCAG ATGACCAGATATTTACGTTTTATGTGCAAGGTGAAGTGTCGCTCACTGCAGCGCTAGCTAA CGCGCAAGAAGGCGATTCAATTGGTATCGCGGATGTATTAAATACAAGTGATACTGCAGA TGATTATGAAGATATGGCTGAGCTTTCTATCGCACAAAATAATCTTCTTATTAAACGGGTA GCAGAAACTAACGCGGTCATTTCAGGCACTACGTGTATTGCATTCAGTTCGTCAGTCAGCG GTGTAGTATTAGATGGTCTTGTGTTTGAAGAGTTAGTGATACCCGTTGCGGGGAGCTGCGG TGAAGGTCGTGGTTCAATTGACCTAAACGGCTCTGGCAATACTATTAAAAACGCTAGTTTC TTGAGCGACTCAGGTGCTACGCGACCCAATTTAGGTTCAAGTGATGAGTCTCACTACATCA CGGTTAGTGGTACCGACAATATTATTGAACGTAACCTATTTACTGGTAAAAGCGTCAACGA AGCTGAAGAAGGCTCTGCTATTAGCATGTTCCTAGGTGTCGGTGACACGCCTAACTCATTG GGCGATCATCAGCGTAACATTGTTCAATACAATCTGTTCAAAGACTTCCTACCTACCACTA TTGACGGTGACGGAGAGTTCGACACTGACTCAGGTAGTCACGCTGTTCAGGTTGGTCGCT CTGGTAGTGGCGATGGCGCGGGTCGCGGCGAACATGTGGTTCAATATAACCGTTTCGATC GCGTACTTGTGGATCGTGGTCTTATTATTGTTCAAGGTGGCGGTAATAGTATTCATGCCAA CACGATTGTAAACTCTTGGGGGAATGTCGAGTTGCGAAATGGCTATGGTAATACCGTGTCG CAAAATATCATTATCTCAAGCGGAGAACCTTATACGGCAACCGTTGGCGGAGTAGAAGGT ACTAATAATAAAGACGGTGGTATTGCTTTCACGCCTTTAGGCCATGCAATTACCGACAACT

	TTGTTGCTAACATCATTACTAATTCTTCAGACCGCGCAGCACTGCATATCGATTCTGATTAT ATCGACAGCGGTAACTCATCTACGCAAACACTGATTGATGCAGGCCTTGATTTAAATACGG TTATTGCTCGTAACACGATATTAAATACAACTAACGCCATTCAGTTTGAAGATGATTCTTCT CGCGACGGCGCAGAAAACTGTACTAATCTTGATTACACCTTGGACTTCGACAGTAACCTTA TTGCTAATCAAAGCGCAGACAACAACATCTTCGGCACGGCTTCTGGTGCTGGTGCTACAGC GATTAAGCAAGATGAATATCCTGCTCATGGTTGTGCATTAGATAACGATTCTGACTATGAT AATAACCATATTTATGCTCAAACCGTTGCTGATTTAACACCGATAATGCCAAAGCGCGATA ACACATCTTTGGTTGATGGTGTTGATGGCAACATATTGGCTGACAATTCAGAAGACGGTGC AAGCTTGAGTGAACCCACTGCGAATAAGTTAGTGGAAGGTACGGGTAGCGATGCCGGTAT TGGTGCAGCGCTGGACGACCTTATCTTTATTGAAGAAAACATGGTTGGGCCTTATTCAACG TGGGAAGCACCGGCTCTGAGTAACTAA

B)

Ulvan lyase	MFLAVVTAQTAPDEDTSAITRCTAEGTNPVRETDIPNPVNVGTIDDRSCYANYKESTVY GKTWGVYNITFDSNDFDTSLQPRIERSLSRSSETGIGSYARLTGVFRILEVGDTSGTSQDG TYLAQAKGKHTGGGGSPDPAICLYLAKPVYGTGEDADKQVSFDIYAERILYRGGEGDG REIVFLKNVKKDEETNFELEVGFKEDPNDVSKKIQYCNAVIGGDTFNWNIPEPERGTESG IRYGAYRVKGGRAQIRWANTTYQKVENVEVTNPGPIGDVYKLKNVATGQYLSDSGVS ASAVIMSDSGEAQNNYWTFVESGSLFNIDNETFGILRAPGAGGPGGAYVVVSTTKEGPS SDGDKVWTIHYNESNDTYRFESGSSGRFMYQEINGNVTHISAMNTDDRSVWKAIAVES LSVDENAILASDVRVFPNPASDSFTISLKTINHVTVNIYDVLGNTIFKSEFNGDTIQIRNKG QFKAGVYLIQLTDKNNNKYHKKLIVK

Table S2. Primer sequences of alginate lyases.

Name	Primer sequence 5'→3'	Cloning vector
PL7-1 F	TACTTCCAATCCAATGCA TCCACAACCTCGCAAACGCCTTTACC	pet 28a, GFP, SUMO
PL7-1 R	TTATCCACTTCCAATGTTATTA CTAGTTACCATGTTCATTCTCAATTG	pet 28a, GFP, SUMO
PL6-1 F	TACTTCCAATCCAATGCA AAACAATATAACGTTAGCTCACCAGA	pet 28a, GFP, SUMO
PL6-1 R	TTATCCACTTCCAATGTTATTA TTACCTCTTGTTCGCTTTCGTGGAAA	pet 28a, GFP, SUMO
PL17 F	TACTTCCAATCCAATGCA GCTCACCCTAACTTGGTGATCACGCA	pet 28a, GFP, SUMO
PL17 R	TTATCCACTTCCAATGTTATTA TTACAGCGCATACACAGCGAAACGGC	pet 28a, GFP, SUMO
PL7-2 F	TACTTCCAATCCAATGCA GAAGACCTCGCGCTGCATGCACAACA	pet 28a, GFP, SUMO
PL7-2 R	TTATCCACTTCCAATGTTATTA GTTCTCTTCTGGTGTACTTTCTGTCAC	pet 28a, GFP, SUMO
PL6-2 F	TACTTCCAATCCAATGCA TTACCTCTTGTTCGCTTTCGTGGAAA	pet 28a, GFP, SUMO
PL6-2 R	TTATCCACTTCCAATGTTATTA TTAGTTACTCAGAGCCGGTGCTTCCC	pet 28a
CBM32 F	CTGGTGCCGCGCGGCAGCCATATGGCTAGC GCGTTAC-CATTAACAGGGTTAAGCGC	pet 28a
CBM32 R	ATCTCAGTGGTGGTGGTGGTGCTCGAGCT AGTCGCCTTCAGTG-CAATTGAATAACT	pet 28a
PL7-1 F2	GCGGCAGCCATATGGCTAGC TCCACAACCTCGCAAACGCCTTTACC	pet 28a
PL7-1 R2	TGGTGGTGGTGGTGCTCGAG GTTACCATGTTCATTCTCAATTGAAT	pet 28a

Table S3. PCR-amplification of alginate lyases from *Alteromonas macleodii* 83-1. Shown are (A) the composition of the PCR master mix and (B) the thermocycler conditions for PCR-amplification.

A) PCR master mix.

Reagent	Concentration	Amount (µl)
2x Q5 Master Mix (New England Biolabs)	1x	12.5
Forward primer	10 pmol/µl	1.25
Reverse primer	10 pmol/µl	1.25
Plasmid DNA	/	1
Autoclaved MilliQ	/	9

B) Thermocycler conditions for PCR-amplification.

Step	Time	Temperature (°C)	cycles
Initial denaturation	30 sec	98	1
Denaturation	7 sec	98	
Annealing	20 sec	50	30
Elongation	1 min	72	
Final elongation	2 min	72	1
Pause	∞	4	∞

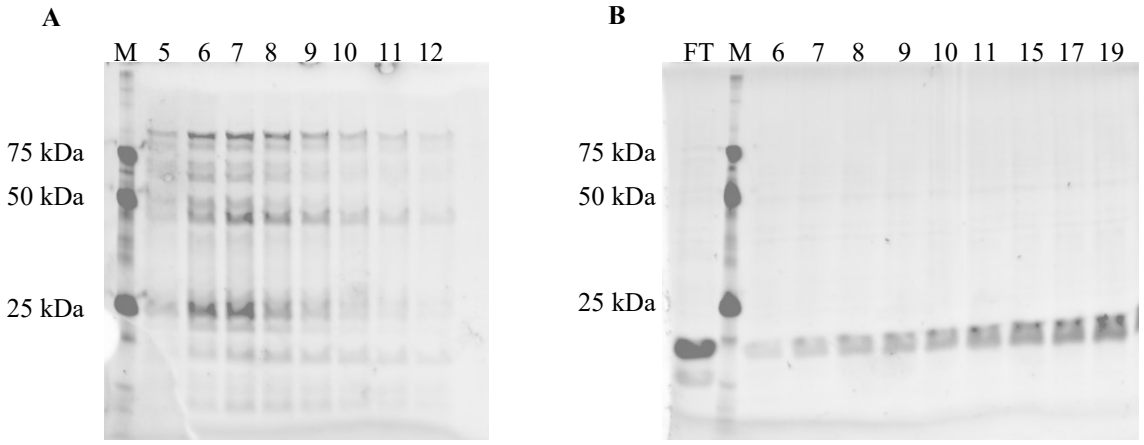

Figure S1. Purified CBM32 of Aly PL7-1 from *Alteromonas macleodii* 83-1. (A) Soluble protein purified via IMAC and (B) refolded protein purified after IMAC. 10 µl of each fraction were used for SDS-PAGE. FT: flow through of chromatography, M: protein marker.

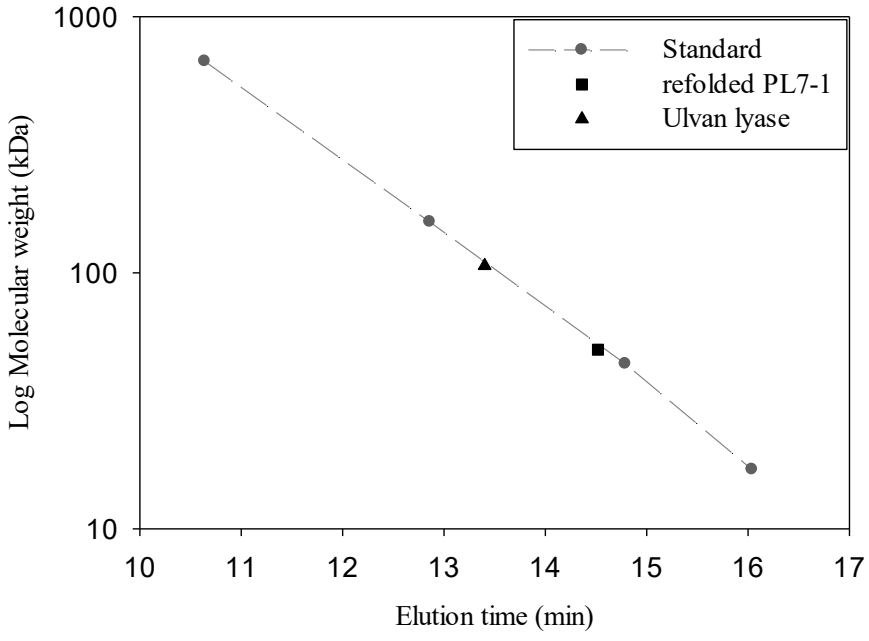

Figure S2. Calibration curve for analytical size exclusion chromatography. Logarithmic application of the molecular weight of 60 µl Gel Filtration Standards (1511901, Bio Rad) against the elution time of 20 mM Tris pH 8, 0.25 M NaCl. SEC was performed in NGC™ Chromatography System (Bio Rad) using an ENrich™ SEC 650 10 x 300 Column (Bio Rad) and 1 ml/min flow rate.

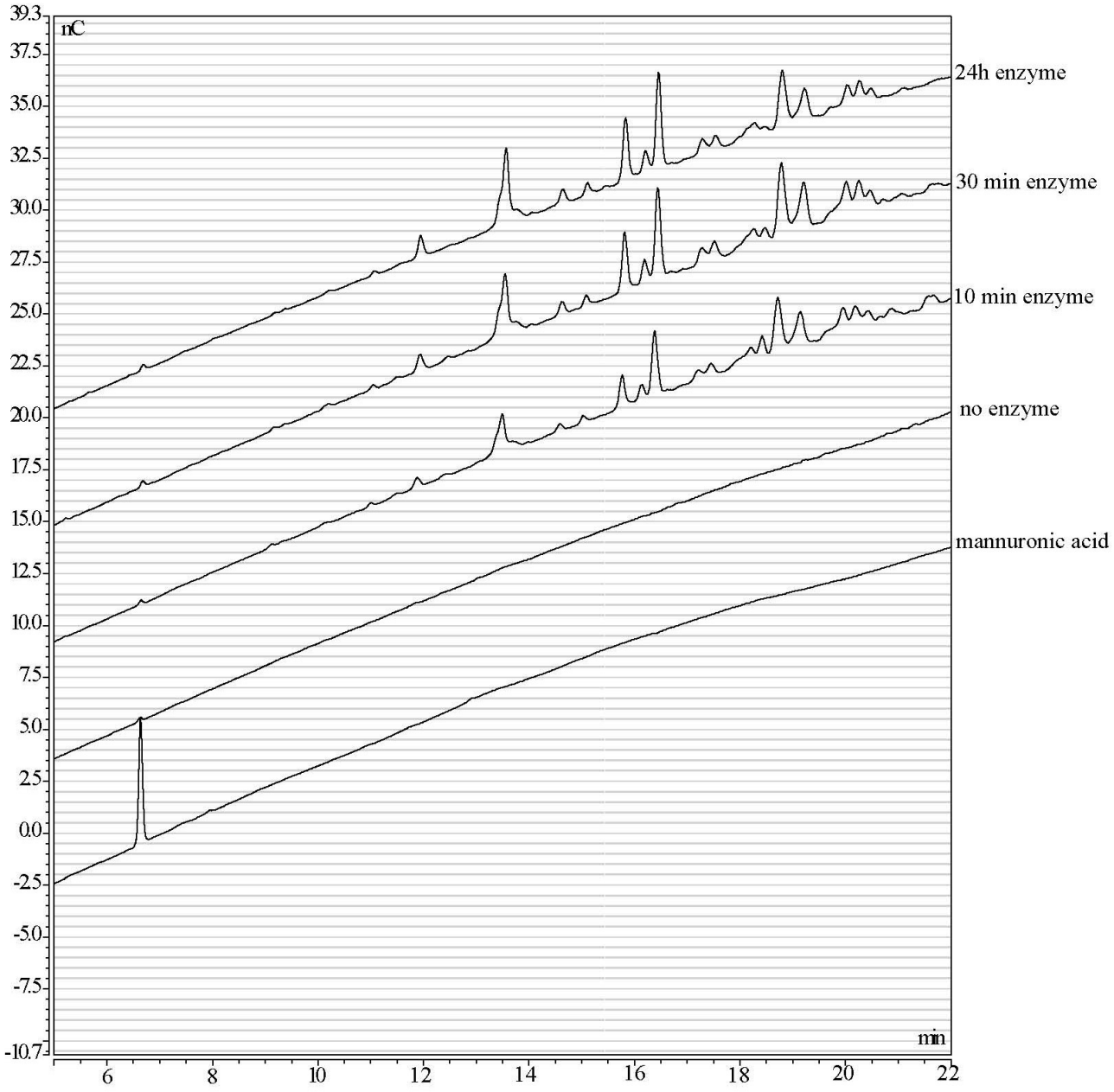

Figure S3. HPLC chromatogram of alginate degradation by refolded PL7-1. Elution time of mannuronic acid, enzymatic digest of 0.1 % algal alginate for four different time intervals (24 h, 30 min, 10 min) as well the control without enzyme. The chromatogram was illustrated using software Chromeleon Dionex version 7.2.3.75533.

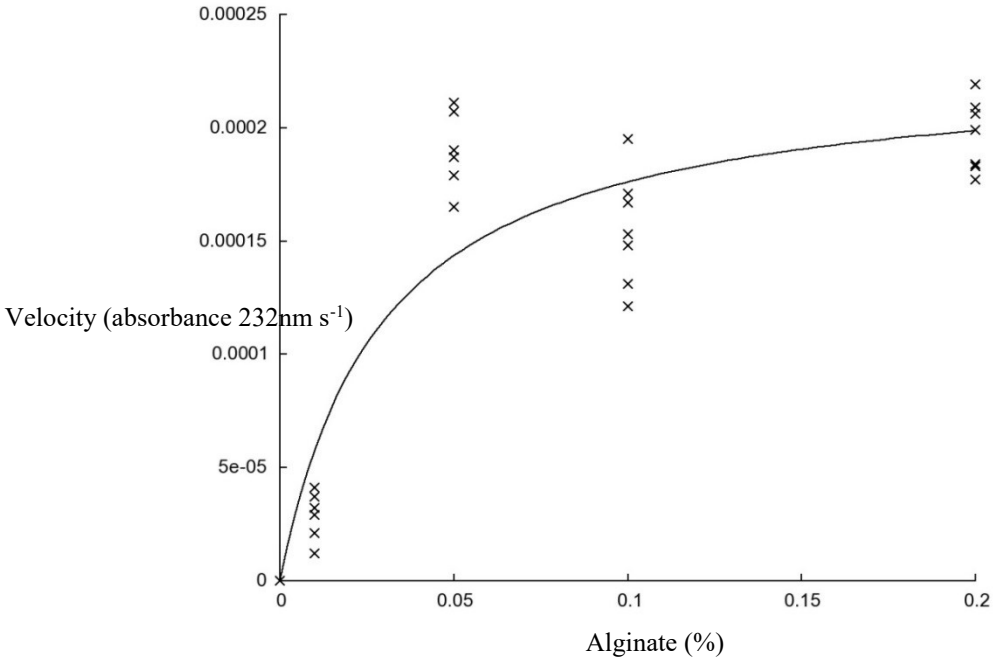

Figure S4. Activity of refolded PL7-1 on alginate. Enzymatic assay was performed using 50 mM HEPES pH 9.0, 0.3 M NaCl, and 1 mM $CaCl_2$ at 25 °C. The curve fitted to the Michaelis-Menten equation.

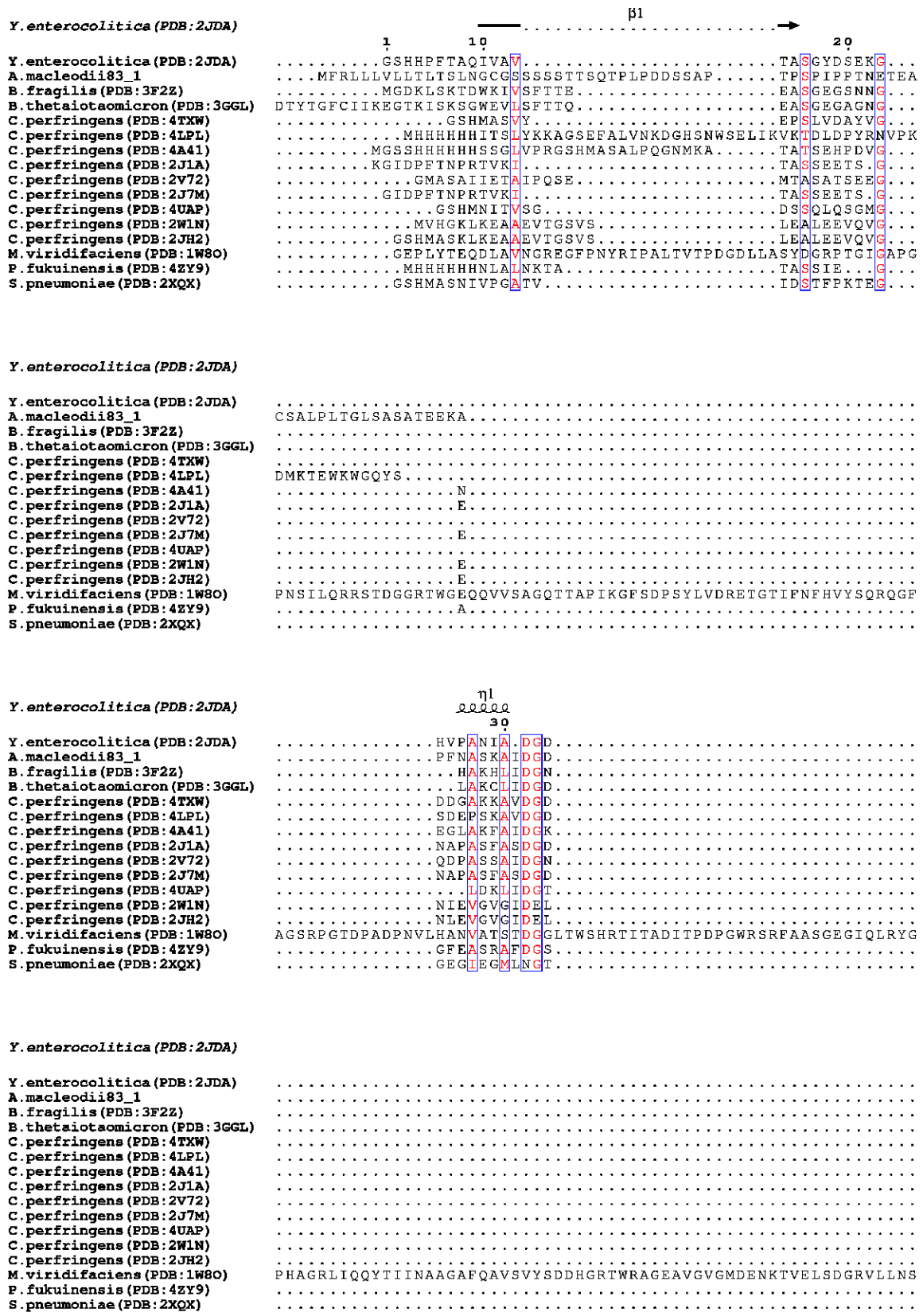

Figure S5. Structure-based alignment of putative CBM32 of PL7-1 from *Alteromonas macleodii* 83-1 and crystallized homologues. Multiple protein alignment of alginate lyases PL7 as well as a secondary structure prediction of the closest homologue of *Yersinia enterocolitica* (PDB code: 2JDA, Abbott *et al*., 2007). Conserved residues in the homologues are colored in red and putative binding residues are indicated by a star.

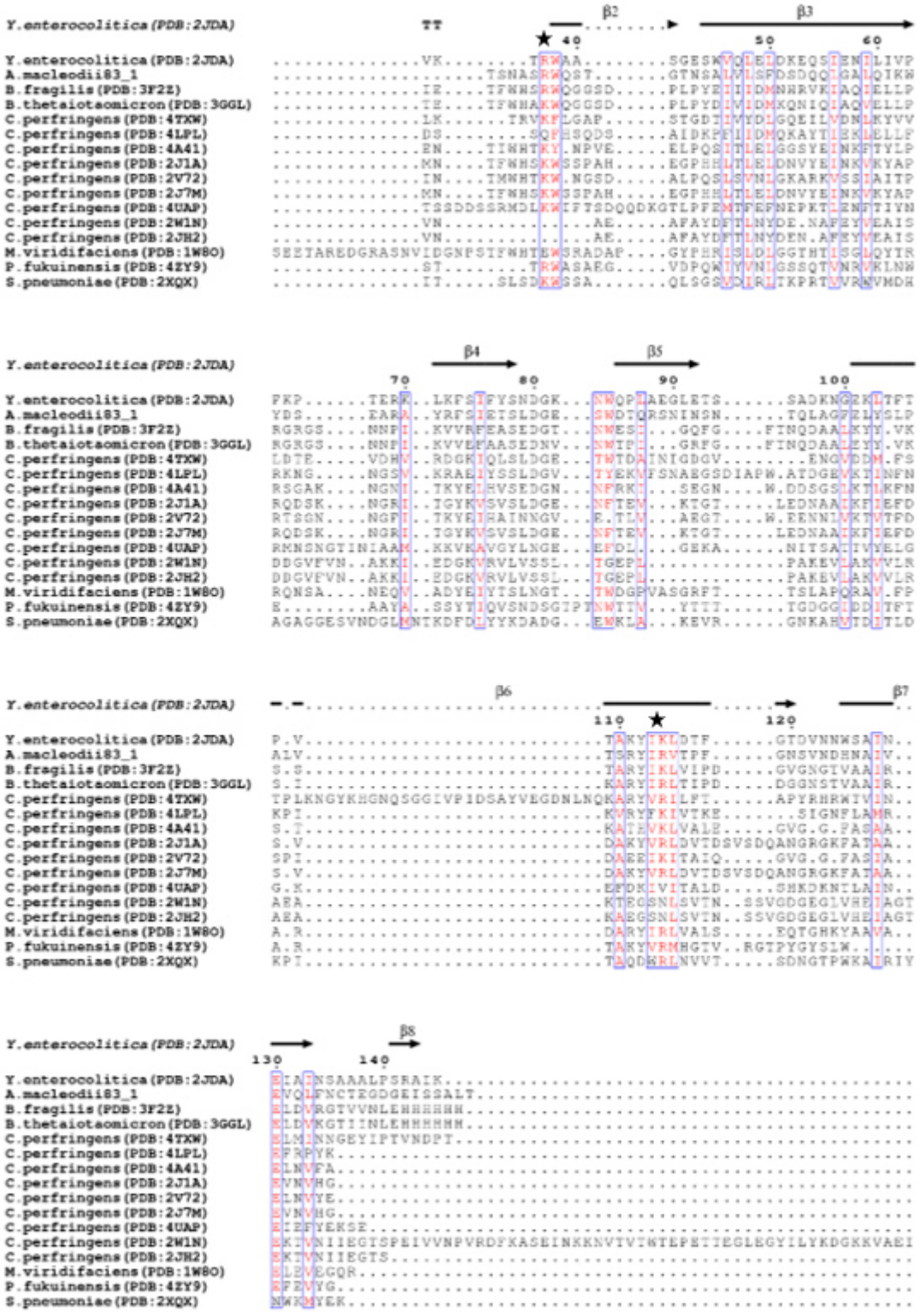

Figure S5. Continued.

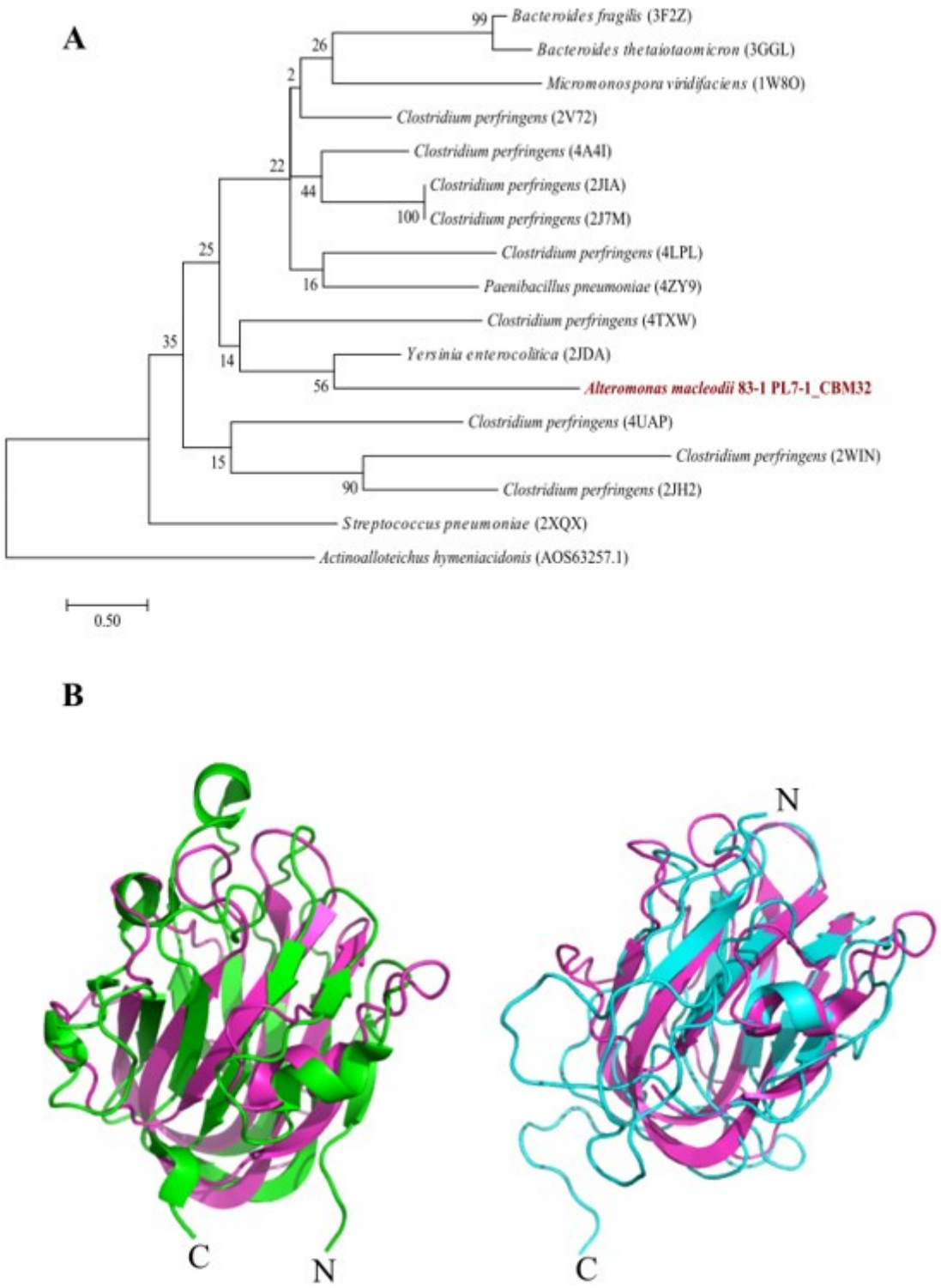

Figure S6. Phylogenetic tree of crystallized CBM32 from bacteria. (A) Maximum likelihood tree based on the WAG+G model (Whelan & Goldman, 2001) using all sites as well as a MUSCLE protein alignment (Edgar, 2004) calculated in MEGA 7.02 (Kumar *et al*., 2016). The indicated values at each branch derive from 1000 bootstrap replications. PDB code of proteins in brackets. Putative CBM32 of PL7-1 from *A. macleodii 83-1* is highlighted in red. Carbohydrate esterase from *Actinoalloteichus hymeniacidonis* (AOS63257.1) was used as out-group. Putative CBM of alginate lyse PL7-1 from *A. macleodi*i 83-1 is highlighted in magenta. Superimposition of CBM32 from (B) *Y. enterocolitica* (magenta) and PL7-1 (green) as well as (C) *Y. enterocolitica* (magenta) and *C. perfringens* (blue, PDB code: 4TXW).

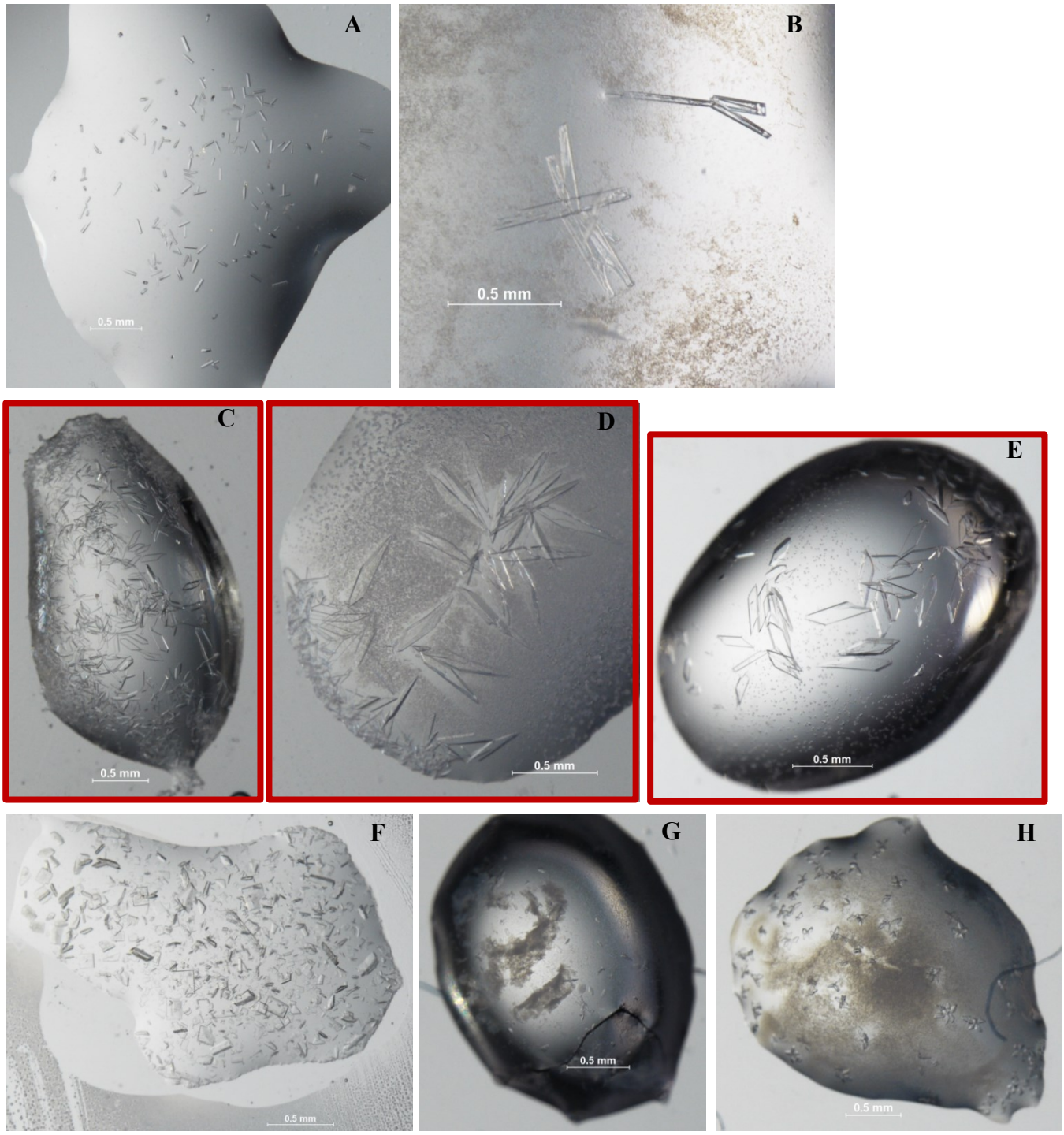

Figure S7. Optimized crystal conditions of ulvan lyase from *Formosa agariphila* KMM3901^T. Crystals from images marked with a red outline were chosen to determine protein structure with X-ray crystallography.

A: 18 mg/ml protein in 20 mM Tris pH 8, 250 mM NaCl 0.1 M Tris pH 8.5, 0.4 M $MgCl_2$, 14 % PEG8000

B: 18 mg/ml protein in 20 mM Tris pH 8, 0.1 M Tris pH 8.5, 0.4 M $MgCl_2$, 22 % PEG8000

C: 29 mg/ml protein in 20 mM Tris pH 8, 0.02 M KH_2PO_4 pH 4, 17 % PEG 3350

D: 29 mg/ml protein in 20 mM Tris pH 8, 0.02 M KH_2PO_4 pH 4:Na_2HPO_4 pH 9 (1:1), 18 % PEG 3350

E: 29 mg/ml protein in 20 mM Tris pH 8, 0.02 M KH_2PO_4 pH 4:Na_2HPO_4 pH 9 (1:4), 19 % PEG 3350

F: 29 mg/ml protein in 20 mM Tris pH 8, 0.02 M KH_2PO_4 pH 4:Na_2HPO_4 pH 9 (1:4), 22 % PEG 3350

G: 29 mg/ml protein in 20 mM Tris pH 8, 20 % glycerol, 24 % PEG 4000, 0.08 M Tris pH 8.5, 0.16 M $MgCl_2$

H: 29 mg/ml protein in 20 mM Tris pH 8, 0.08 M Bis-Tris-propane pH 9, 23 % PEG 1500.

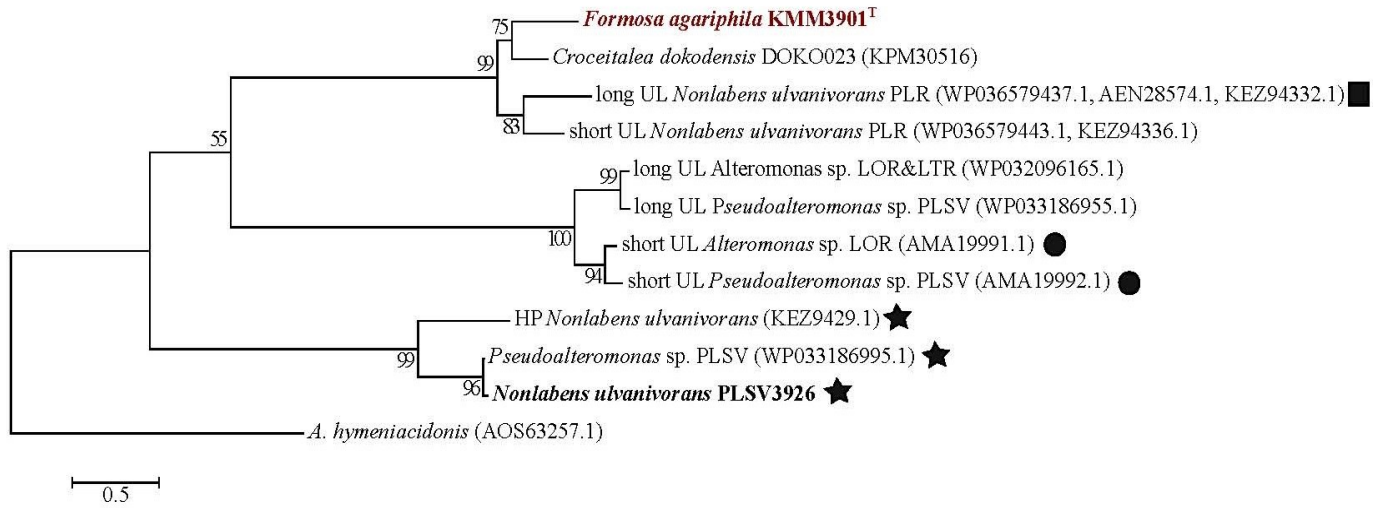

Figure S8. Phylogenetic relatedness of bacterial ulvan lyases. The indicated values at each branch derive from 1000 bootstrap replications. Ulvan lyase (UL) from *F. agariphila* KMM3901^T is colored in red. Carbohydrate esterase from *Actinoalloteichus hymeniacidonis* (AOS63257.1) was used as an out-group. PL families 24 and 25 are indicated by dots and stars, respectively. Unclassified polysaccharides are marked with a square. The lyase with known structure is highlighted in bold. HP: hypothetical protein.

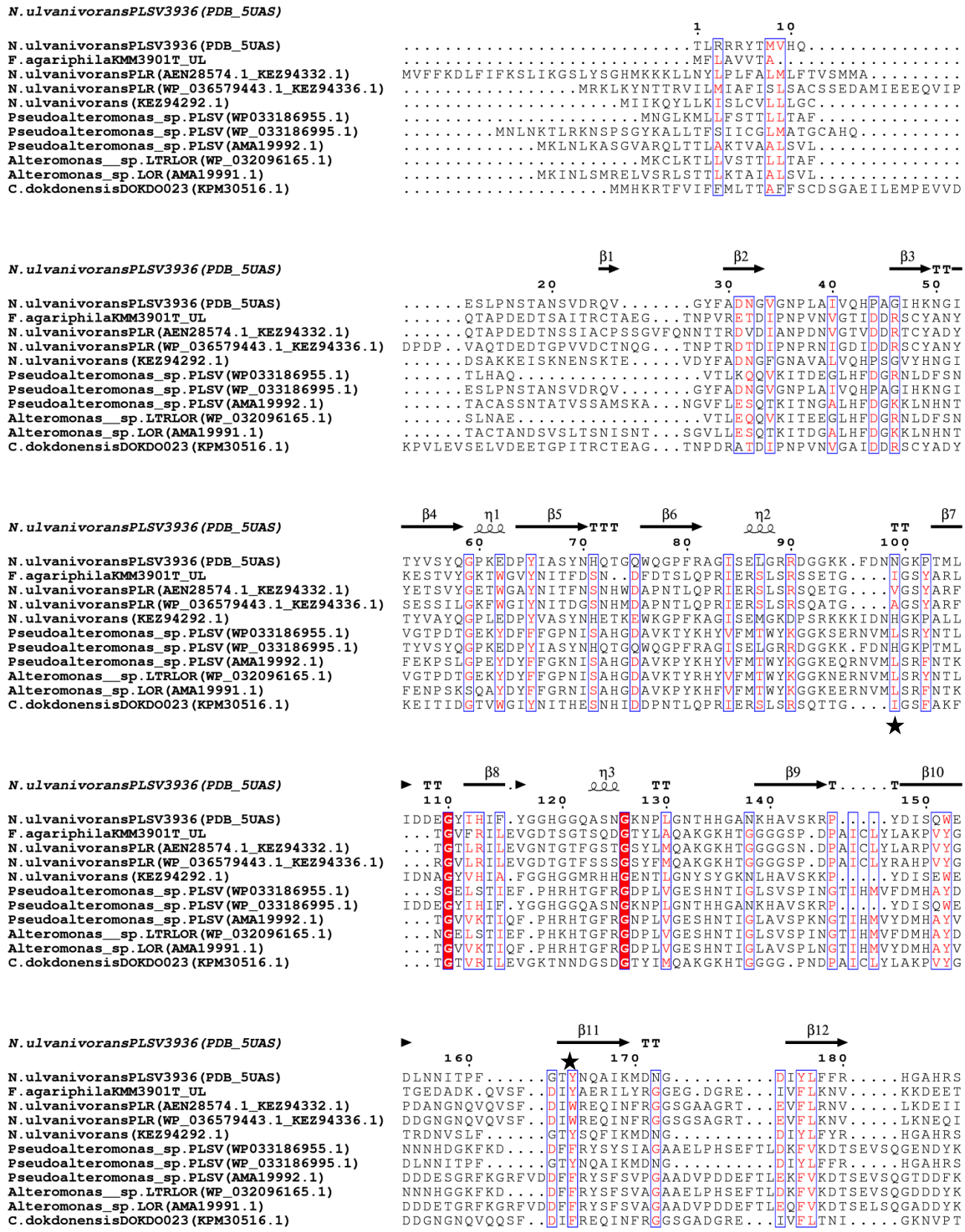

Figure S9. Multiple sequence alignment of bacterial ulvan lyases. Multiple protein alignment of ulvan lyases as well as a secondary structure prediction of *Nonlabens ulvanivorans* PLSV3936 (PDB code: 5UAS, Ulaganathan *et al*., 2017). Conserved residues in the homologues are colored in red and putative catalytic residues are indicated by a star.

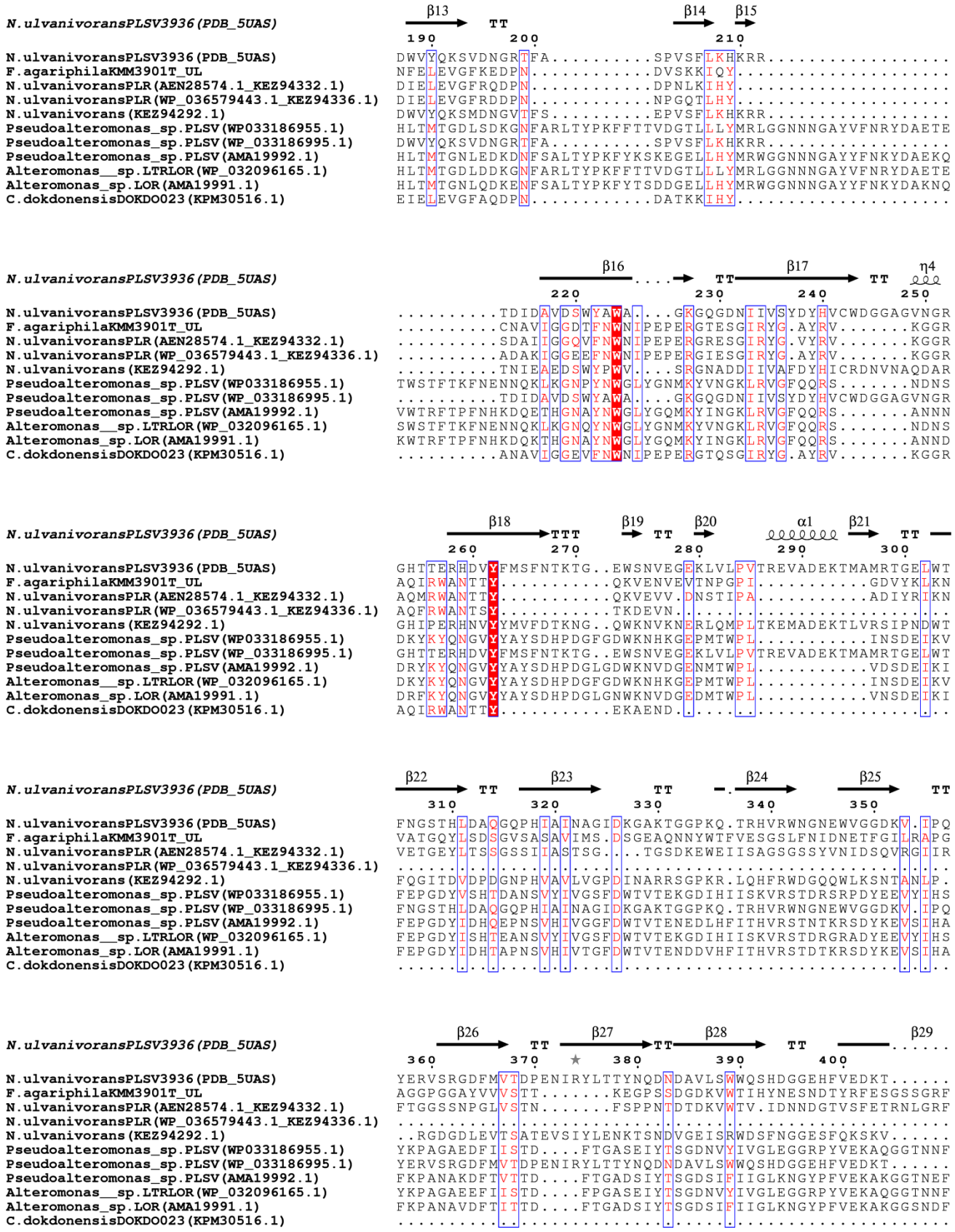

Figure S9. Continued.

```
N.ulvanivoransPLSV3936(PDB_5UAS)                    β30              β31          β32
                                                ..━━━━►TT ━━━►     TT      ━━━━━►     ━.━━━━►
                                                      410 ★     420       430         440

N.ulvanivoransPLSV3936(PDB_5UAS)                ..VLRKDNASFAISAFIKDAIPDAQMLVAEKVSDEGI.KMYLVGE.........
F.agariphilaKMM3901T_UL                         ..MYQEINGNVTHISAMNTDDRSVWKAIAVESLSVDE.NAILASD.........
N.ulvanivoransPLR(AEN28574.1_KEZ94332.1)        ..LYHDTNNMITHSA..NIDDRSKWNLESTTLSVDSQ.QIASVGV.........
N.ulvanivoransPLR(WP_036579443.1_KEZ94336.1)    ......................................................
N.ulvanivorans(KEZ94292.1)                      ..FLQRENSGFVISSLIDNPHPDARIIVAEKEEGTDFRKMYLLGD.........
Pseudoalteromonas_sp.PLSV(WP033186955.1)        VRVYEASDGPTFDHGTLYIKDGKVYYYLMERTSGNAM.PLYLQIIDLDLDLESD
Pseudoalteromonas_sp.PLSV(WP_033186995.1)       ..VLRKDNASFAISAFIKDAIPDAQMLVAEKVSDEGI.KMYLVGE.........
Pseudoalteromonas_sp.PLSV(AMA19992.1)           EVVYQQTSGVKFDHGTIHIENGKAYYYLMEKGAGNSL.PLHLQVI.........
Alteromonas__sp.LTRLOR(WP_032096165.1)          IRVYEASDGPVFDHGTLYIKDGKVYYYLMERTSGTAM.PLYLQII..DLDLESD
Alteromonas_sp.LOR(AMA19991.1)                  EVVYQQASGVKFDHGTIHIENGKAYYYLMEKGAGNAL.PLHLQVI.........
C.dokdonensisDOKDO023(KPM30516.1)               ......................................................


N.ulvanivoransPLSV3936(PDB_5UAS)

N.ulvanivoransPLSV3936(PDB_5UAS)                ......................................................
F.agariphilaKMM3901T_UL                         ......................................................
N.ulvanivoransPLR(AEN28574.1_KEZ94332.1)        ......................................................
N.ulvanivoransPLR(WP_036579443.1_KEZ94336.1)    ......................................................
N.ulvanivorans(KEZ94292.1)                      ......................................................
Pseudoalteromonas_sp.PLSV(WP033186955.1)        ANAPIVSFPSPSLTVEQGFEKLSLNIAAESPVEVRTIQSVTLYINDELVRTDTS
Pseudoalteromonas_sp.PLSV(WP_033186995.1)       ......................................................
Pseudoalteromonas_sp.PLSV(AMA19992.1)           ......................................................
Alteromonas__sp.LTRLOR(WP_032096165.1)          ANAPIVSFPSPSVTVNQGYEKLSLNISAESPVEGRSIQSVSLYIDDELVRTDDS
Alteromonas_sp.LOR(AMA19991.1)                  ......................................................
C.dokdonensisDOKDO023(KPM30516.1)               ......................................................


N.ulvanivoransPLSV3936(PDB_5UAS)

N.ulvanivoransPLSV3936(PDB_5UAS)                ......................................................
F.agariphilaKMM3901T_UL                         ......................................................
N.ulvanivoransPLR(AEN28574.1_KEZ94332.1)        ......................................................
N.ulvanivoransPLR(WP_036579443.1_KEZ94336.1)    ......................................................
N.ulvanivorans(KEZ94292.1)                      ......................................................
Pseudoalteromonas_sp.PLSV(WP033186955.1)        LPYLFGHGSKPHETGAMGWLDTHEPNPSPLPAGRHIFKAVAVDSEGDSSVATMM
Pseudoalteromonas_sp.PLSV(WP_033186995.1)       ......................................................
Pseudoalteromonas_sp.PLSV(AMA19992.1)           ......................................................
Alteromonas__sp.LTRLOR(WP_032096165.1)          LPFLFGHGSKPHETGALGWLDRHEPNPSPLSAGRHVFKAVAVDSEGDSSTATMI
Alteromonas_sp.LOR(AMA19991.1)                  ......................................................
C.dokdonensisDOKDO023(KPM30516.1)               ......................................................


N.ulvanivoransPLSV3936(PDB_5UAS)

N.ulvanivoransPLSV3936(PDB_5UAS)                ......................................................
F.agariphilaKMM3901T_UL                         ......................................................
N.ulvanivoransPLR(AEN28574.1_KEZ94332.1)        ......................................................
N.ulvanivoransPLR(WP_036579443.1_KEZ94336.1)    ......................................................
N.ulvanivorans(KEZ94292.1)                      ......................................................
Pseudoalteromonas_sp.PLSV(WP033186955.1)        LTVNSNAPIISFPQESLEVDEGFEKLSLNISAESAVEGRTIESVSLYIDGEFVR
Pseudoalteromonas_sp.PLSV(WP_033186995.1)       ......................................................
Pseudoalteromonas_sp.PLSV(AMA19992.1)           ......................................................
Alteromonas__sp.LTRLOR(WP_032096165.1)          LNVNSNAPIVSFPQESLEVDEGFERLSLNISAESAVEGRTIESVSLYIDGGLVR
Alteromonas_sp.LOR(AMA19991.1)                  ......................................................
C.dokdonensisDOKDO023(KPM30516.1)               ......................................................


N.ulvanivoransPLSV3936(PDB_5UAS)

N.ulvanivoransPLSV3936(PDB_5UAS)                ......................................................
F.agariphilaKMM3901T_UL                         ......................................................
N.ulvanivoransPLR(AEN28574.1_KEZ94332.1)        ......................................................
N.ulvanivoransPLR(WP_036579443.1_KEZ94336.1)    ......................................................
N.ulvanivorans(KEZ94292.1)                      ......................................................
Pseudoalteromonas_sp.PLSV(WP033186955.1)        TDTSLPYLFGHASKPHETGAMGWLDTHSPNPSPLTSGTYEFTAVAIDSEGEEST
Pseudoalteromonas_sp.PLSV(WP_033186995.1)       ......................................................
Pseudoalteromonas_sp.PLSV(AMA19992.1)           ......................................................
Alteromonas__sp.LTRLOR(WP_032096165.1)          TDTSLPYLFGHASKPHETGAMGWLDTHSPNPSPLAAGSYEFTAVATDNEGEETT
Alteromonas_sp.LOR(AMA19991.1)                  ......................................................
C.dokdonensisDOKDO023(KPM30516.1)               ......................................................
```

Figure S9. Continued.

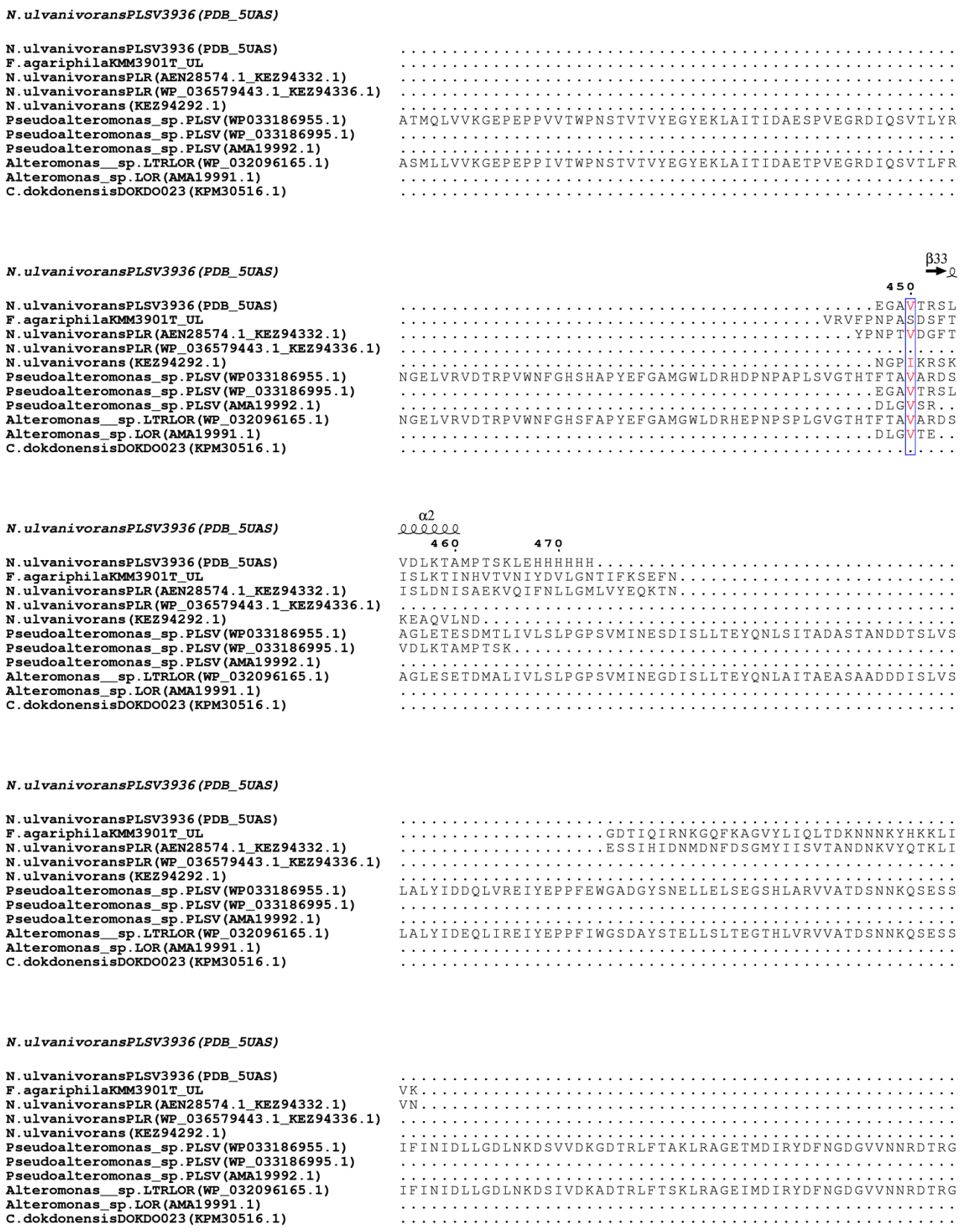

Figure S9. Continued.

Statement

Bremen, May 24th, 2017

I, Nadine Gerlach, hereby confirm that I have written this thesis unaided and that I used no other resources than those mentioned. All passages taken either verbatim or in adapted form from publications are indicated as such.

Nadine Gerlach